Горение атомных ядер:

Гидростатическое горение

FBS2014

В.Н. Кондратьев

Киевский национальный университет имени Тараса Шевченко, UA-03022 Киев, Украина

ЛТФ, ОИЯИ, 141980, Дубна Россия

Energy vs Work

in Comparison

	– Energy (joules)
Average daytime solar energy on Earth/m^2 sec	$1.3\ 10^{3}$
Energy from metabolism of a candy bar	$1\ 10^{6}$
Energy spend at 1 hour walking (adult)	$1\ 10^{6}$
Kinetic energy of a car at 100 km/hr	$1\ 10^{6}$
Daily energy needs of an adult	$1\ 10^{7}$
Energy released at burning 1 liter oil	$1.2\ 10^{7}$
Energy released at fission of 1kg ^{235}U	$5.6\ 10^{13}$
Energy from fusion of hydrogen in 1l water	$7\ 10^{13}$
Energy released by 1 megaton H-bomb	$5\ 10^{15}$
Energy at major earthquake (magnitude 8)	$2.5\ 10^{16}$
Annual energy generation by Sun	10^{34}
Energy released at supernova (star explosion)	10^{44}--10^{46}

Nuclear Reactors

Fusion

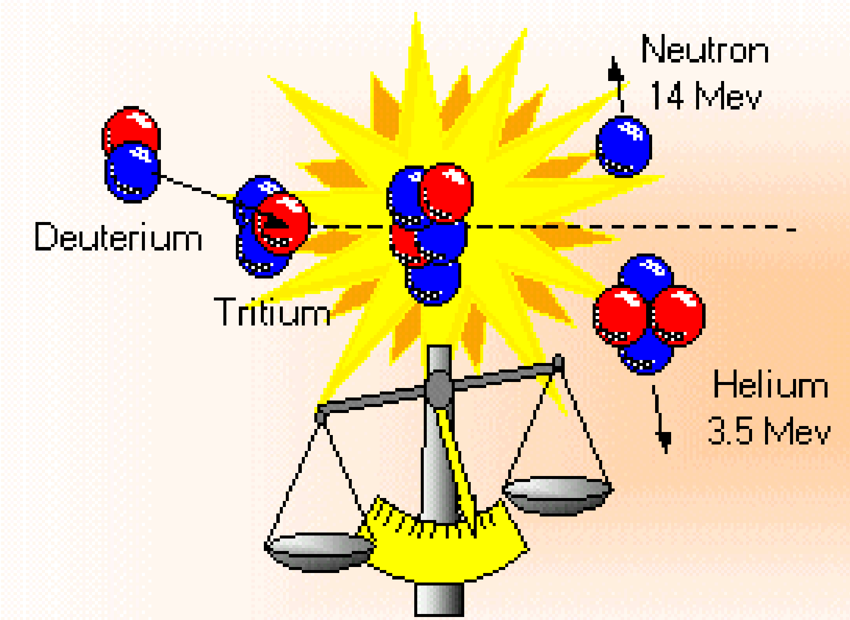

D + T –

Fission

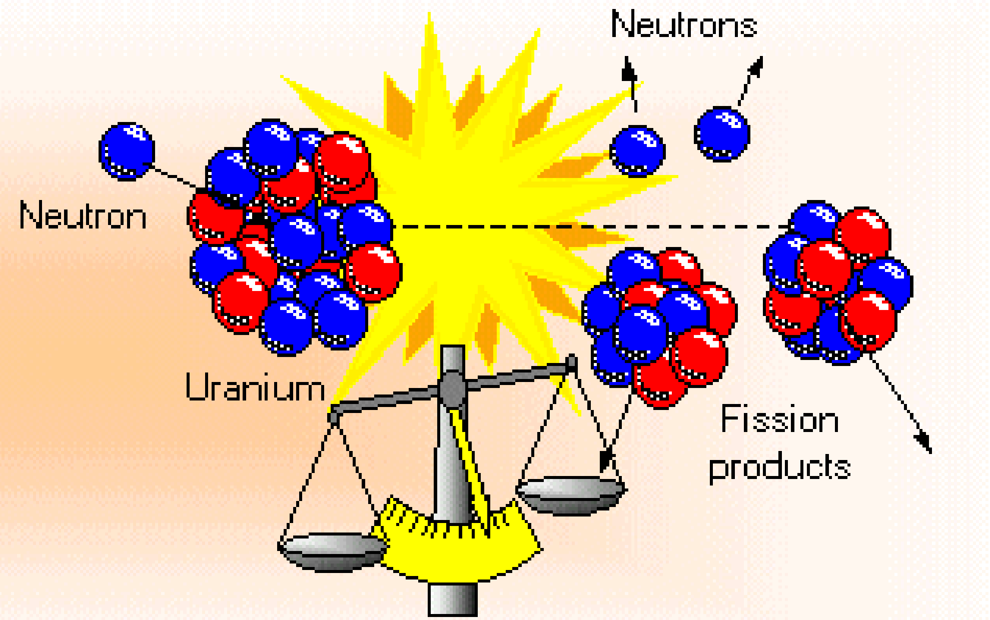

$n + U^{235} \longrightarrow 2.5\ n + \text{fission products} + 200\ \text{MeV}$

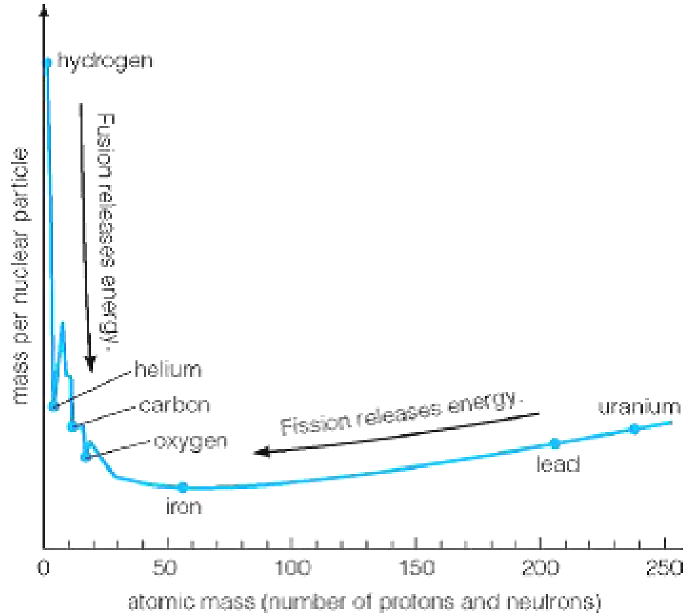

Nuclear Binding Energy Map

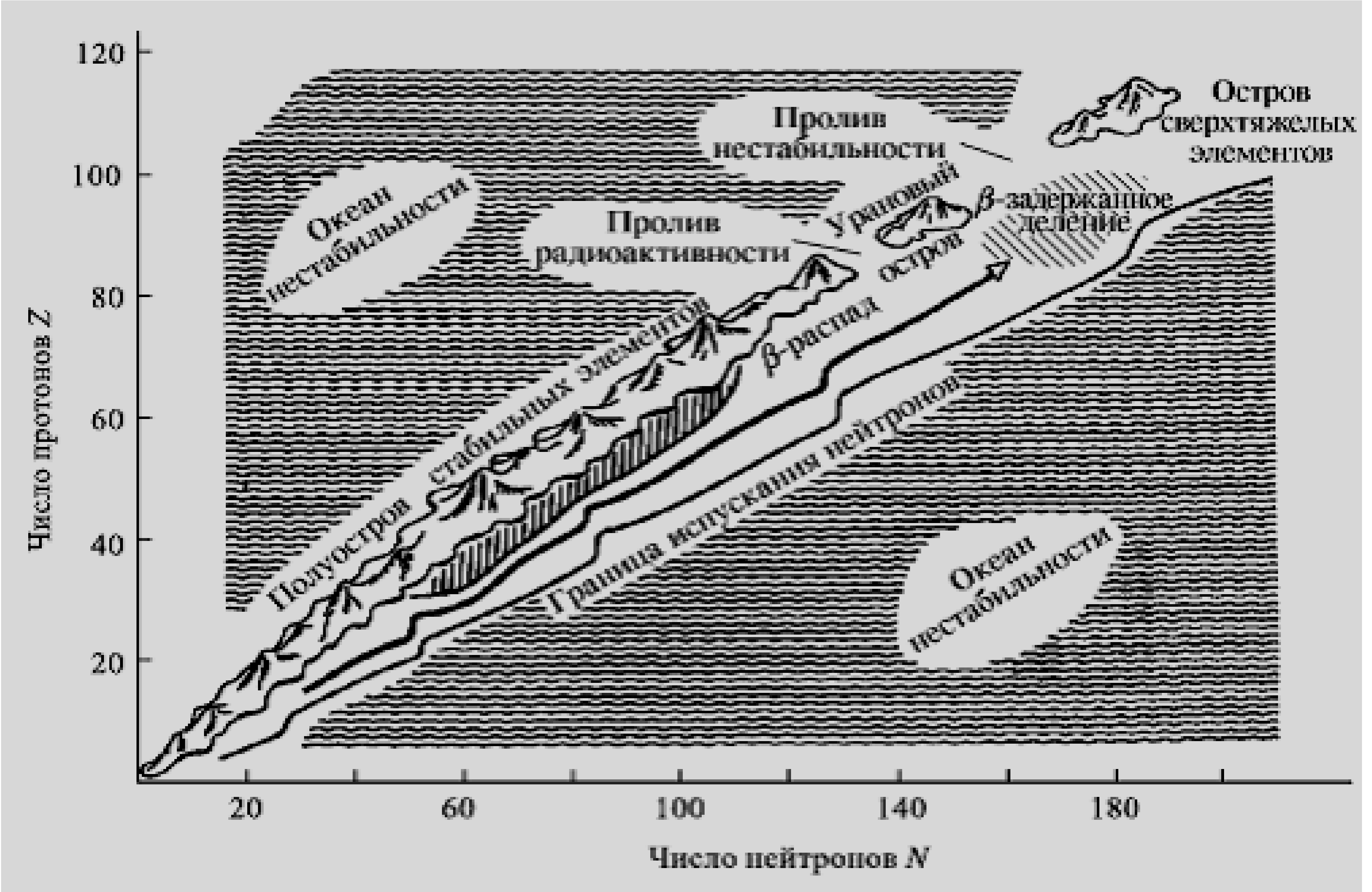

Solar Abundances

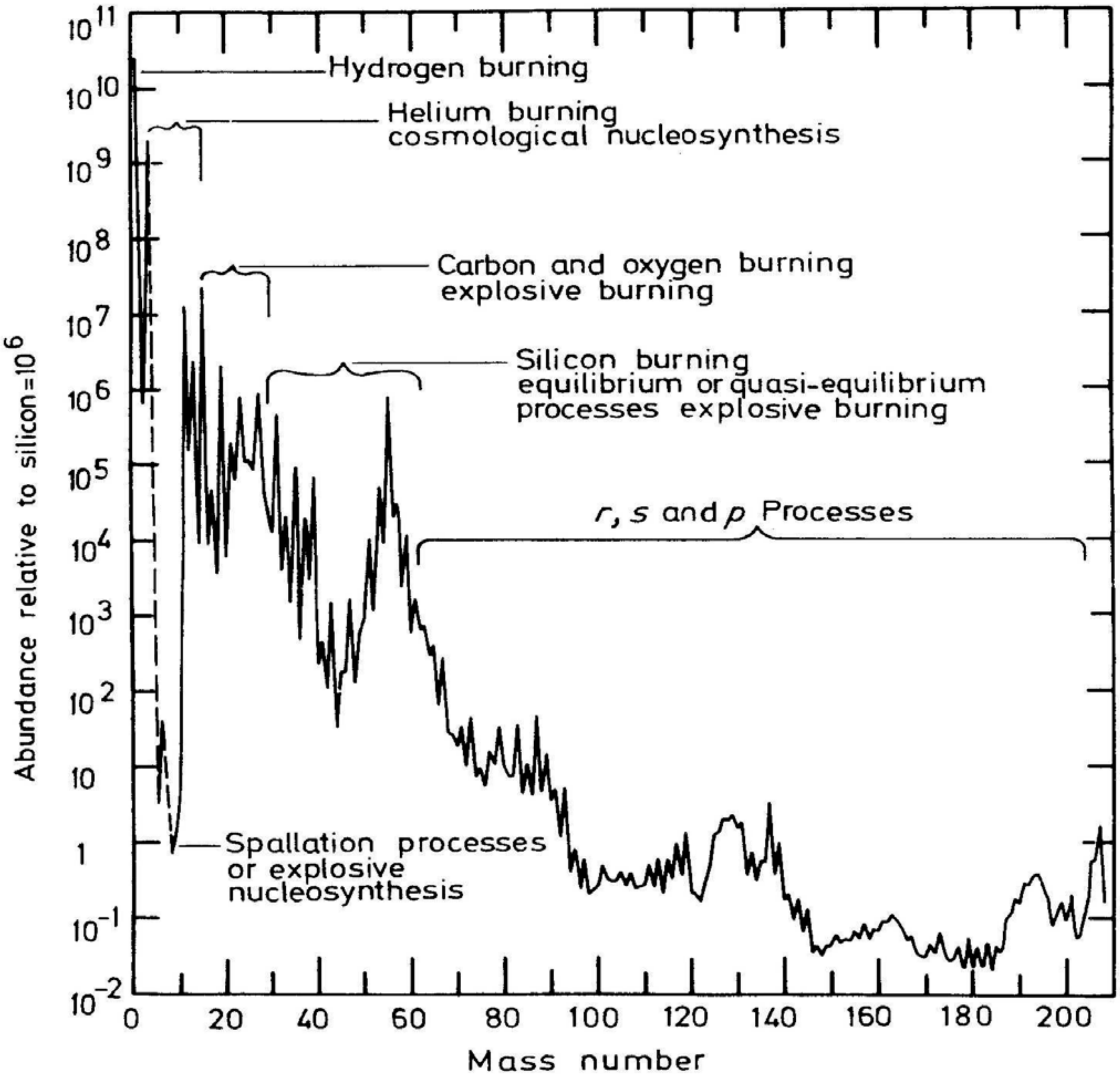

Hertzsprung- Russell (H-R) diagram

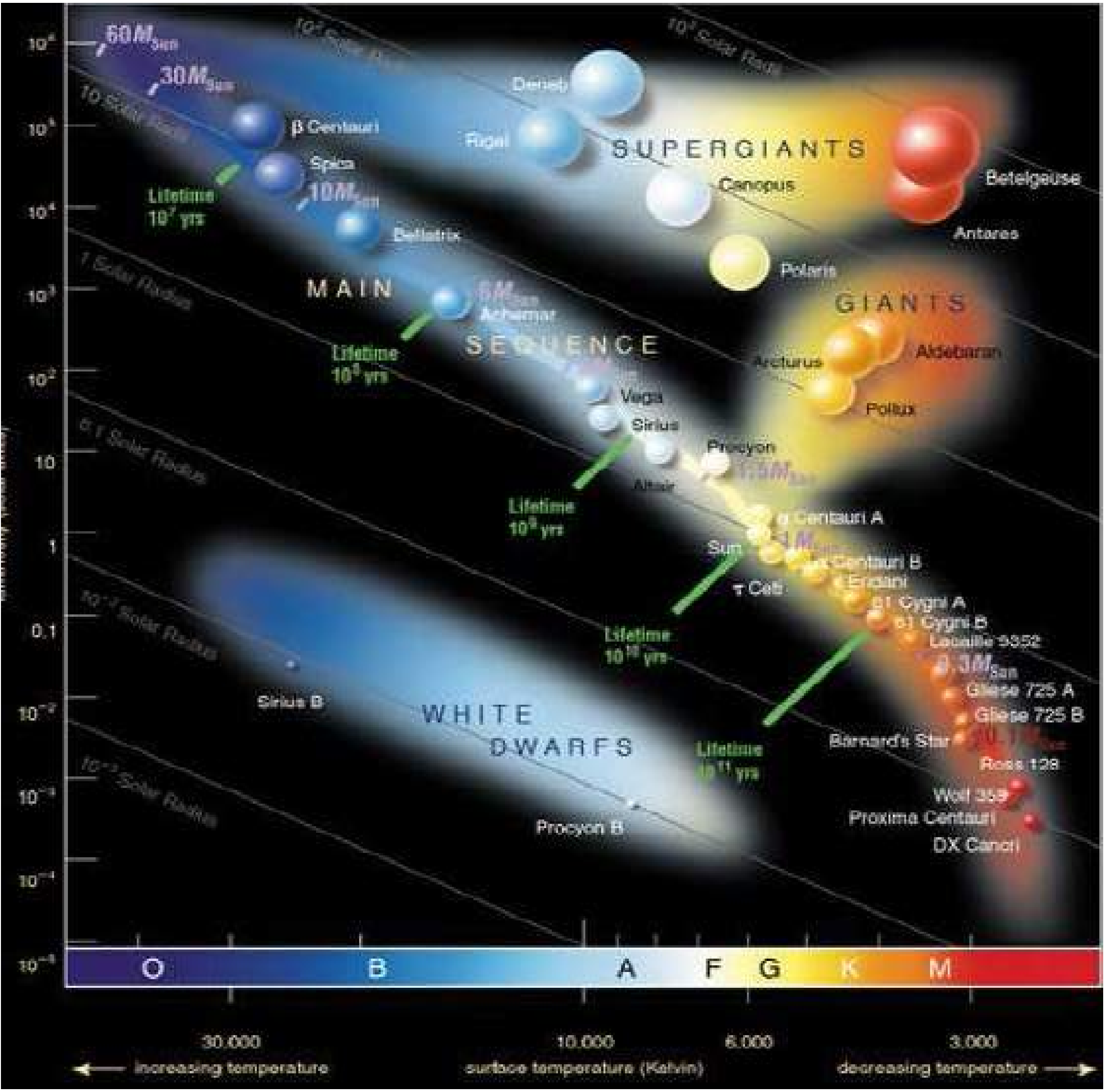

Stefan-Boltzmann
Law for flux

luminosity L
of a star with
radius R **&**
surface temperature T
$L \sim (\text{Surface}) T^4 \sim R^2 T^4$

Solar System

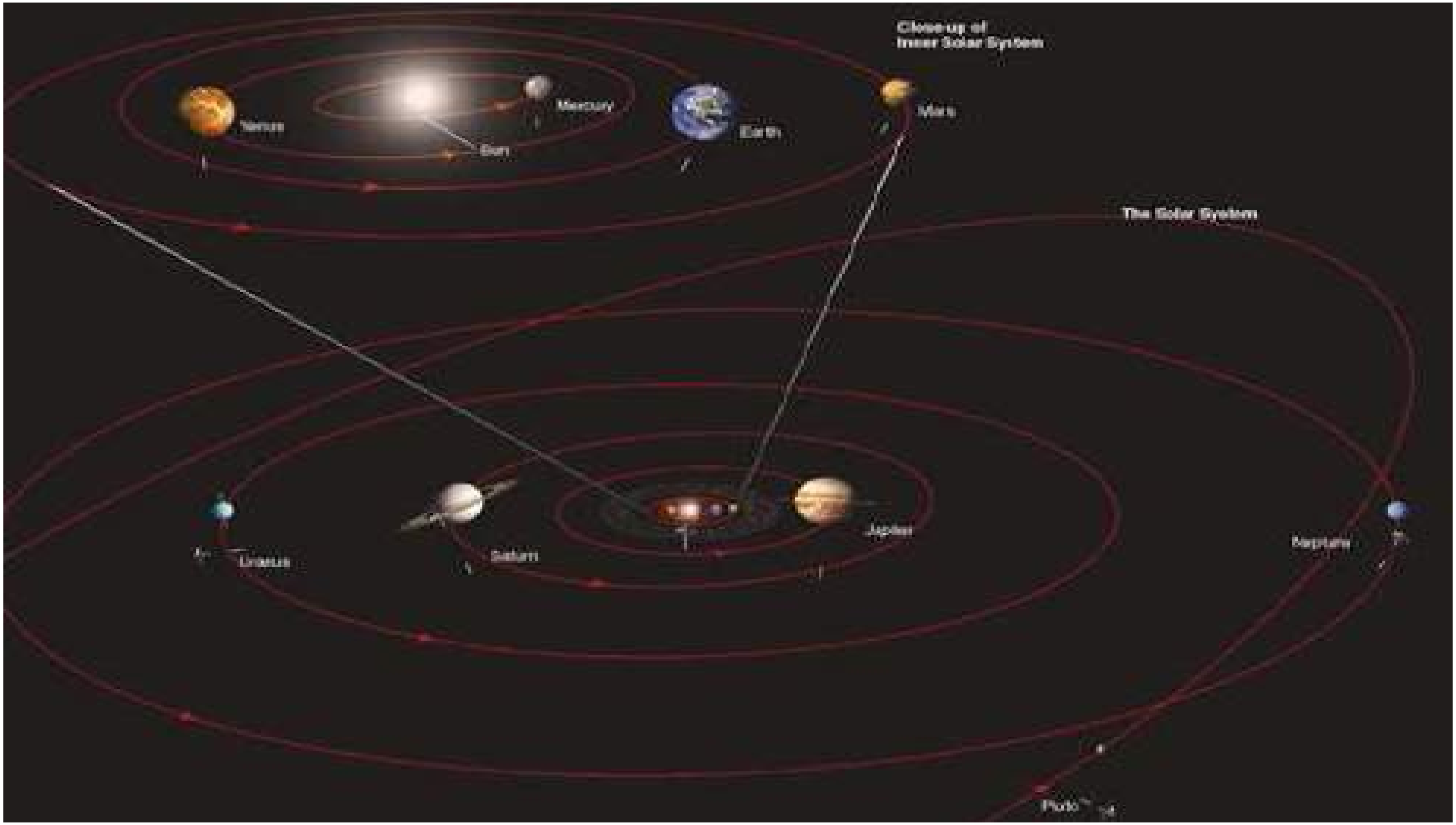

- Sun(star) + 9 planets - ***M, V, E, Mars, J S N U***
  - (P= dwarf planet)
- Distance Earth to Sun= 1.5x 10^{11} m= 1AU
  - Pluto-Sun= 39. 5 AU

Structure of low mass star, e.g. the Sun

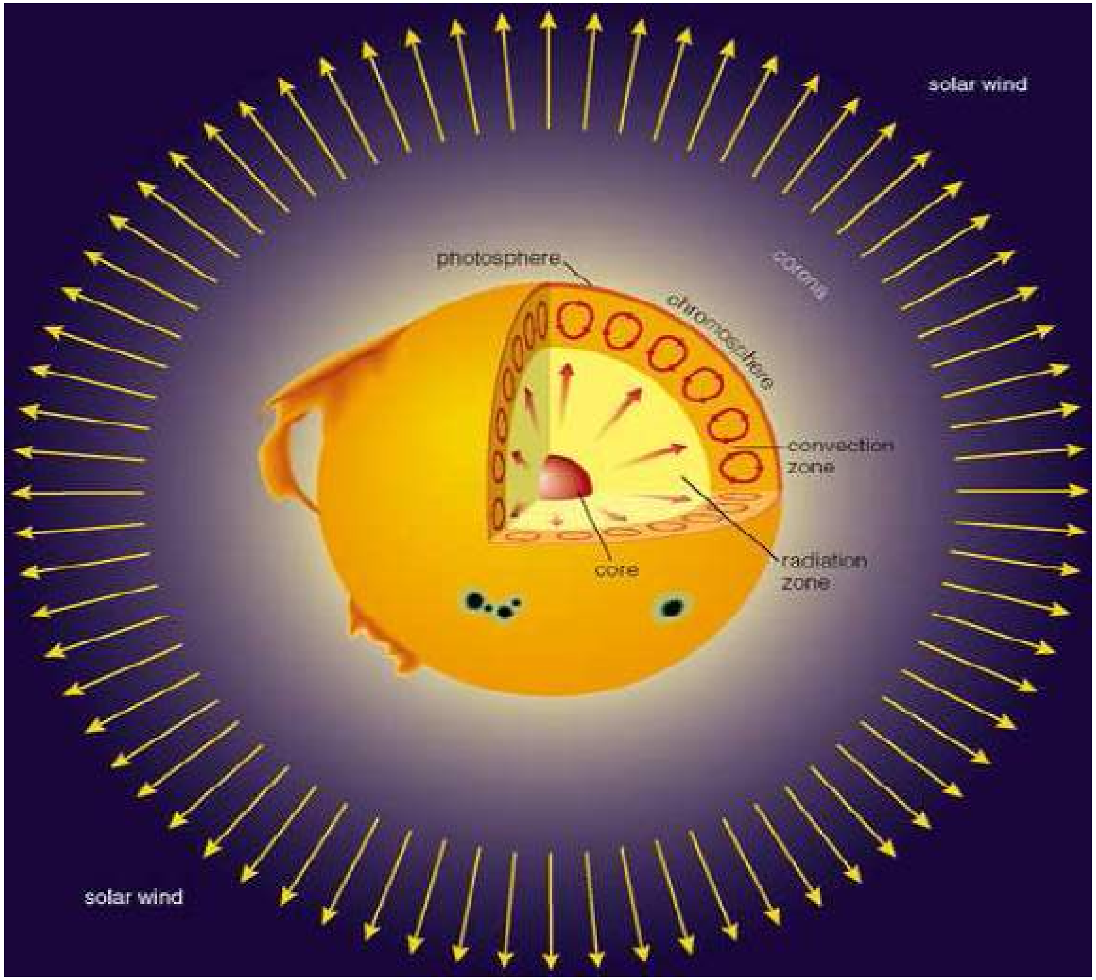

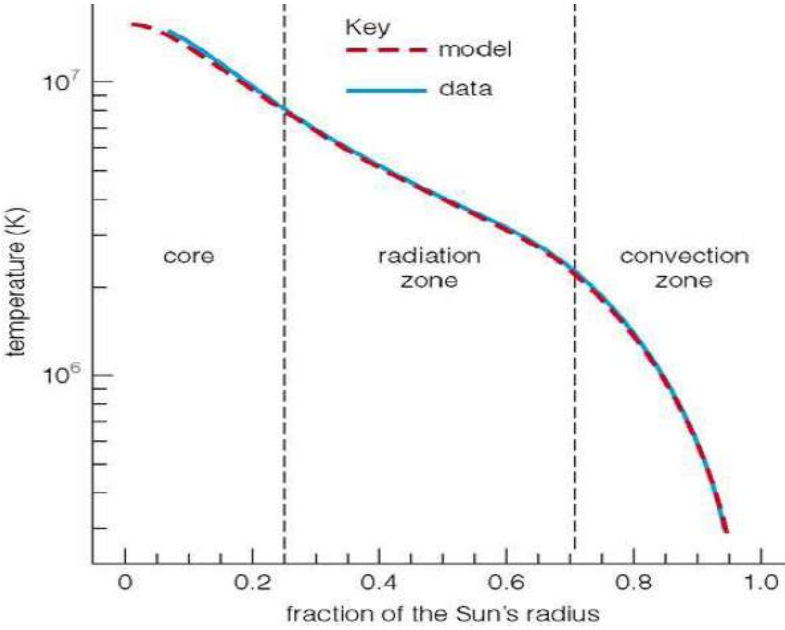

- Nuclear fusion in core with high temperature & pressure
- released energy that is transported to photosphere & emitted

$$4p \rightarrow {}^{4}He + 2e^{+} + 2\nu_e$$

pp chains

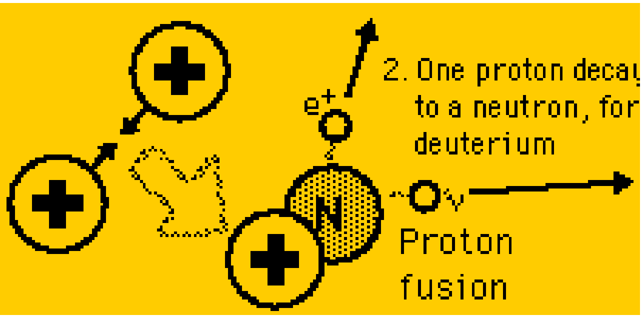

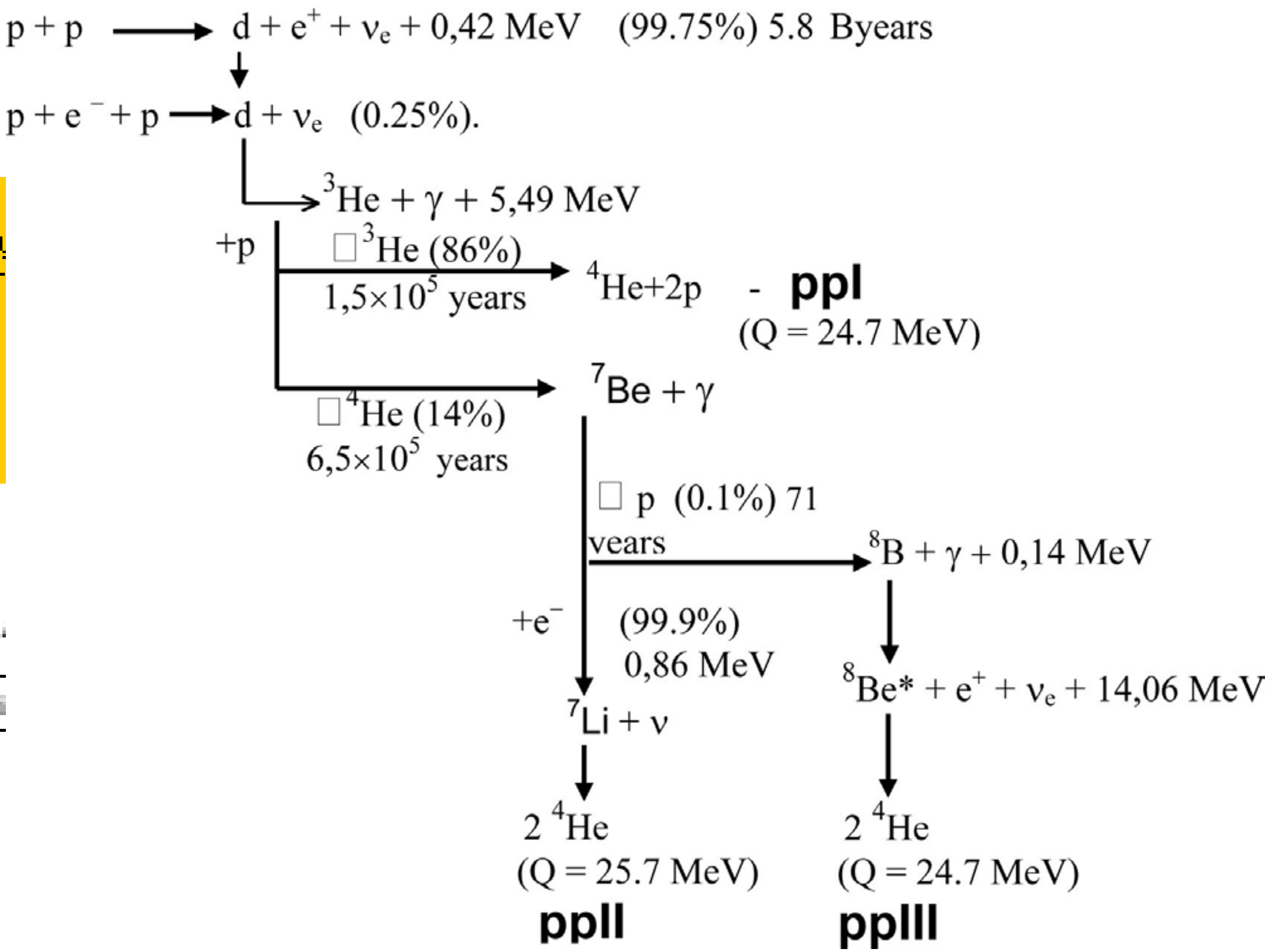

$p + p \longrightarrow d + e^{+} + \nu_e + 0{,}42$ MeV (99.75%) 5.8 Byears

$p + e^{-} + p \longrightarrow d + \nu_e$ (0.25%).

$\longrightarrow {}^{3}He + \gamma + 5{,}49$ MeV

+p

□ ^{3}He (86%) $\longrightarrow$ ^{4}He+2p - **ppI**

$1{,}5\times10^{5}$ years

(Q = 24.7 MeV)

□ ^{4}He (14%) $\longrightarrow$ ^{7}Be + γ

$6{,}5\times10^{5}$ years

□ p (0.1%) 71 years $\longrightarrow$ $^{8}B + \gamma + 0{,}14$ MeV

$\downarrow$

$^{8}Be^{*} + e^{+} + \nu_e + 14{,}06$ MeV

$\downarrow$

2 ^{4}He

(Q = 24.7 MeV)

ppIII

+e^{-} (99.9%) 0,86 MeV

$\downarrow$

$^{7}Li + \nu$

$\downarrow$

2 ^{4}He

(Q = 25.7 MeV)

ppII

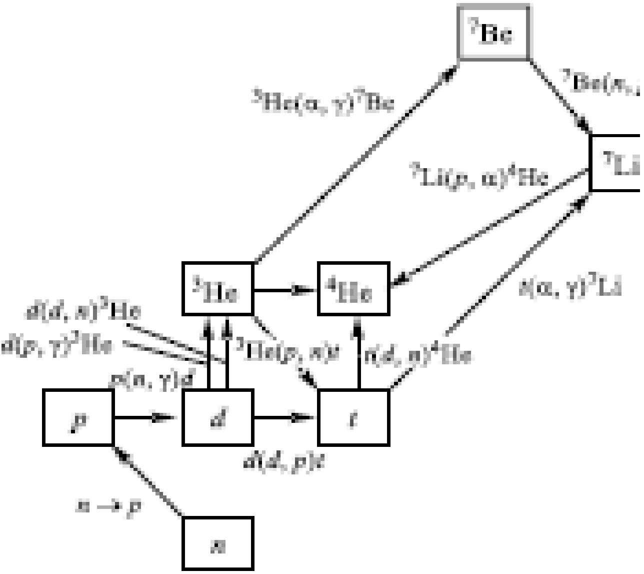

Competition pp chains *vs* temperature

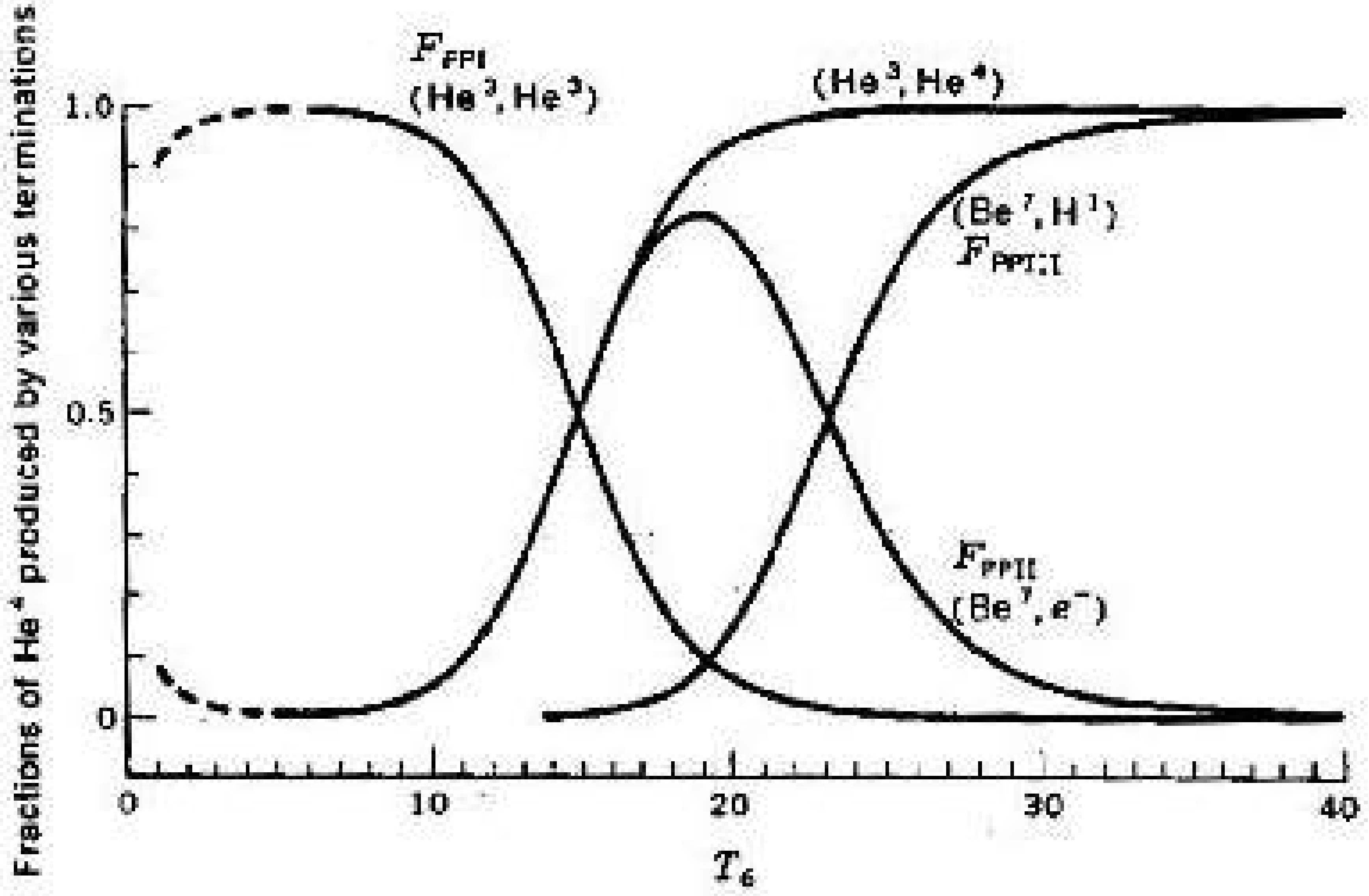

pp & CNO cycles *vs* temperature

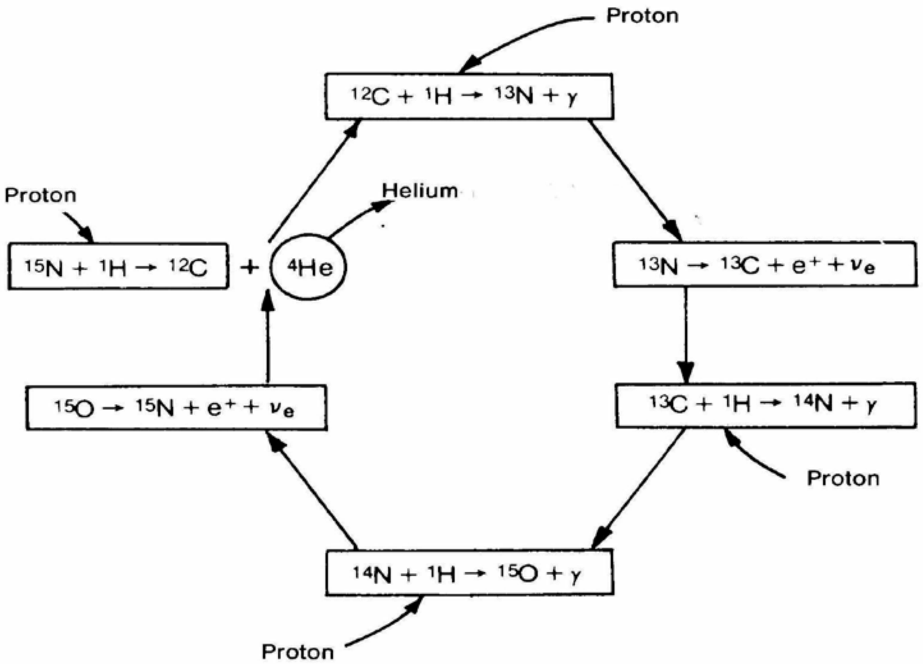

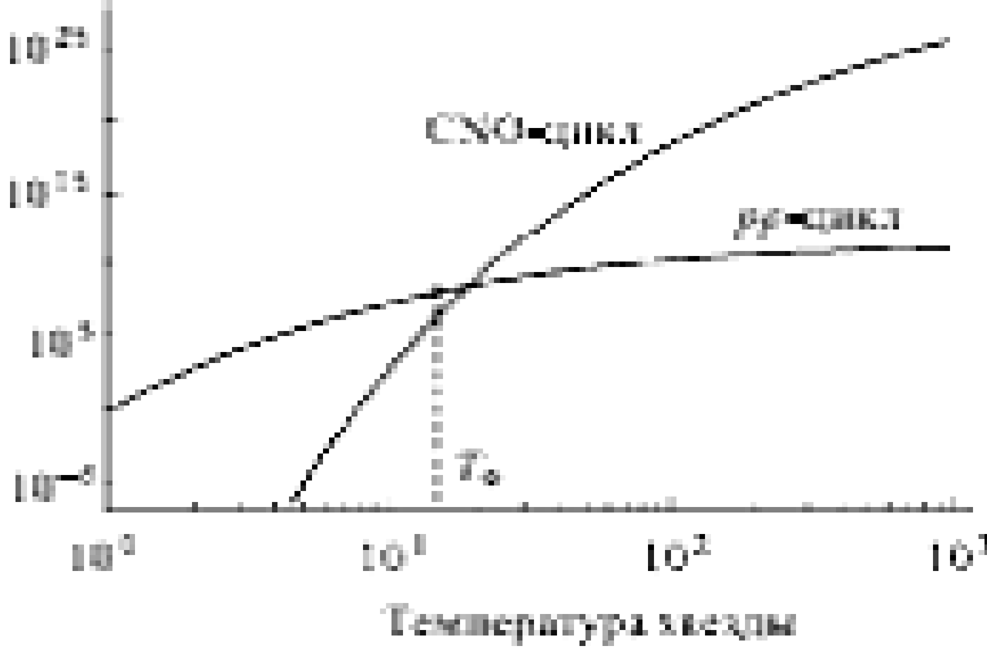

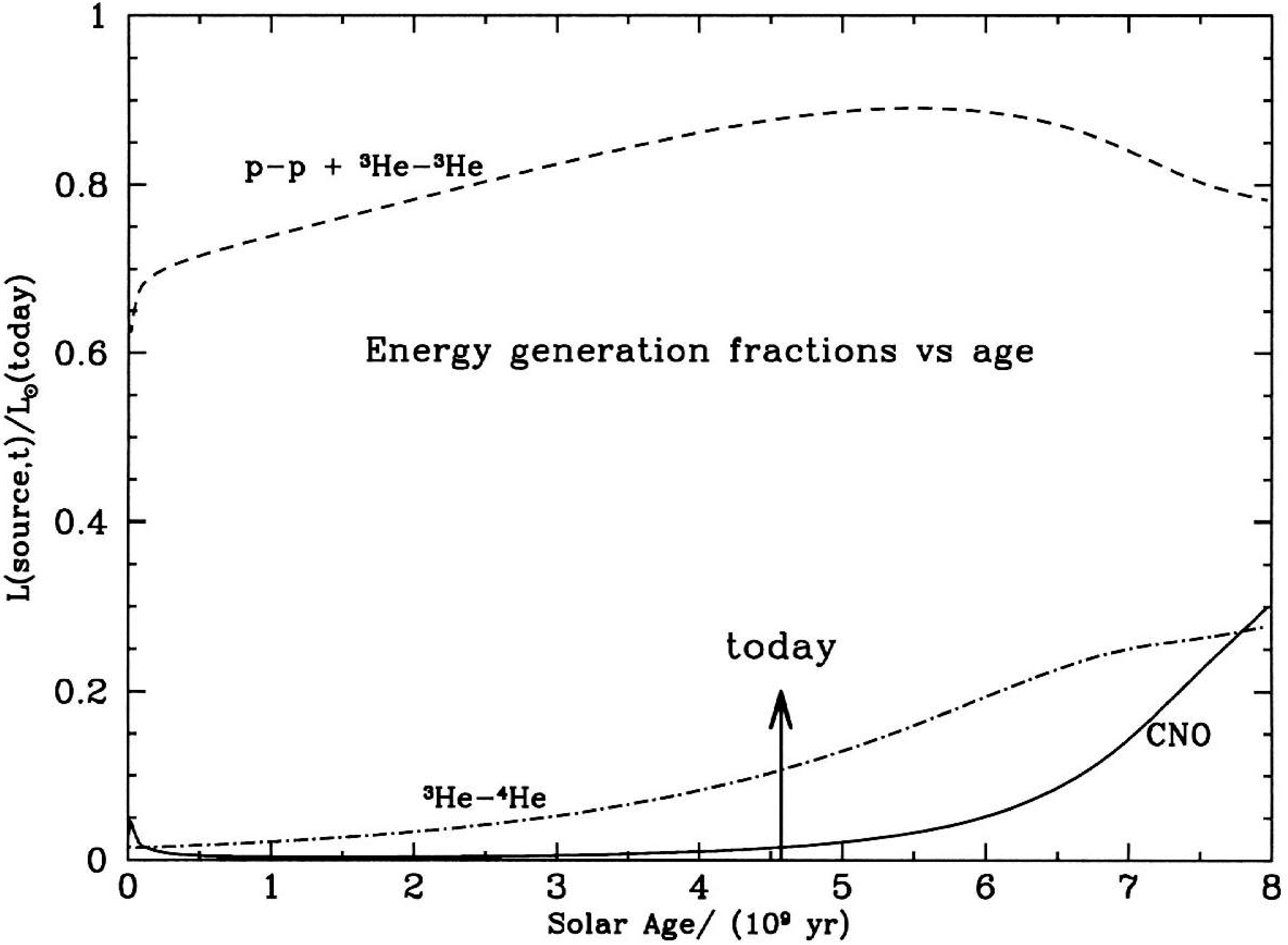
Energy generation fractions vs age
p–p + ^{3}He–^{3}He
^{3}He–^{4}He
CNO
today
L(source,t)/L$_\odot$(today)
Solar Age/ (10^9 yr)
0
0.2
0.4
0.6
0.8
1
0
1
2
3
4
5
6
7
8

solar neutrino spectrum

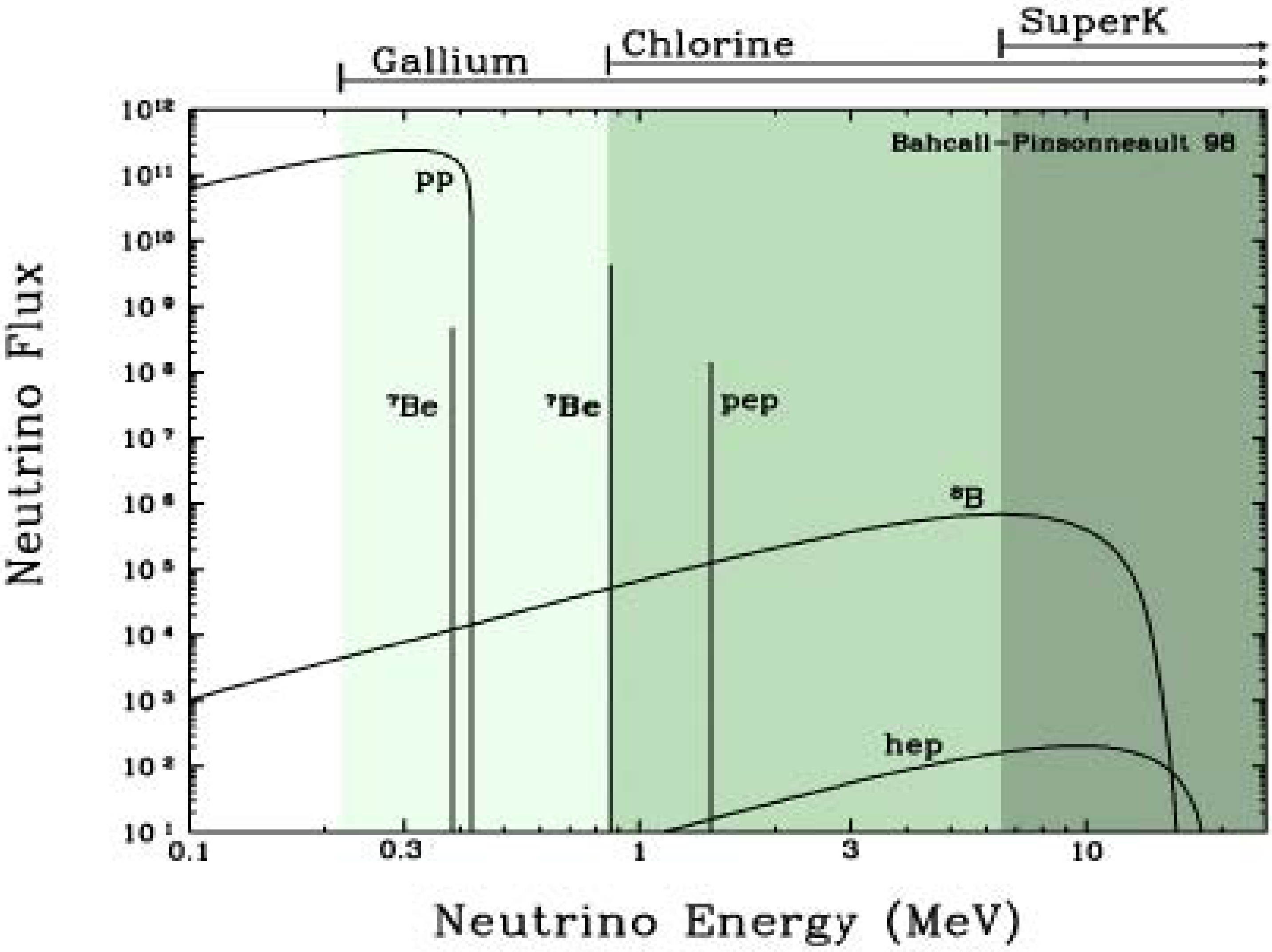

Solar (& other) Neutrino

different fluxes

↙ ↘

observations **expectations** from

standard solar model (**SSM**)

Fluxes

$$\phi({}^{7}Be) \approx 0 \quad \phi({}^{8}B) \approx 0.43\phi^{\mathrm{SSM}}({}^{8}B)$$

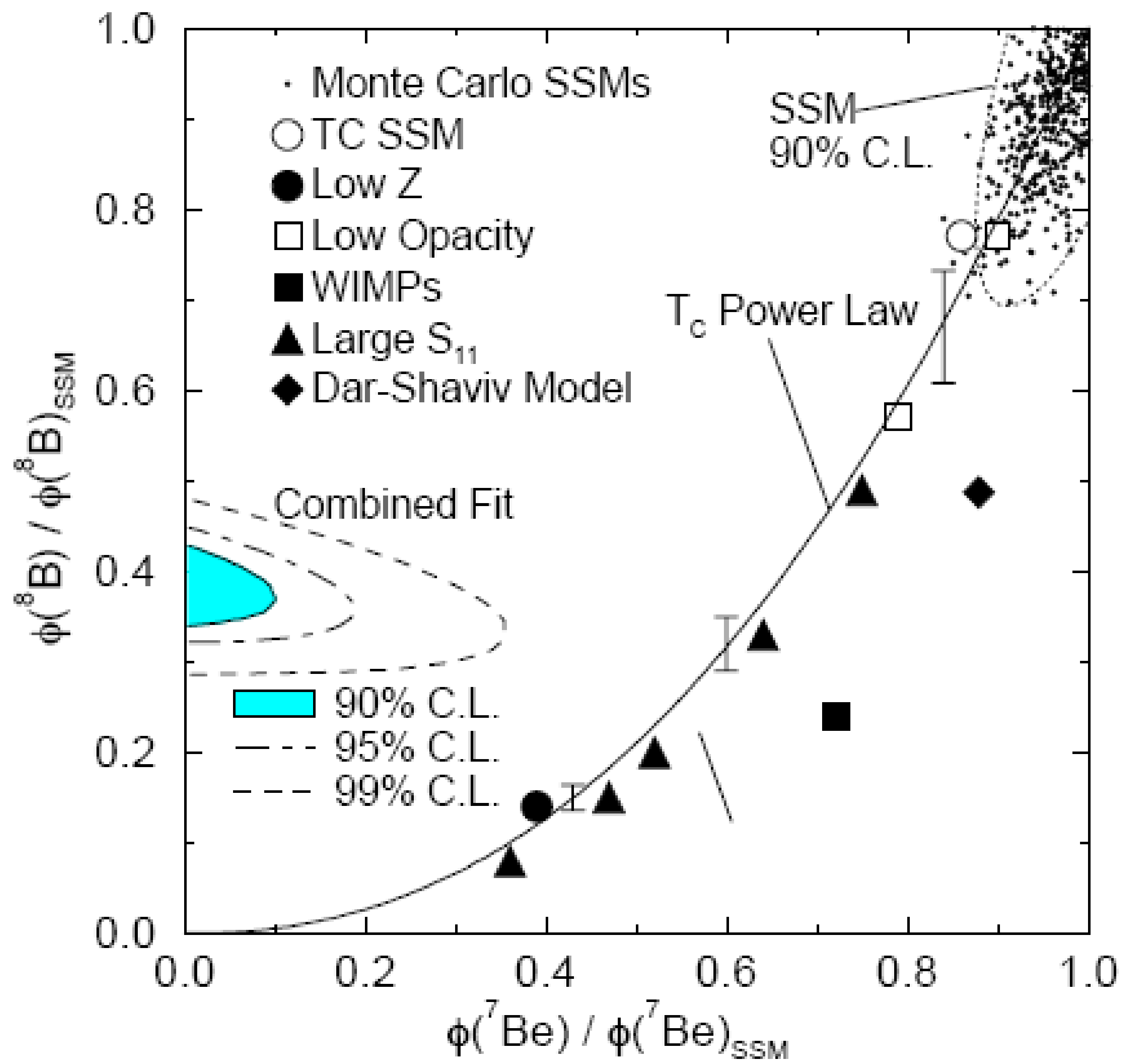
· Monte Carlo SSMs
○ TC SSM
● Low Z
□ Low Opacity
■ WIMPs
▲ Large S_{11}
◆ Dar-Shaviv Model
SSM 90% C.L.
T_C Power Law
Combined Fit
90% C.L.
95% C.L.
99% C.L.
$\phi(^8B) / \phi(^8B)_{SSM}$
$\phi(^7Be) / \phi(^7Be)_{SSM}$
0.0
0.2
0.4
0.6
0.8
1.0

Neutrino masses & vacuum neutrino Oscillations

weak interaction eigenstates

NEUTRINO $\nu_e \leftrightarrow$ positron

$\nu_\mu \leftrightarrow$ muon

MASS eigenstates $|\upsilon_1\rangle$ & $|\upsilon_2\rangle$ with masses m_1 & m_2

$$|\upsilon_e\rangle = \cos\theta_\upsilon\ |\upsilon_1\rangle + \sin\theta_\upsilon\ |\upsilon_2\rangle$$

$$|\upsilon_\mu\rangle = \sin\theta_\upsilon\ |\upsilon_1\rangle + \cos\theta_\upsilon\ |\upsilon_2\rangle$$

(vacuum) mixing angle θ_υ **.**

time t=0 → $|\upsilon(\mathrm{t{=}0})\rangle = |\upsilon_{\mathrm{e}}\rangle = \cos\theta_\upsilon\ |\upsilon_1\rangle + \sin\theta_\upsilon\ |\upsilon_2\rangle$

Each eigenstate propagates with a phase ↘

$$\exp\left\{i\left(\vec{k}\vec{x} - \omega t\right)\right\} = \exp\left\{i\left(\vec{k}\vec{x} - t\sqrt{m_i^2 + k^2}\right)\right\}$$

neutrino mass<<momentum ↙ $\sqrt{m_i^2 + k^2} \approx k\left(1 + \frac{m_i^2}{2k^2}\right)$

$$|\upsilon(\mathrm{t})\rangle = \exp\left\{i\left(\vec{k}\vec{x} - kt - \frac{m_1^2 + m_2^2}{2k}t\right)\right\}$$

$$\left[\cos\theta_\upsilon\ |\upsilon_1\rangle \exp\left\{i\delta m^2 t/4k\right\} + \sin\theta_\upsilon\ |\upsilon_2\rangle \exp\left\{-i\delta m^2 t/4k\right\}\right]$$

BEAT PHASE $\delta m^2 = m_2^2 - m_1^2$

PROBABILITY for neutrino state to remain $\left|\upsilon_e\right\rangle$ at time $\boldsymbol{t}$

$$P_{\upsilon_e}(t) = \left|\left\langle \upsilon_e \middle| \upsilon(t) \right\rangle\right|^2$$

$$= 1 - \sin^2 2\theta_\upsilon \sin^2\left(\frac{\delta m^2 t}{4k}\right) \quad \rightarrow \quad 1 - \sin^2 2\theta_\upsilon$$

m<< E ~ k →

$$P_\upsilon(x) = 1 - \sin^2 2\theta_\upsilon \sin^2\left(\frac{\delta m^2 c^4 x}{4\hbar c E}\right)$$

oscillation length

$$L_o = \frac{4\pi\hbar c E}{\delta m^2 c^4}$$

E~ 1 MeV: sensitivity to $\delta m_\upsilon^2 \geq 10^{-12}\ \mathrm{eV}^2$

SuperKamiokande

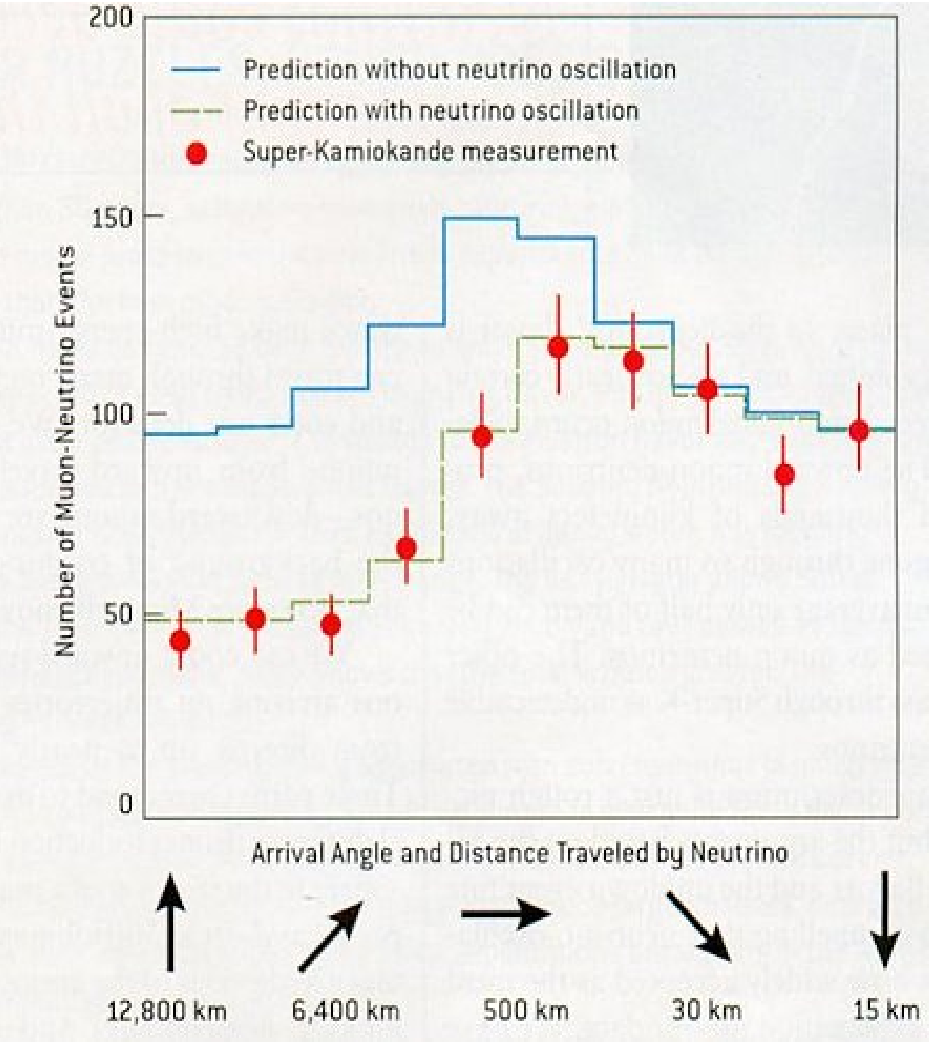

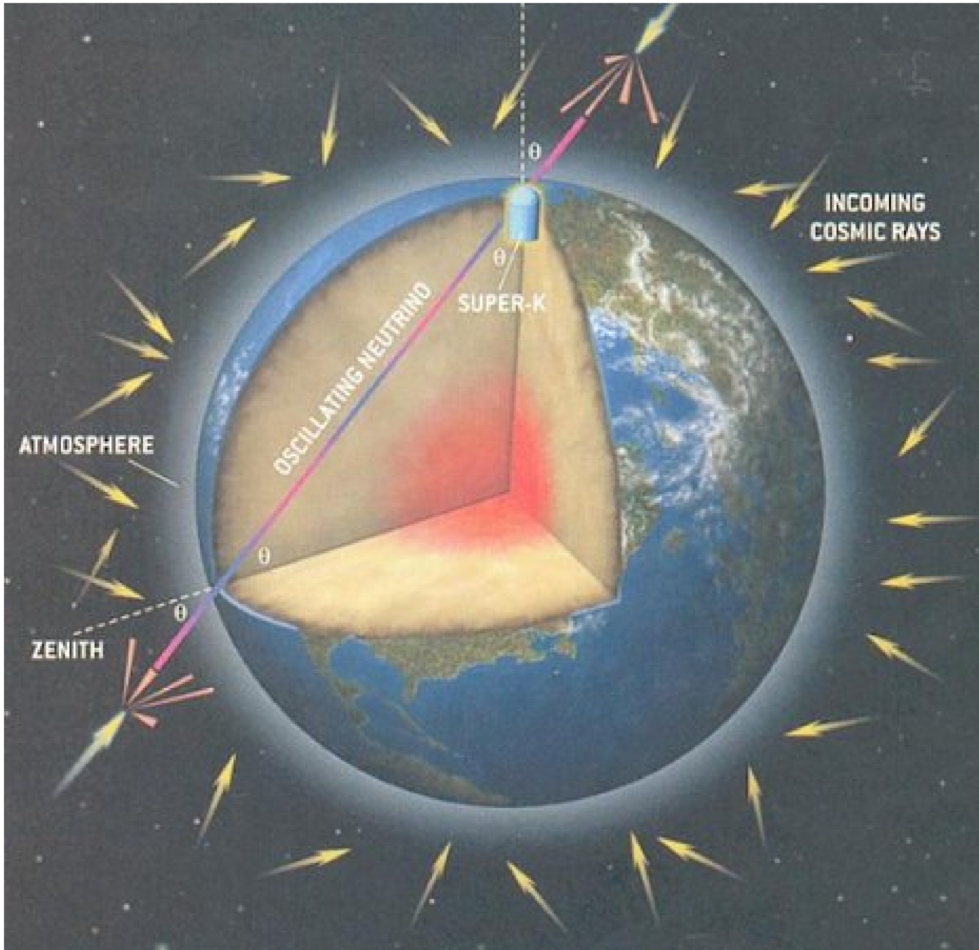

Discovering Mass

The farther neutrinos travel, the more time they have to oscillate. By comparing the ratio of flavors of neutrinos coming "up" through the Earth to those coming from overhead, physicists determined that neutrinos oscillate, which neutrinos can only do if they have mass.

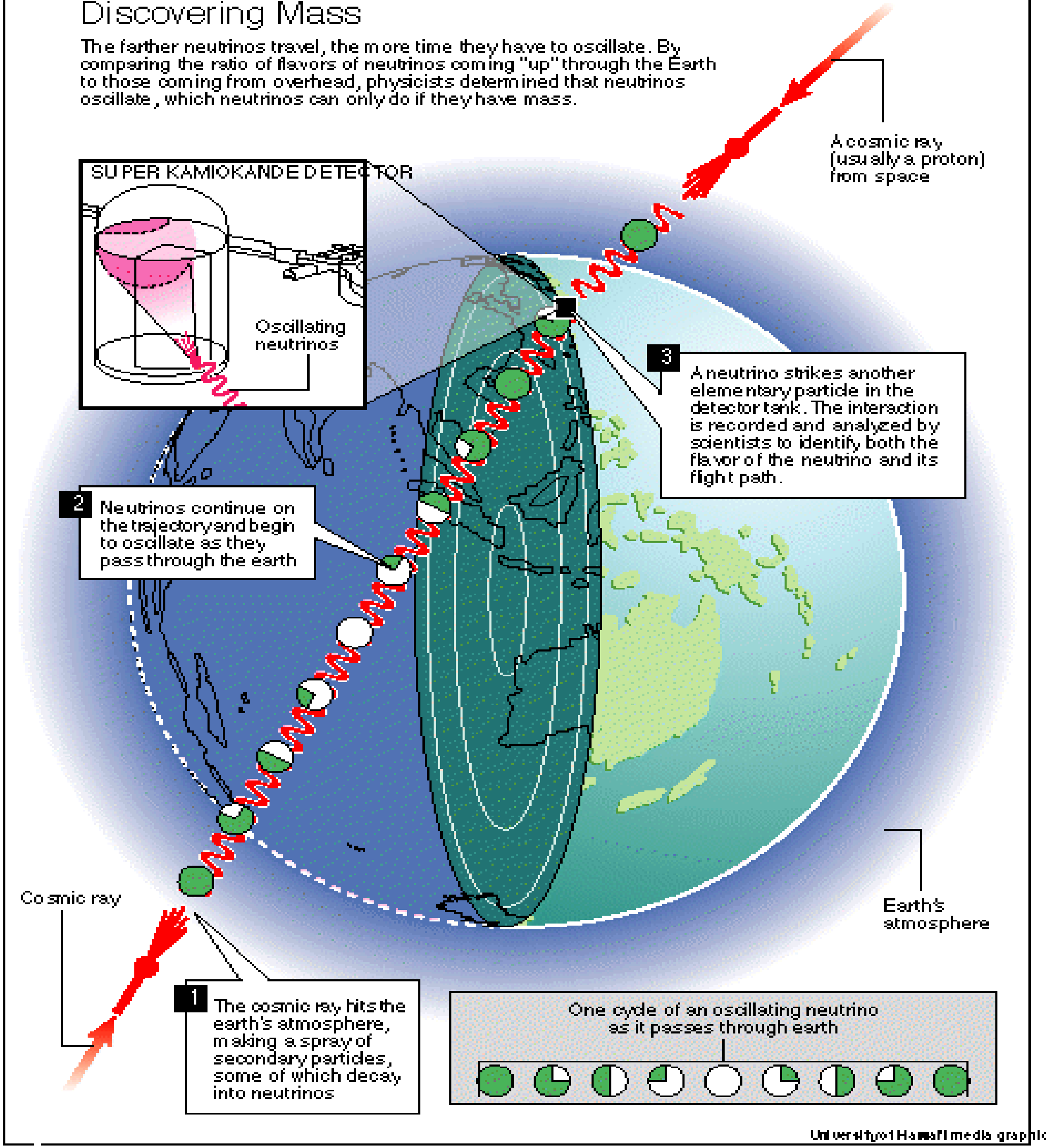

1 The cosmic ray hits the earth's atmosphere, making a spray of secondary particles, some of which decay into neutrinos

2 Neutrinos continue on the trajectory and begin to oscillate as they pass through the earth

3 A neutrino strikes another elementary particle in the detector tank. The interaction is recorded and analyzed by scientists to identify both the flavor of the neutrino and its flight path.

University of Hawaii media graphic

Parameters from Cl/Ga/Kamiokande/Super-Kamiokande neutrino data

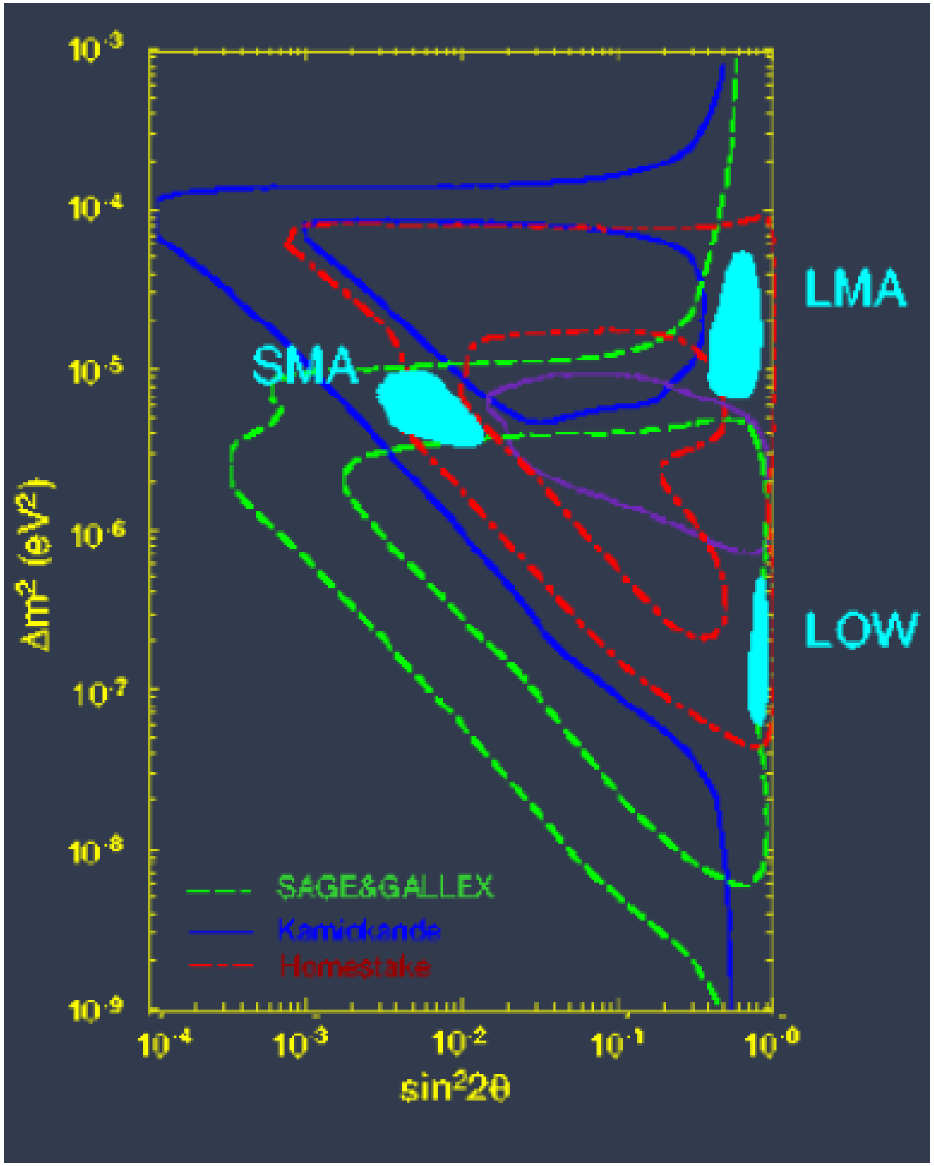

LIGHT & HEAVY local mass *eigenstates*

$$\left|\upsilon_{\mathrm{L}}\right\rangle = \cos\theta(x)\,\left|\upsilon_e\right\rangle - \sin\theta(x)\,\left|\upsilon_\mu\right\rangle$$

$$\left|\upsilon_{\mathrm{H}}\right\rangle = \sin\theta(x)\,\left|\upsilon_e\right\rangle + \cos\theta(x)\,\left|\upsilon_\mu\right\rangle$$

local mixing angle

$$\sin 2\theta(x) = \frac{\sin 2\theta_\upsilon}{\sqrt{X^2(x) + \sin^2 2\theta_\upsilon}}$$

$$\cos 2\theta(x) = \frac{-X(x)}{\sqrt{X^2(x) + \sin^2 2\theta_\upsilon}}$$

$$X(x) = 2E\sqrt{2}G_F\,\rho(x)E/\delta m^2 - \cos 2\theta_\upsilon \;:$$

$$\theta(x) \in \theta_\upsilon \rightarrow \pi/2 \text{ as density } \rho(x)\;\; 0 \rightarrow \infty \;.$$

Mikheyev-Smirnov-Wolfenstein *avoided level crossing*

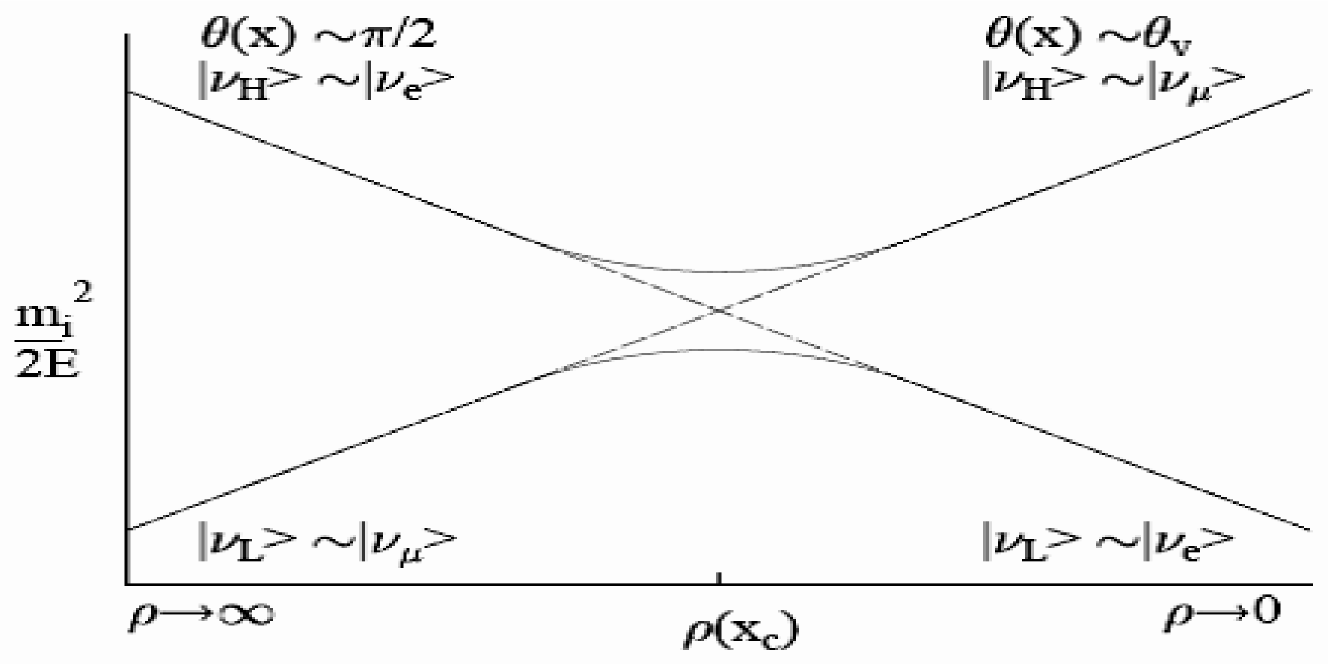

splitting minimum value: -- $\sin 2\theta_\upsilon \delta m^2 / 2E$,

at ***critical density*** $\rho_c = \rho(x_c) \leftarrow 2\sqrt{2}EG_F\rho_c = \delta m^2 \cos 2\theta_\upsilon$
cross point for diagonal elements of original flavor matrix

HR diagr ***evolution:*** **low-mass star *at exhausted H in core***

- Main sequence star core/**reactor fusing H to He** at T>**10^7 °K**

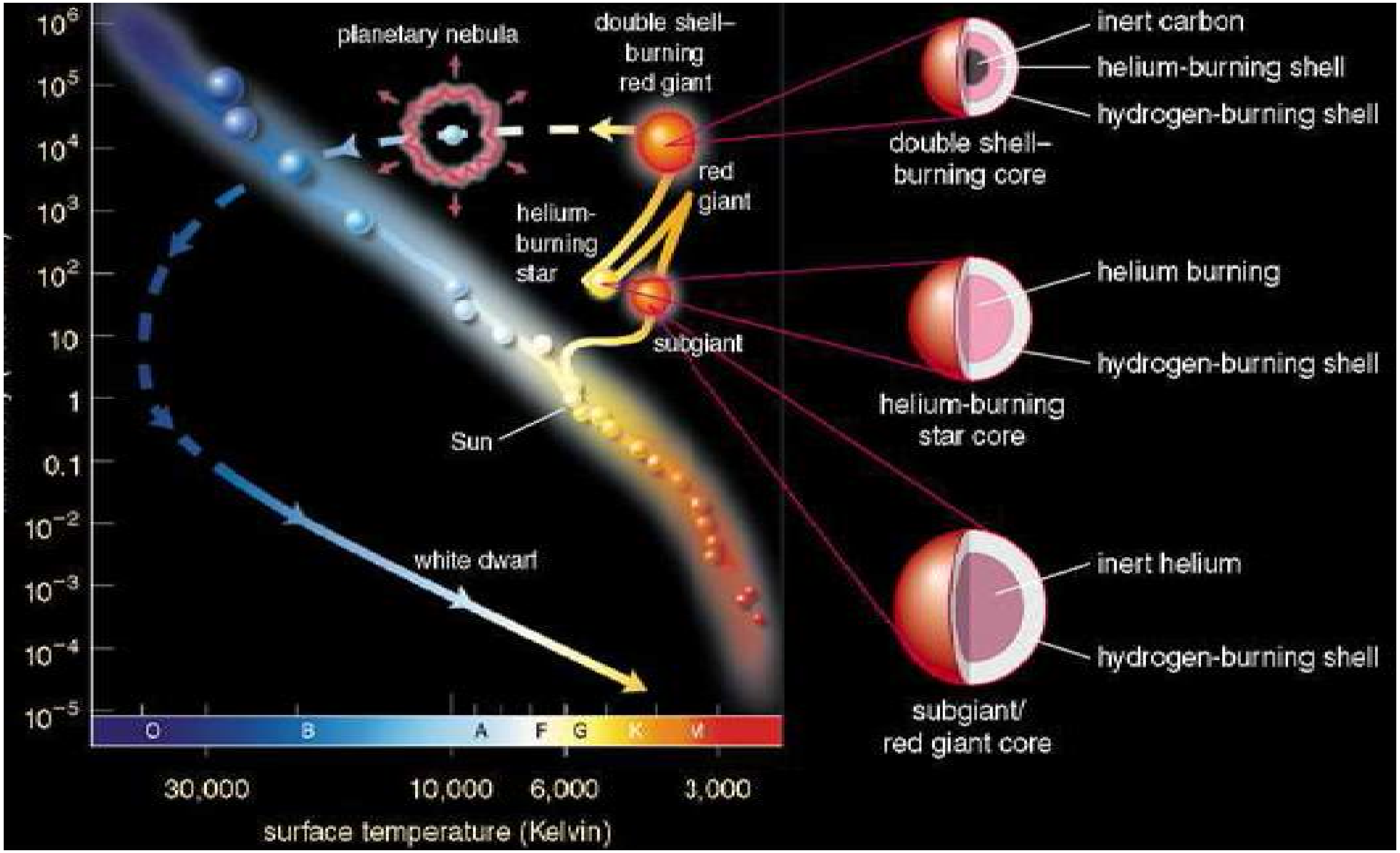

- Subgiant /Red Giant star (inert He core and Hydrogen- fusing shell)
- All the core H converted to He. To fuse He-->Carbon $T_c > 10^8$ K
- inert He core shrinks, heats up H-Shell bringing fusion of H to Helium starts
- star expands & enters subgiant/red giant phase: large and luminous

The Supergiant Star Betelgeuse

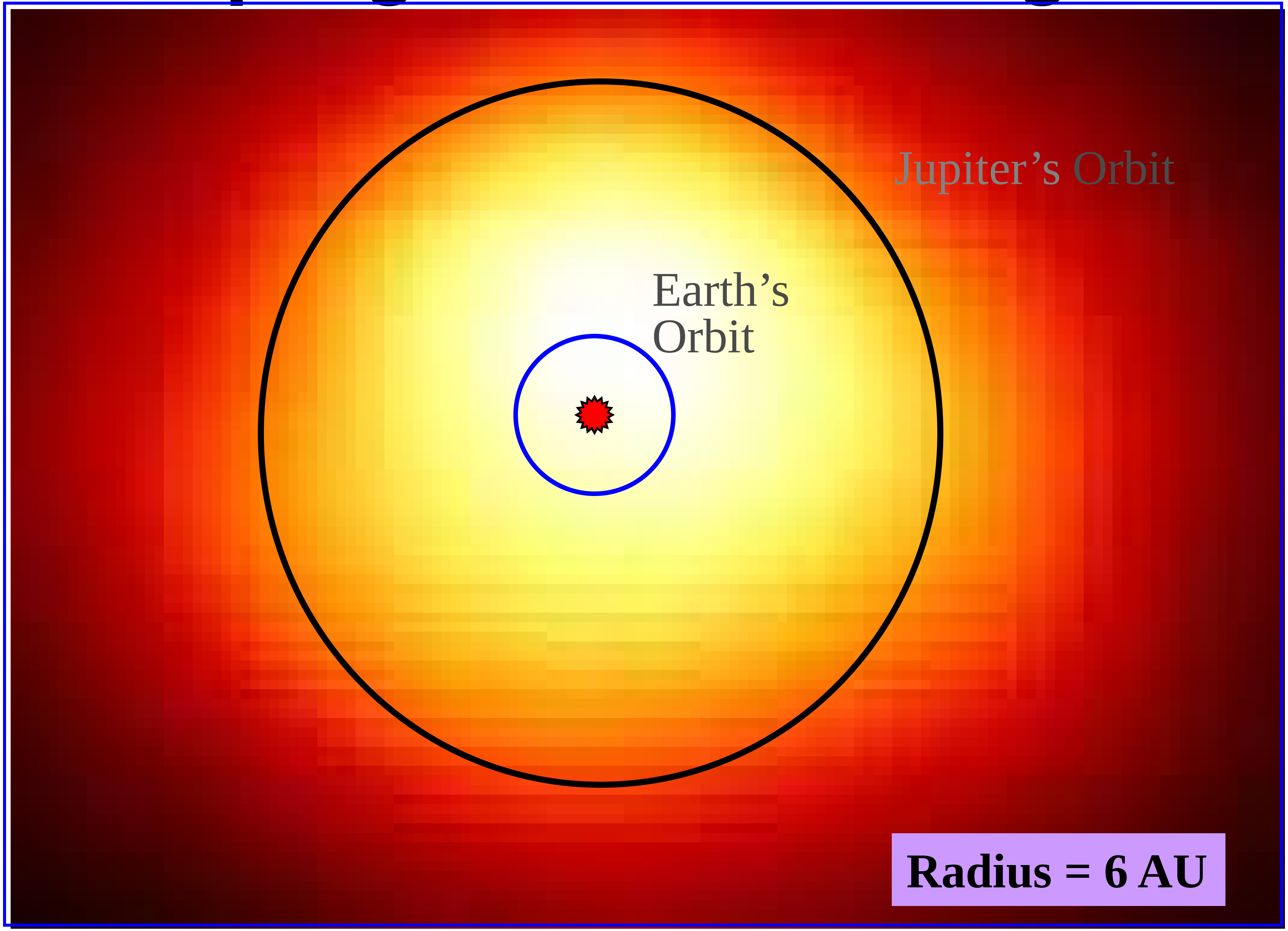

Red giants and helium burning

- helium core densities ~10^6 g/cm^3
- core densities and temperatures allow --> helium burning
- $^4He + ^4He + ^4He \rightarrow ^{12}C + \Gamma$-ray
- red giants evolve along
  - the “horizontal branch”
- Form **Planetary nebulae & white dwarf**

HELIUM-BURNING REACTIONS IN RED GIANTS

(THE START OF NUCLEOSYNTHESIS OF HEAVY ELEMENTS)

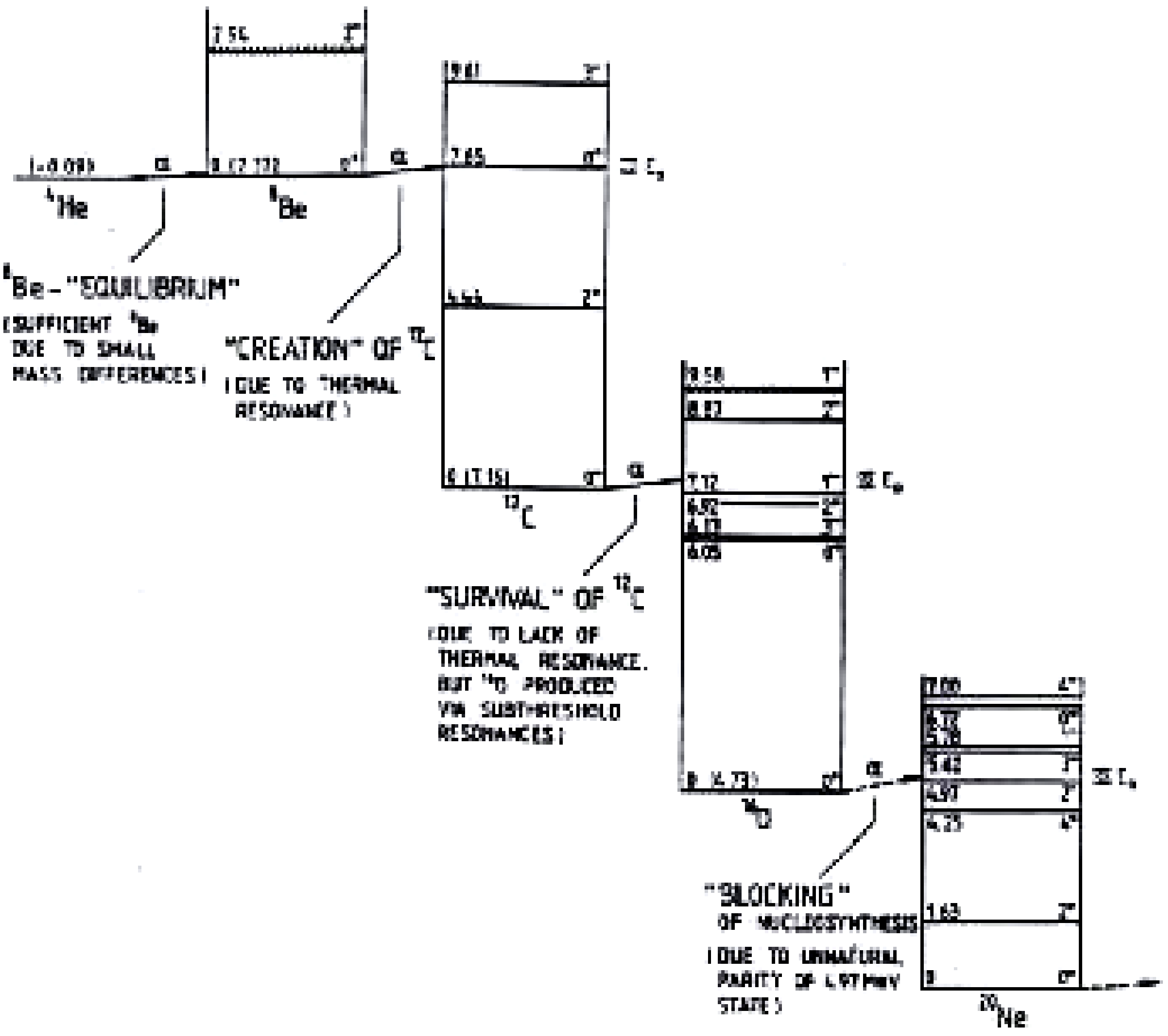

^{8}Be - "EQUILIBRIUM"
(SUFFICIENT ^{8}Be DUE TO SMALL MASS DIFFERENCES)

"CREATION" OF ^{12}C
(DUE TO THERMAL RESONANCE)

"SURVIVAL" OF ^{12}C
(DUE TO LACK OF THERMAL RESONANCE, BUT ^{16}O PRODUCED VIA SUBTHRESHOLD RESONANCES)

"BLOCKING" OF NUCLEOSYNTHESIS
(DUE TO UNNATURAL PARITY OF 4.97 MeV STATE)

Planetary Nebula Formation

Helix

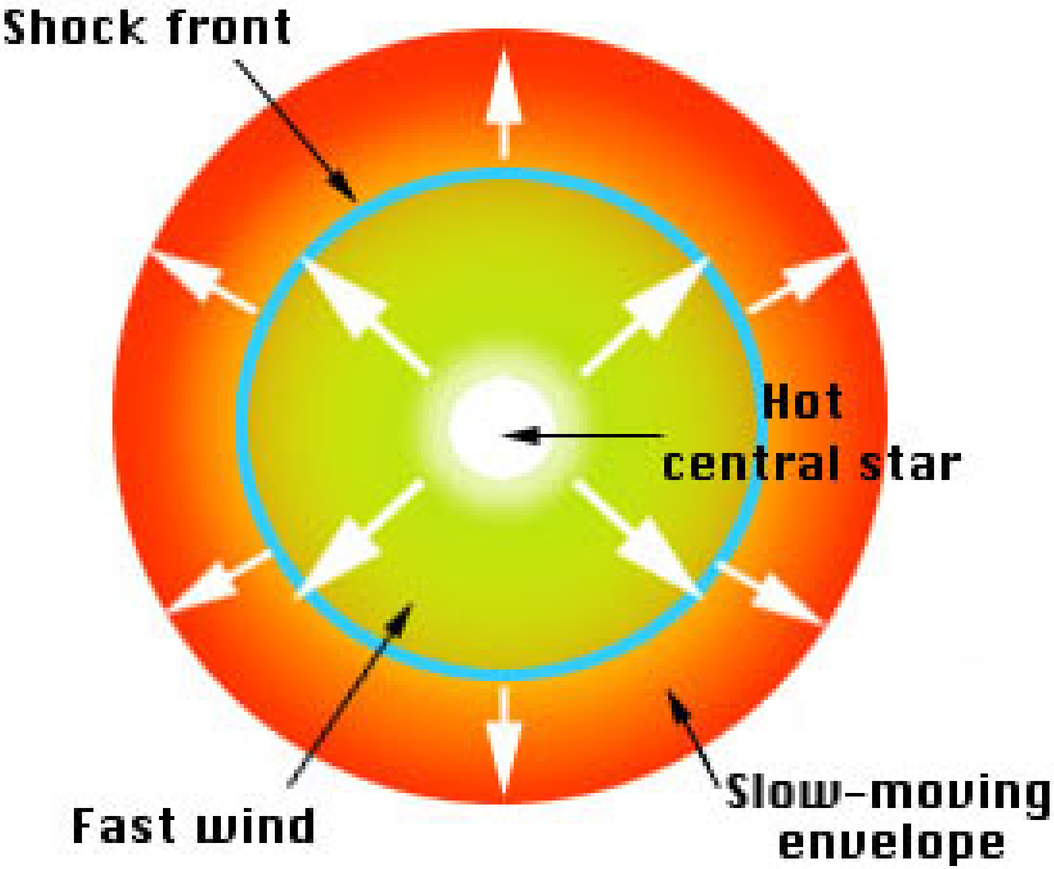

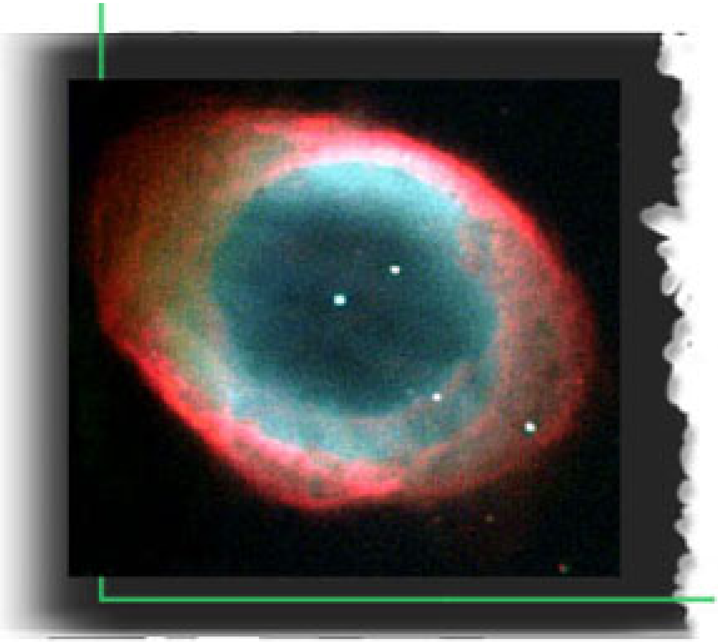

Cosmic Rays flux *vs* solar activity

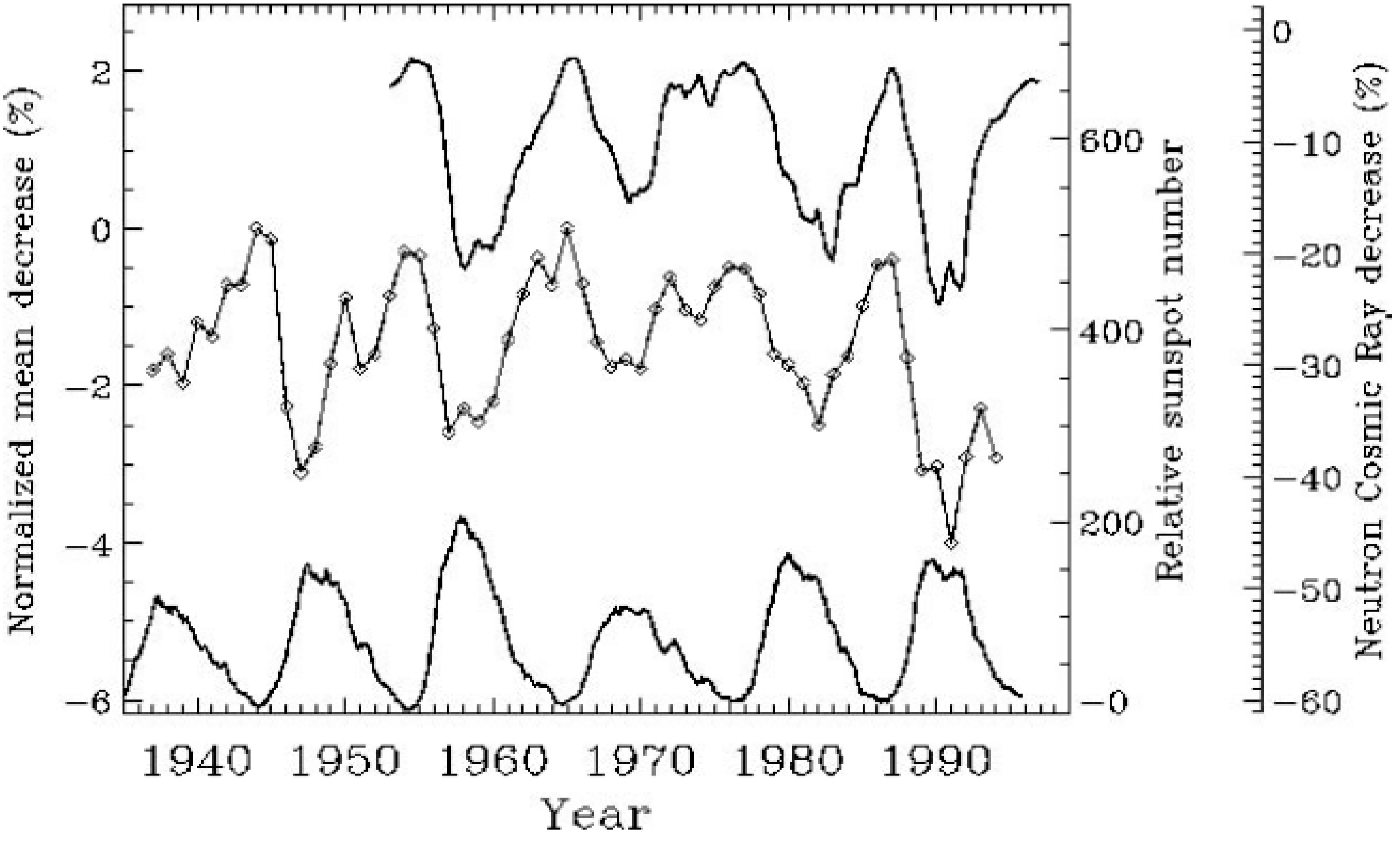

Massive Star, $M > 8\ M_o$ *onion*

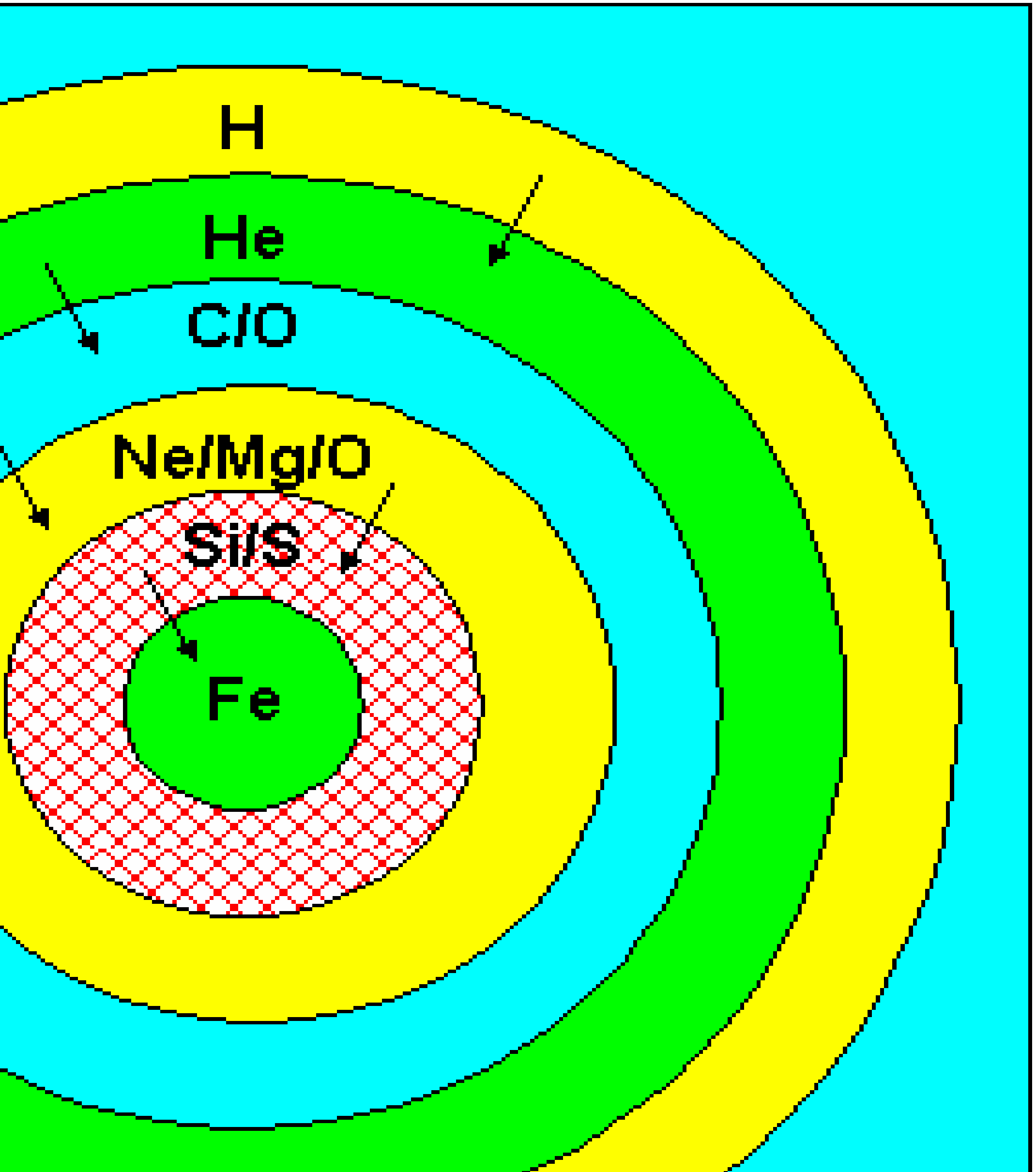

$4H \rightarrow {}^{4}_{2}He$

$3\ {}^{4}_{2}He \rightarrow {}^{12}_{6}C$

${}^{12}_{6}C + {}^{12}_{6}C \rightarrow {}^{20}_{10}Ne + {}^{4}_{2}He$

${}^{12}_{6}C + {}^{12}_{6}C \rightarrow {}^{24}_{12}Mg + \gamma$

${}^{12}_{6}C + {}^{16}_{8}O \rightarrow {}^{28}_{14}Si + \gamma$

${}^{16}_{8}O + {}^{16}_{8}O \rightarrow {}^{32}_{16}S + \gamma$

${}^{28}_{14}Si + {}^{16}_{8}O \rightarrow {}^{44}_{22}Ti(\beta^{+})$

${}^{44}_{21}Sc(\beta^{+})\ {}^{44}_{20}Ca$

${}^{28}_{14}Si + {}^{28}_{14}Si \rightarrow {}^{56}_{28}Ni(\beta^{+})$

${}^{56}_{27}Co(\beta^{+})\ {}^{56}_{26}Fe$

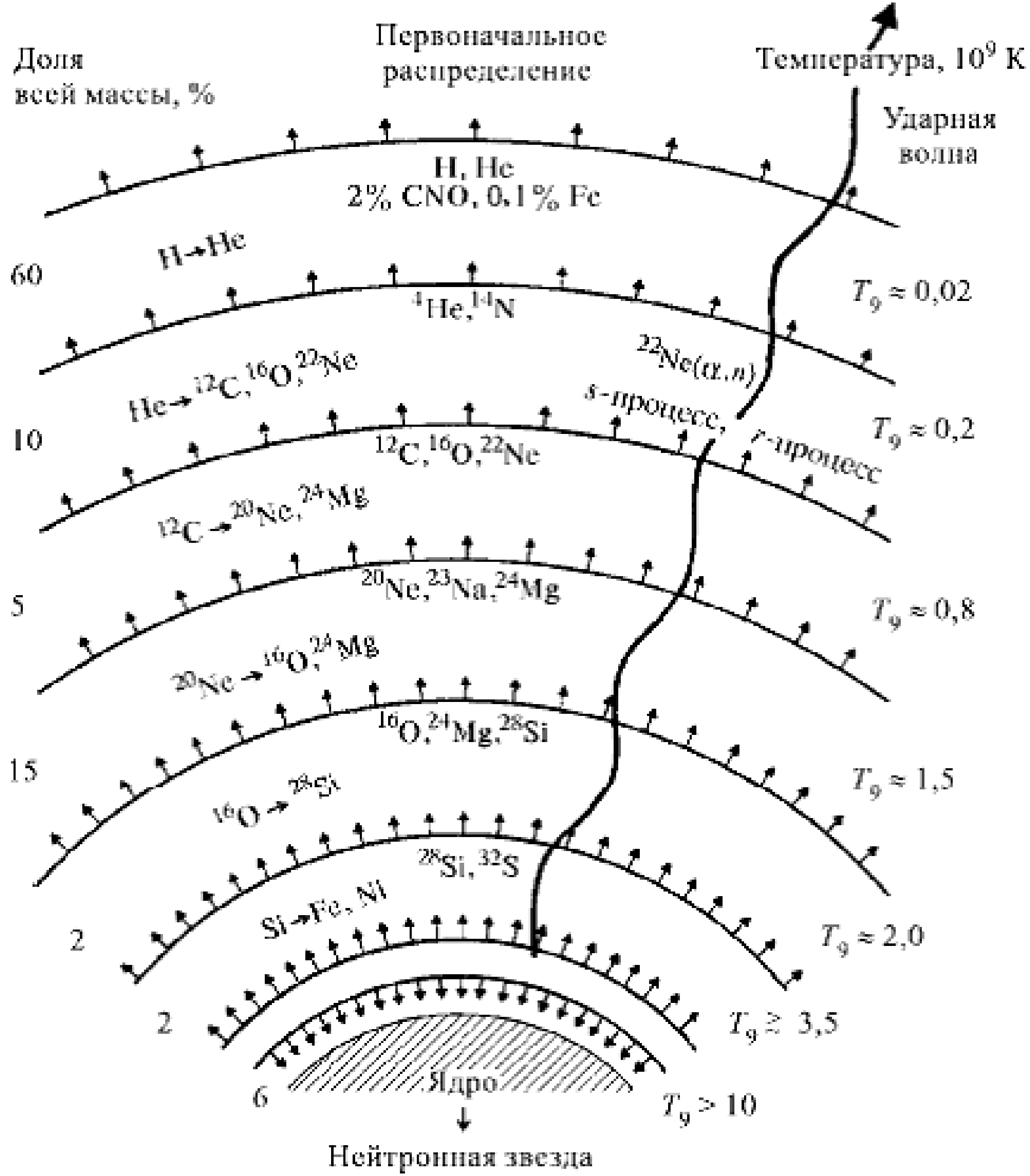

T_7^p	*t*/sec	*R*/cm
7.6	***154***	**10^{11}**
31.3	***19.5***	**10^{10}**
95.	***3.5***	**$10^{9.5}$**
450	***0.19***	**$10^{8.5}$**
609	***0.1***	**10^{8}**

Crab

Supernova remnant called Crab Nebula; VLT/Optical

X-ray (blue) and optical (red) radiation from Crab Nebula's core region. A pulsar near the center propels particles.

Горение атомных ядер:

взрывное горение

Дубна.2014

В.Н. Кондратьев

ЛТФ, ОИЯИ, 141980, Дубна Россия

Киевский национальный университет имени Тараса Шевченко, UA-03022 Киев, Украина

Before and after pictures of SN1987a

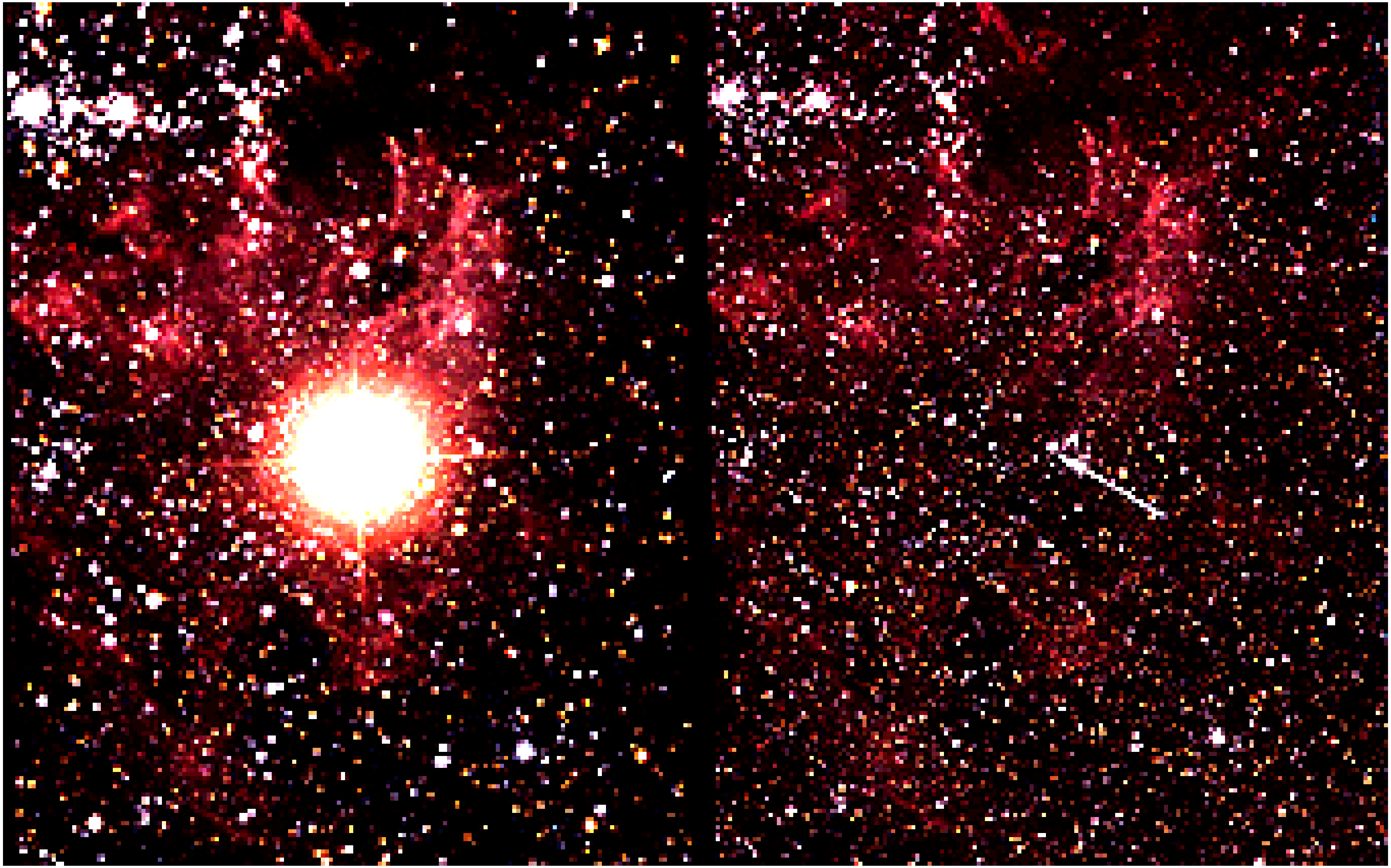

Hertzsprung- Russell (H-R) diagram

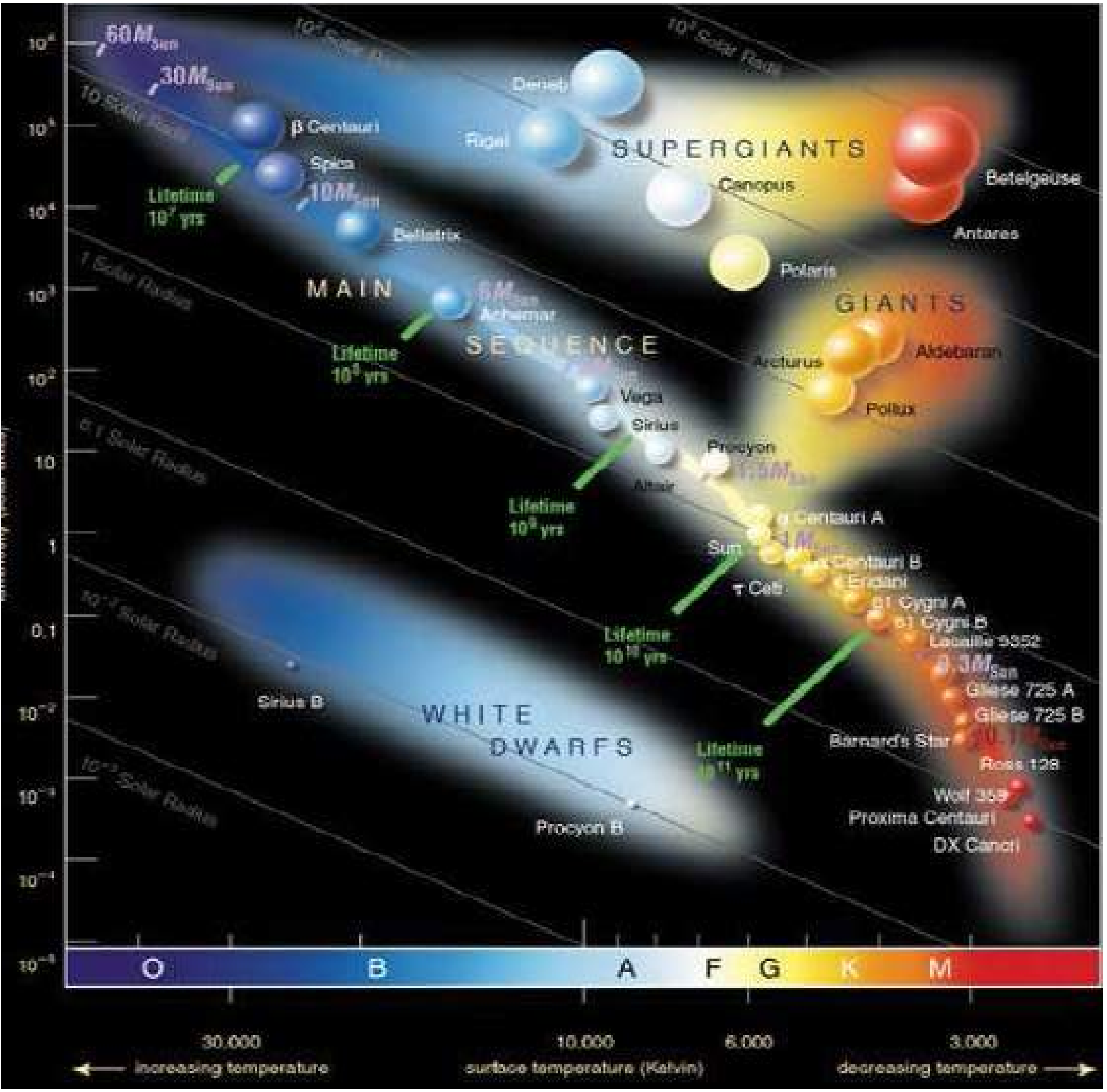

Stefan-Boltzmann
Law for flux

luminosity L
of a star with
radius R **&**
surface temperature T
$L \sim (\text{Surface})T^4 \sim R^2T^4$

Massive Star, $M > 8\ M_o$ *onion*

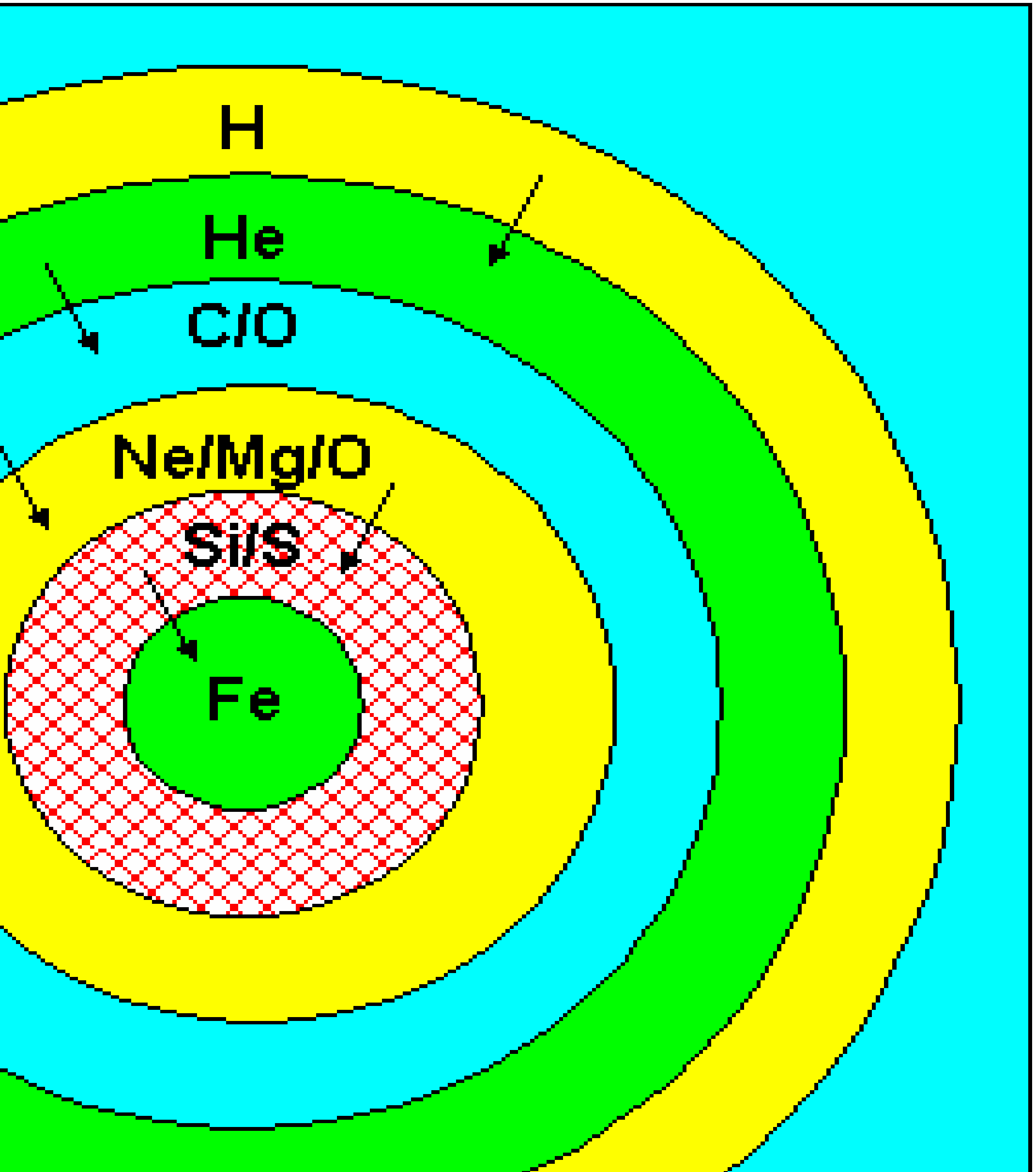

$4H \rightarrow {}^{4}_{2}He$

$3\ {}^{4}_{2}He \rightarrow {}^{12}_{6}C$

${}^{12}_{6}C + {}^{12}_{6}C \rightarrow {}^{20}_{10}Ne + {}^{4}_{2}He$

${}^{12}_{6}C + {}^{12}_{6}C \rightarrow {}^{24}_{12}Mg + \gamma$

${}^{12}_{6}C + {}^{16}_{8}O \rightarrow {}^{28}_{14}Si + \gamma$

${}^{16}_{8}O + {}^{16}_{8}O \rightarrow {}^{32}_{16}S + \gamma$

${}^{28}_{14}Si + {}^{16}_{8}O \rightarrow {}^{44}_{22}Ti(\beta^{+})$

${}^{44}_{21}Sc(\beta^{+})\ {}^{44}_{20}Ca$

${}^{28}_{14}Si + {}^{28}_{14}Si \rightarrow {}^{56}_{28}Ni(\beta^{+})$

${}^{56}_{27}Co(\beta^{+})\ {}^{56}_{26}Fe$

Stellar Collapse and Supernova Explosion

Onion structure

Collapse (implosion)

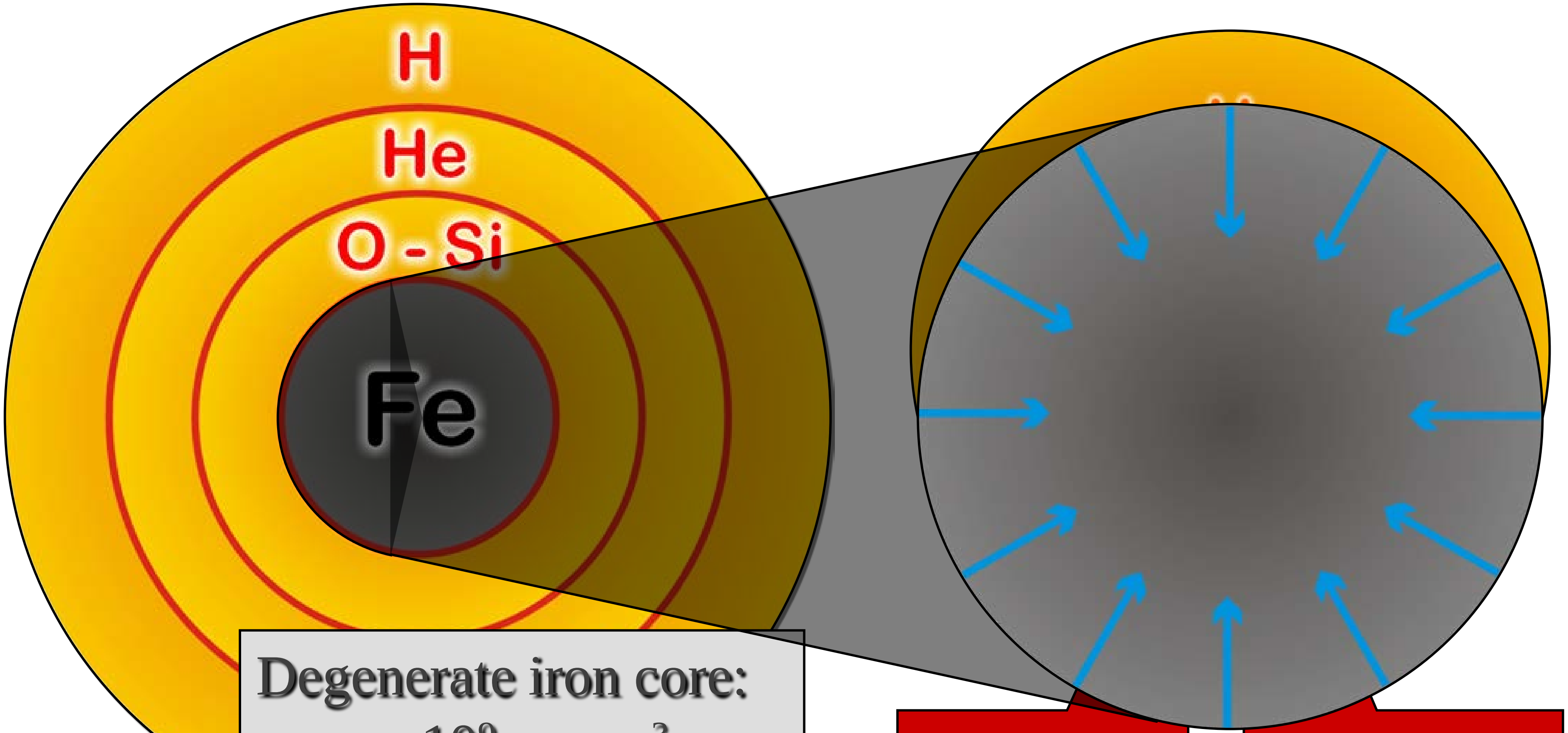

Helium Burning

Hydrogen Burning

Degenerate iron core:

$\rho \approx 10^{9}$ g cm^{-3}

$T \approx 10^{10}$ K

$M_{Fe} \approx 1.5\ M_{sun}$

$R_{Fe} \approx 10^{3,5}$ km

Stellar Collapse and Supernova Explosion

Newborn Neutron Star

Explosion

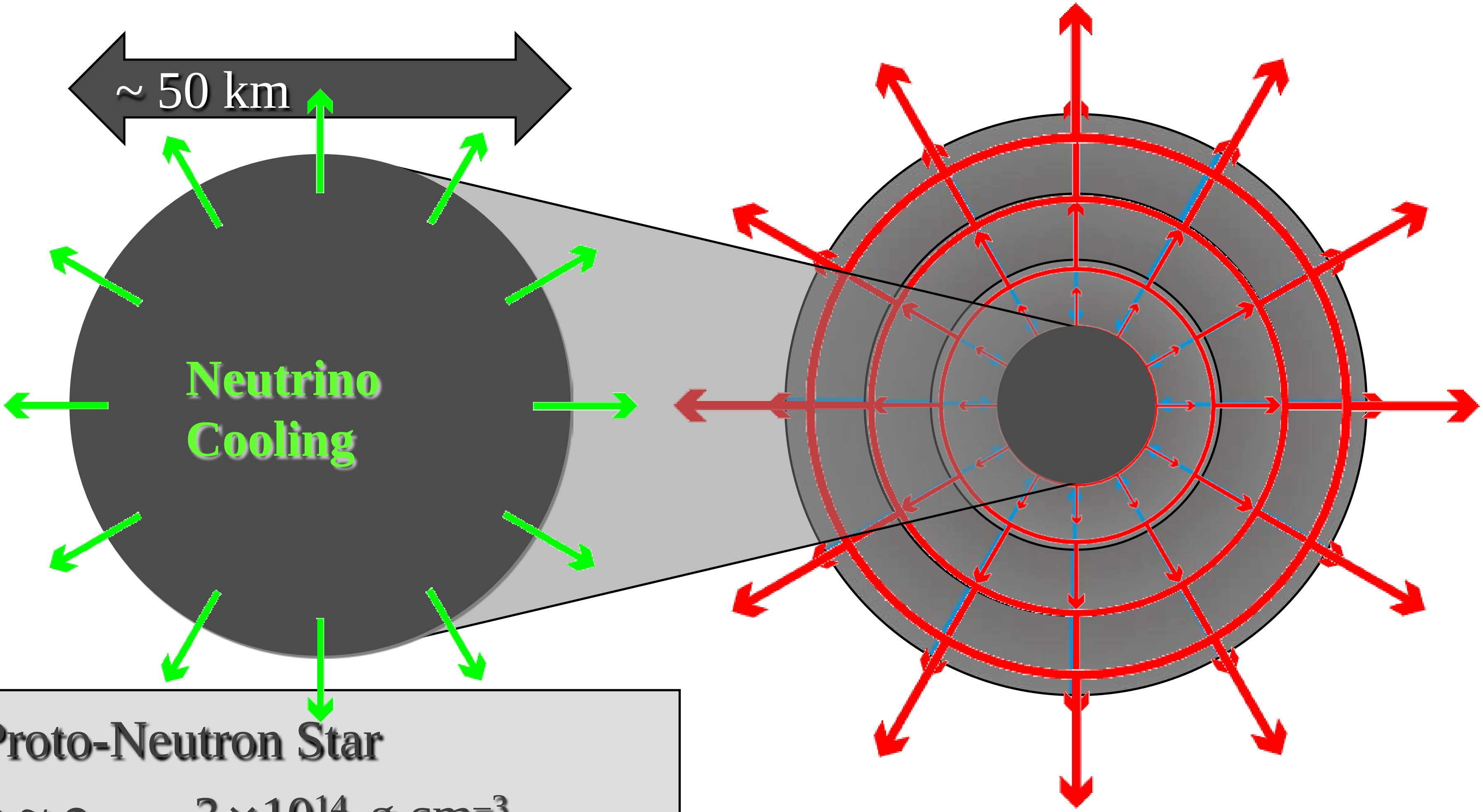

Proto-Neutron Star

$\rho \approx \rho_{\mathrm{nuc}} = 3\times10^{14}\ \mathrm{g\ cm^{-3}}$

$T \approx 30$ MeV

Stellar Collapse and Supernova Explosion

Newborn Neutron Star

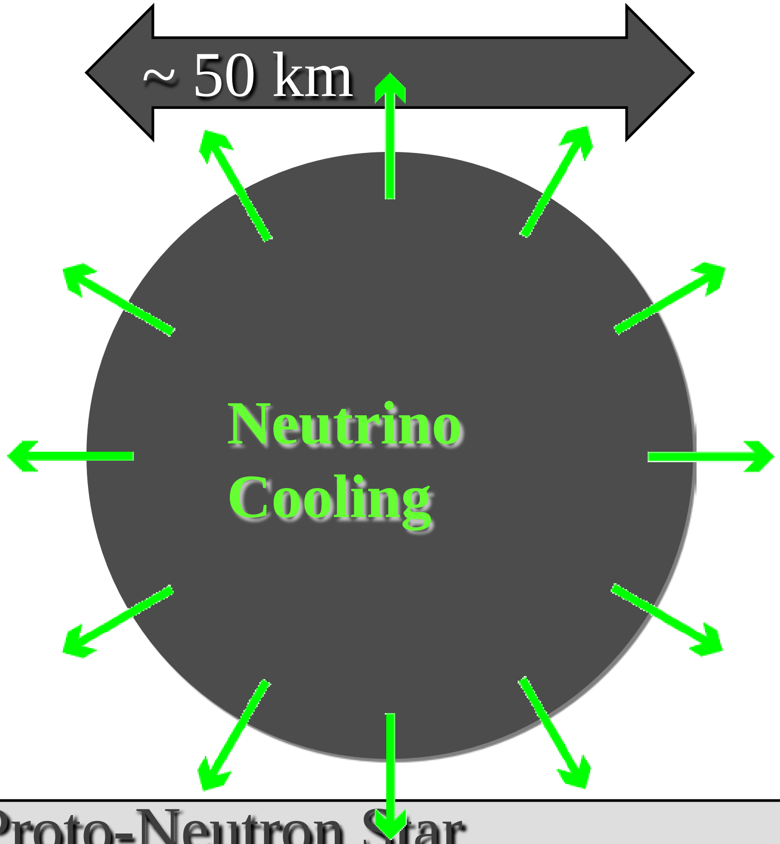

Proto-Neutron Star

$\rho \approx \rho_{\mathrm{nuc}} = 3\times10^{14}\ \mathrm{g\ cm^{-3}}$

$T \approx 10\ \mathrm{MeV}$

Gravitational binding energy

$E_b \approx 10^{53,5}\ \mathrm{erg} \approx 20\%\ M_{\mathrm{SUN}}\, c^2$

This is distributed as

99%	Neutrinos
1%	Kinetic energy of explosion (1% of this into cosmic rays)
0.01%	Photons, outshine host galaxy

Core-collapse supernova

***high-mass(M>8M$_o$)*star**

***Evolution* on HR diagram**

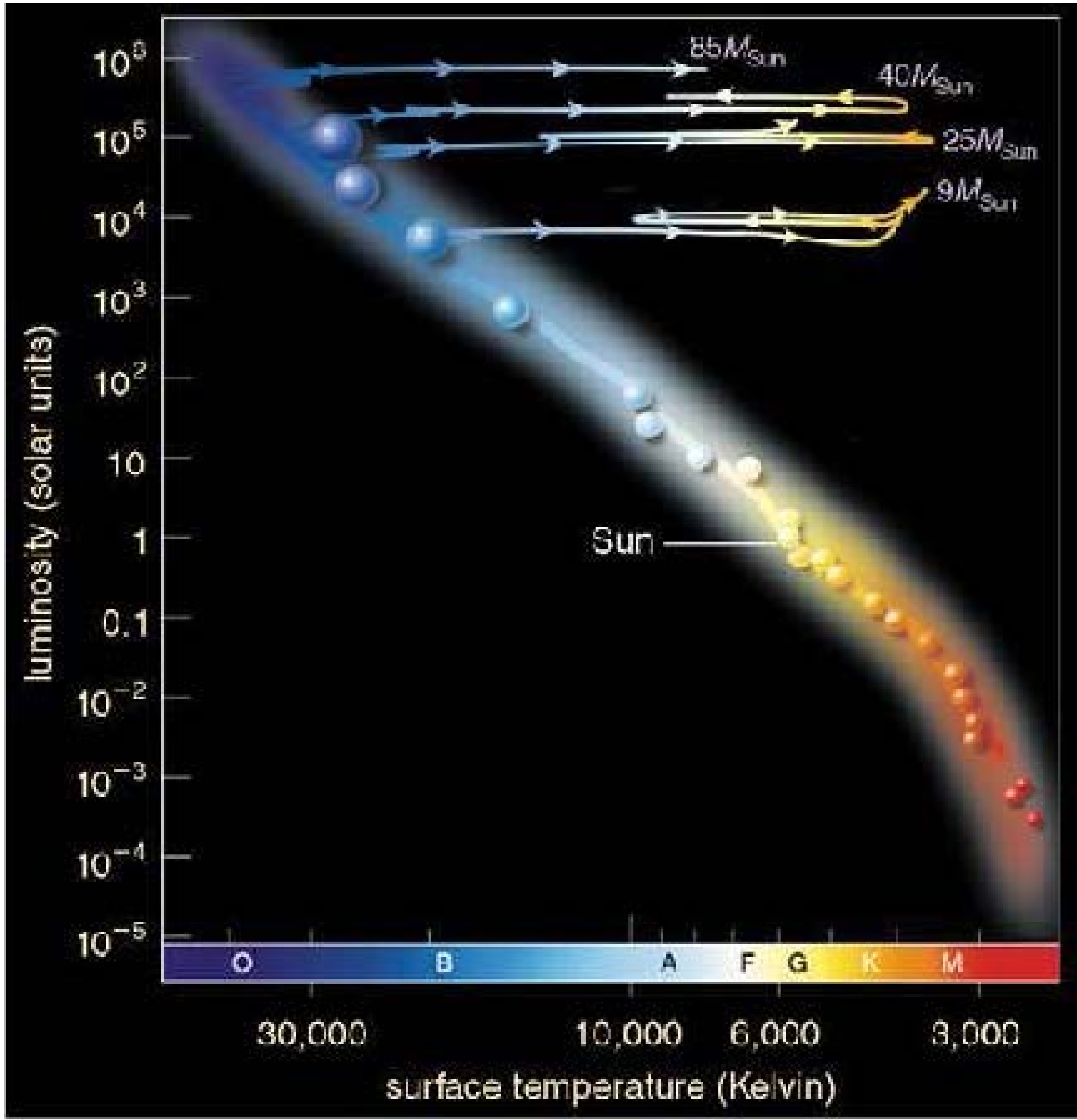

explosive
nucleosynthesis
origin of
Heavy Nuclides

Explosive nucleosynthesis

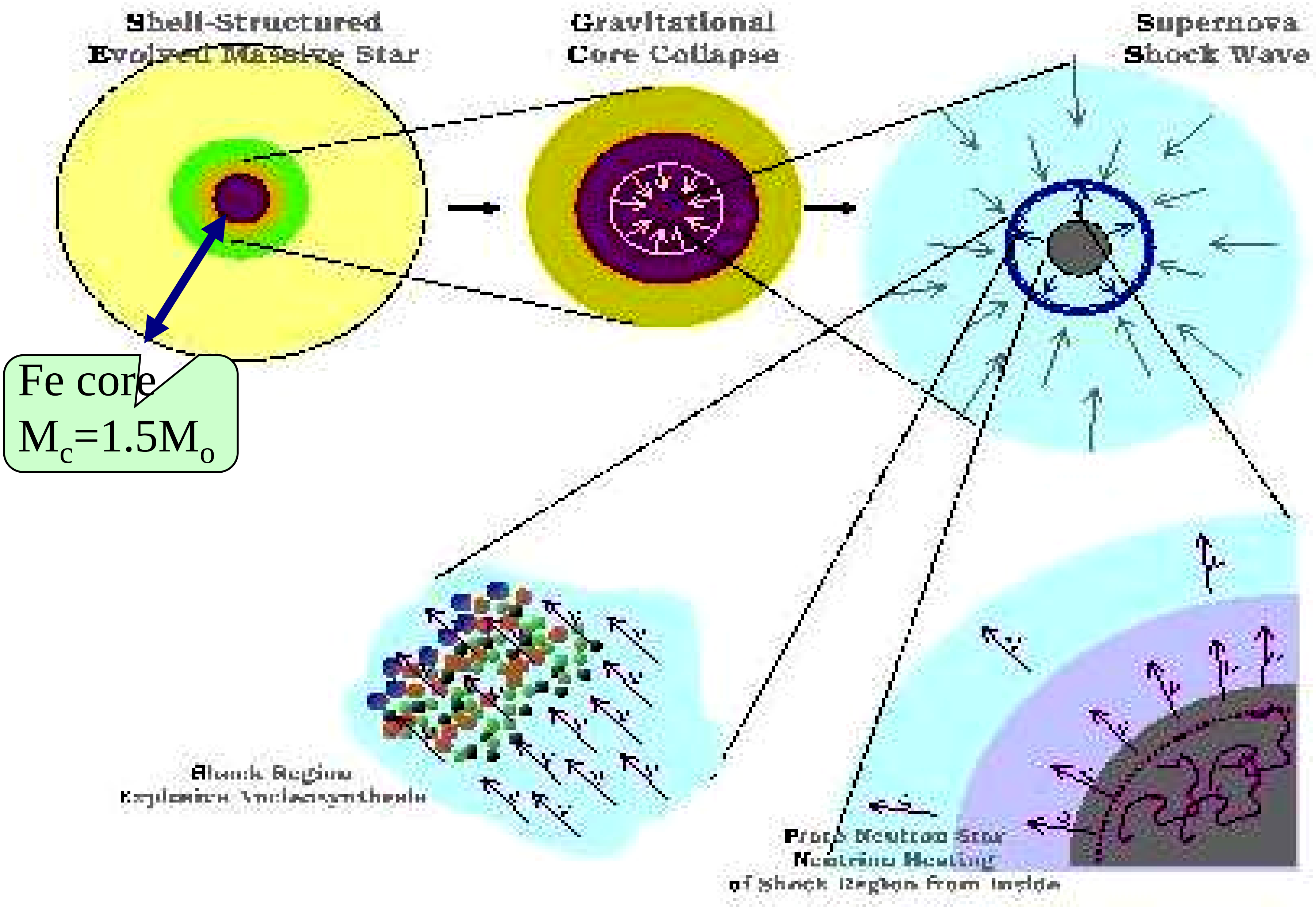

Fe core

M_c=1.5M_o

INTEGRAL
VIRGO.UA

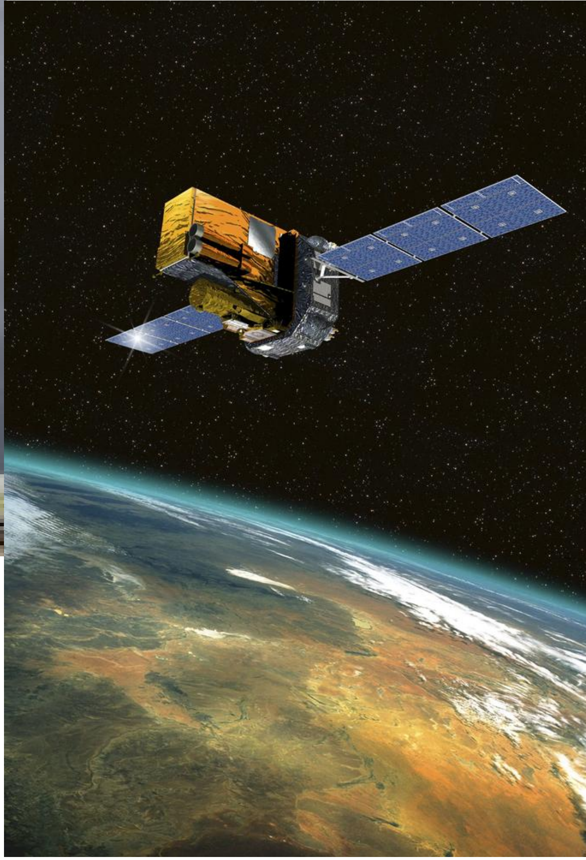

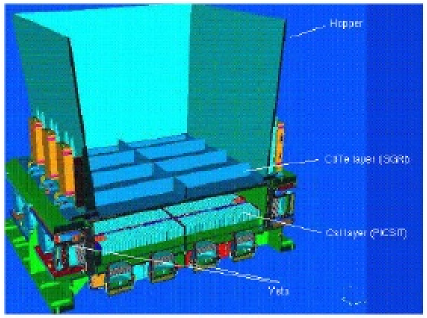

IBIS/ISGRI

Energy range	20 keV – 1 MeV
Energy resolution (FWHM)	7% at 100 keV
Detector area	960 cm2 at 50 keV

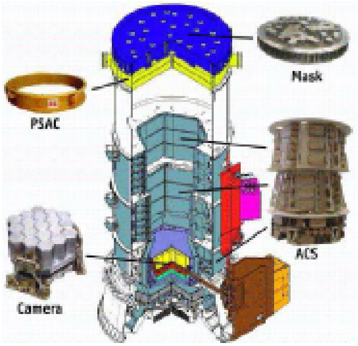

SPI

Energy range	20 keV – 8 MeV
Energy resolution (FWHM)	2.35 keV at 1.33 MeV
Detector area	~ 500 cm^2

Integral IBIS/ISGRI

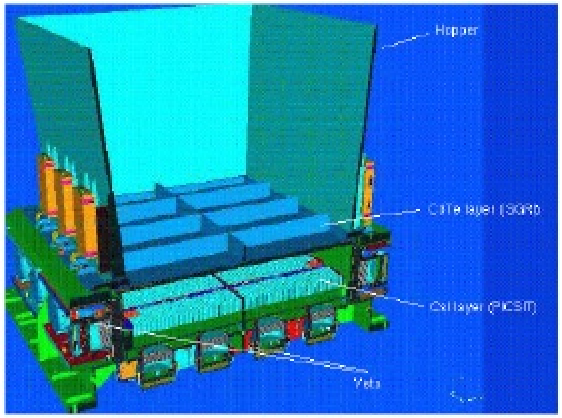

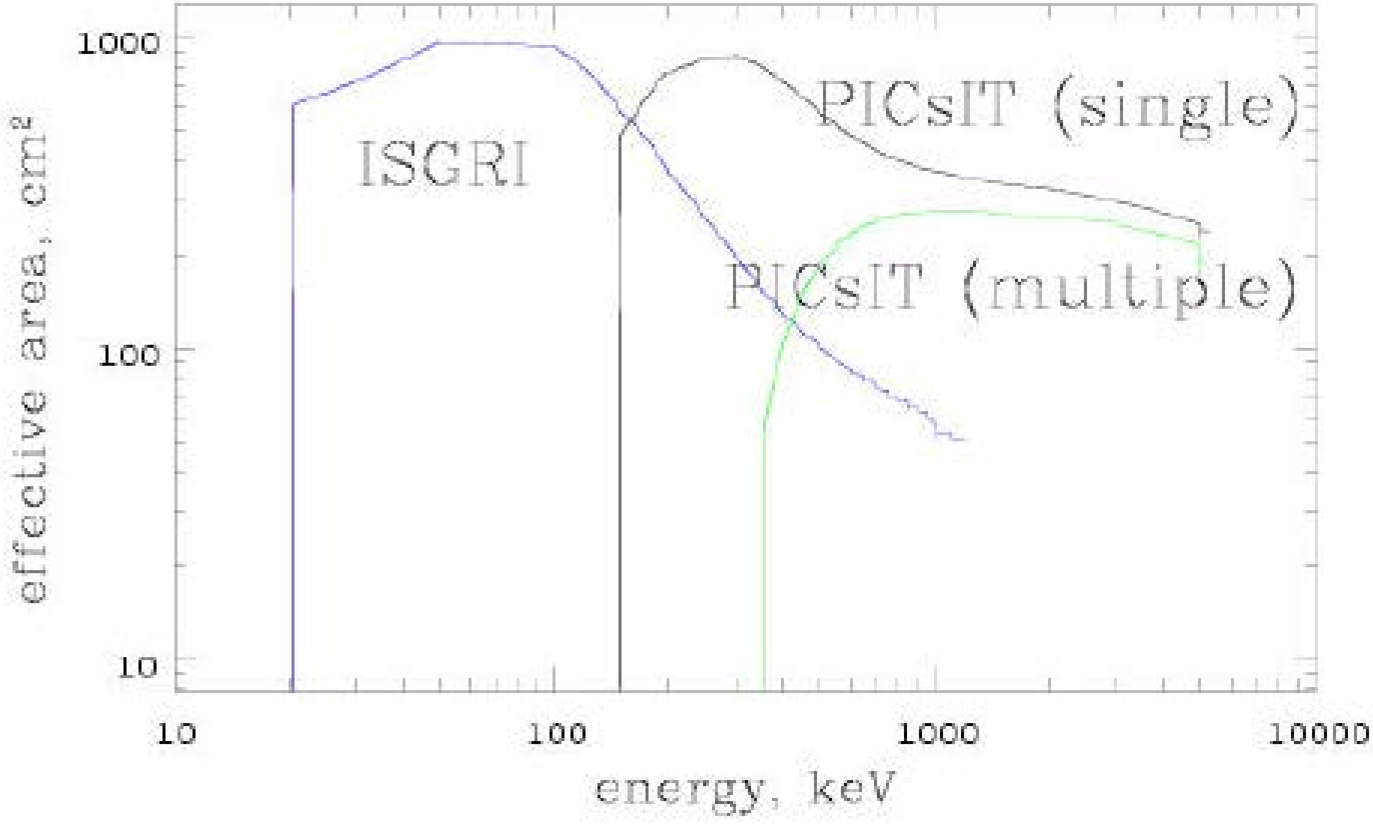

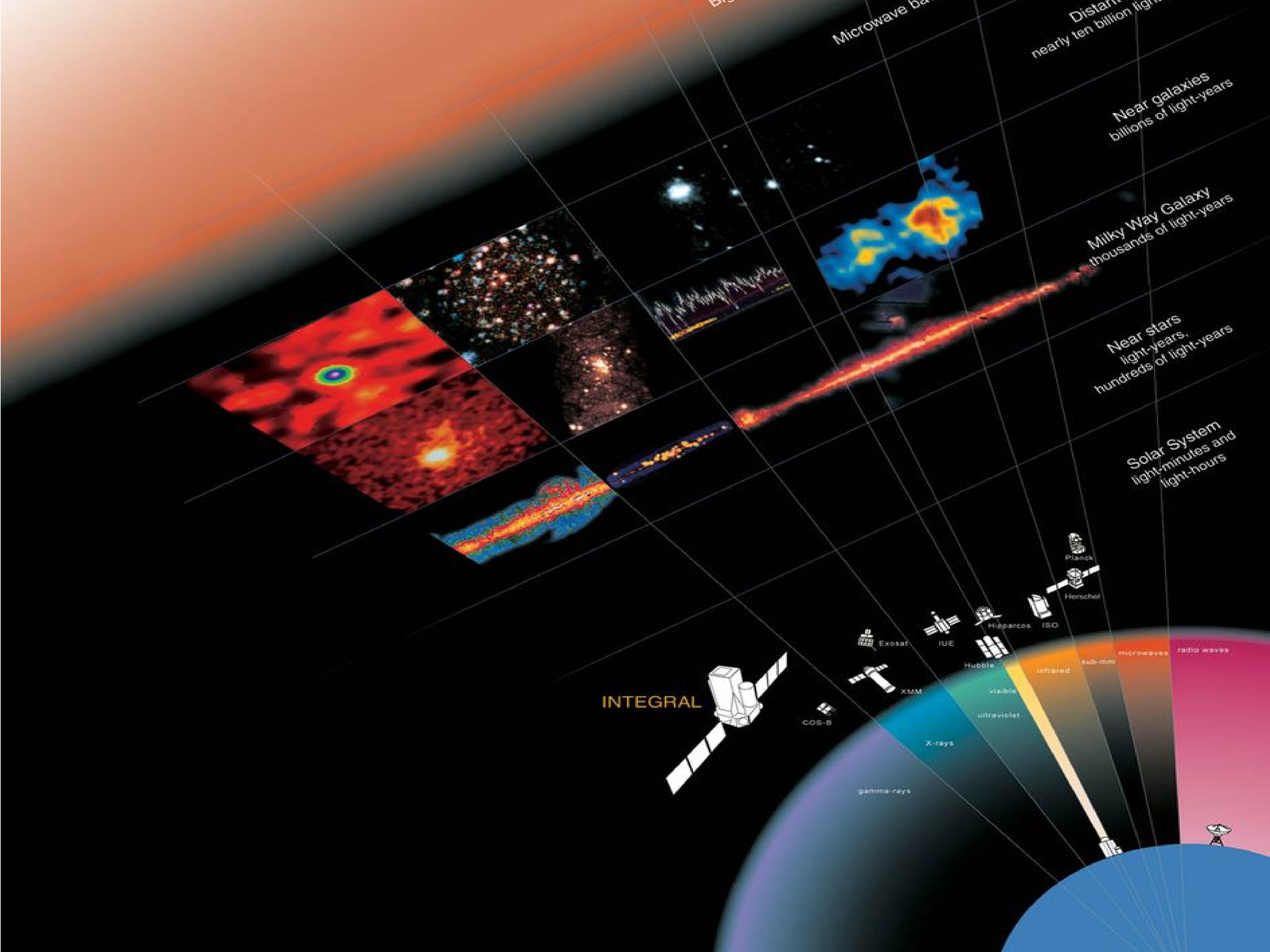
Bi
Microwave ba
Distant
nearly ten billion ligh
Near galaxies
billions of light-years
Milky Way Galaxy
thousands of light-years
Near stars
light-years,
hundreds of light-years
Solar System
light-minutes and
light-hours
Planck
Herschel
Hipparcos
ISO
Exosat
IUE
Hubble
XMM
INTEGRAL
COS-B
radio waves
microwaves
sub-mm
infrared
visible
ultraviolet
X-rays
gamma-rays

INTEGRAL Exposure of sky in Galactic coordinates (ksec)

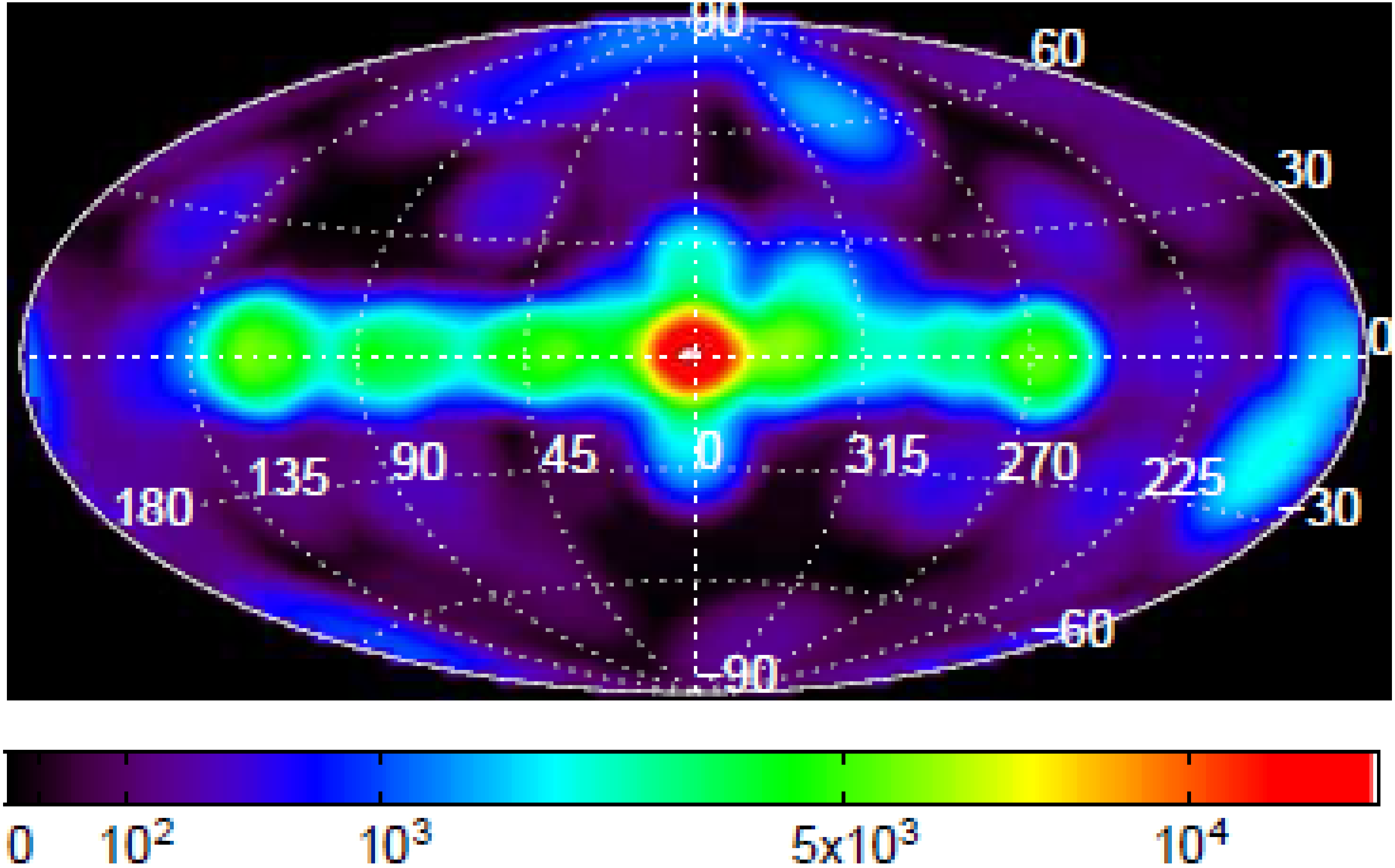

CAS A(3.4+0.3-0.1)kpc, TYCHO(2.2+/-0.3)kpc

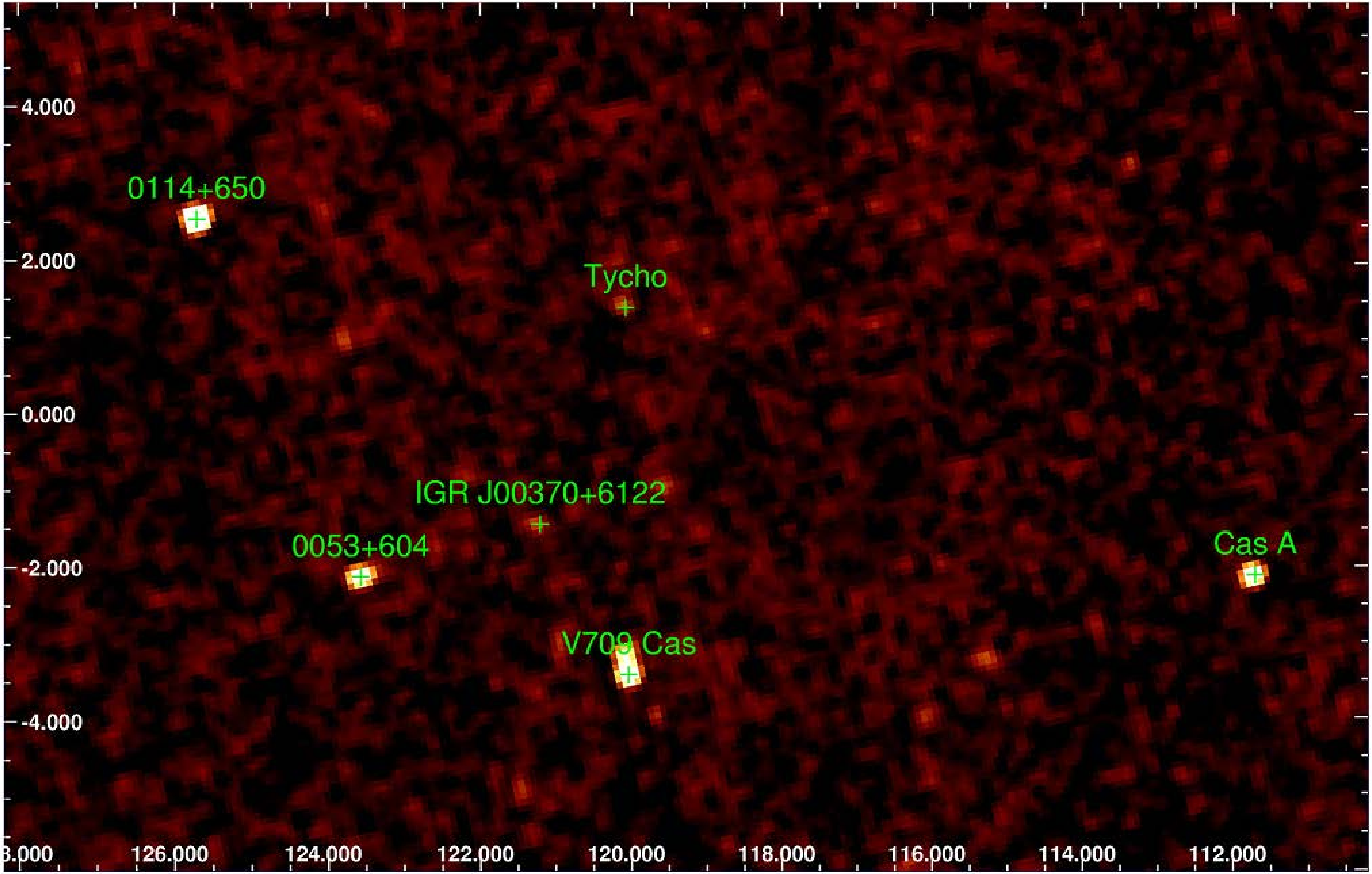

Investigated Supernovas

Name	Coordinate	Age
SN 1987A	**-** 279.7 -31.9,	**20 y**
Cas A	**-** 111.7 -2.1,	**330 y**
TYCHO	**-** 120.1 +1.4,	**440 y**
Vela Junior	**-** 266.3 -1.2	**?**

The scheme of the ^{44}Ti decay

Earth environment

59 y

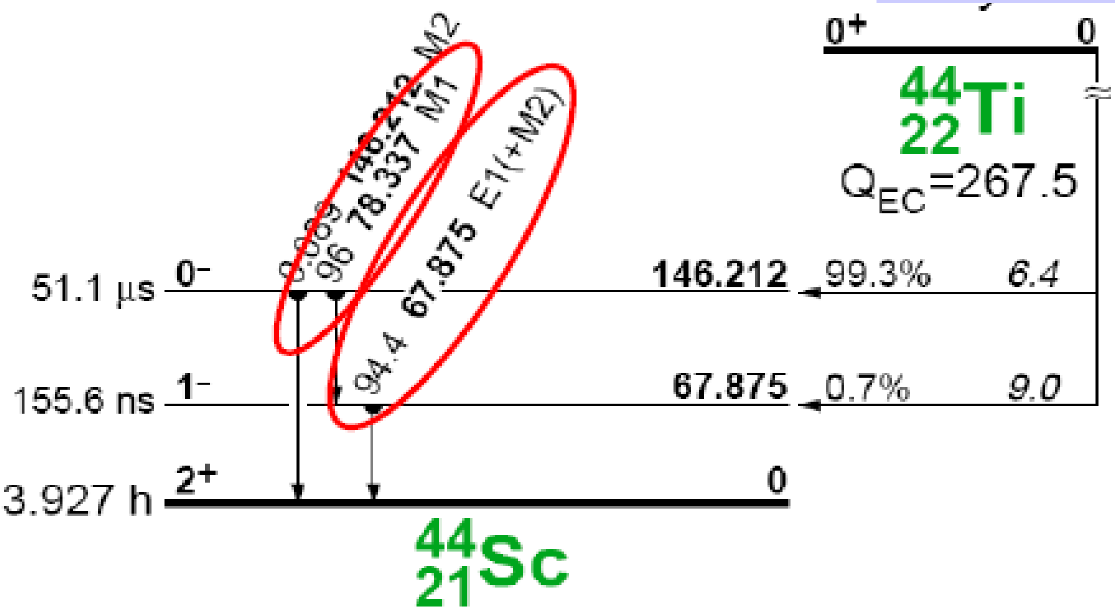

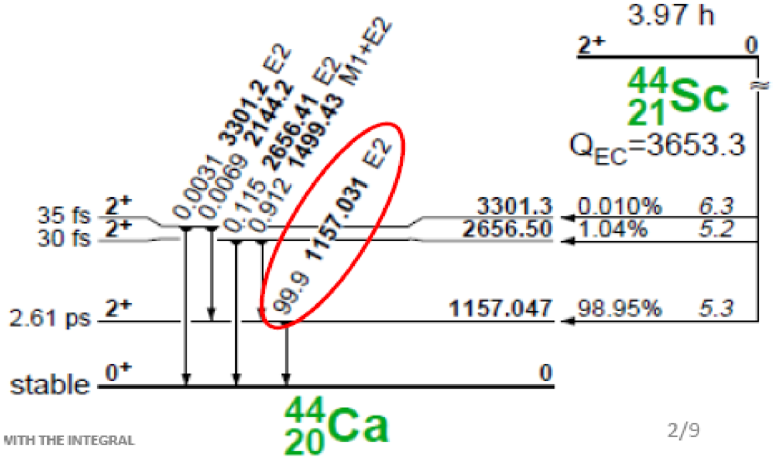

Cassiopeia A (3.4+0.3-0.1)kpc

Energy range (keV): **20-62-72-82-100**

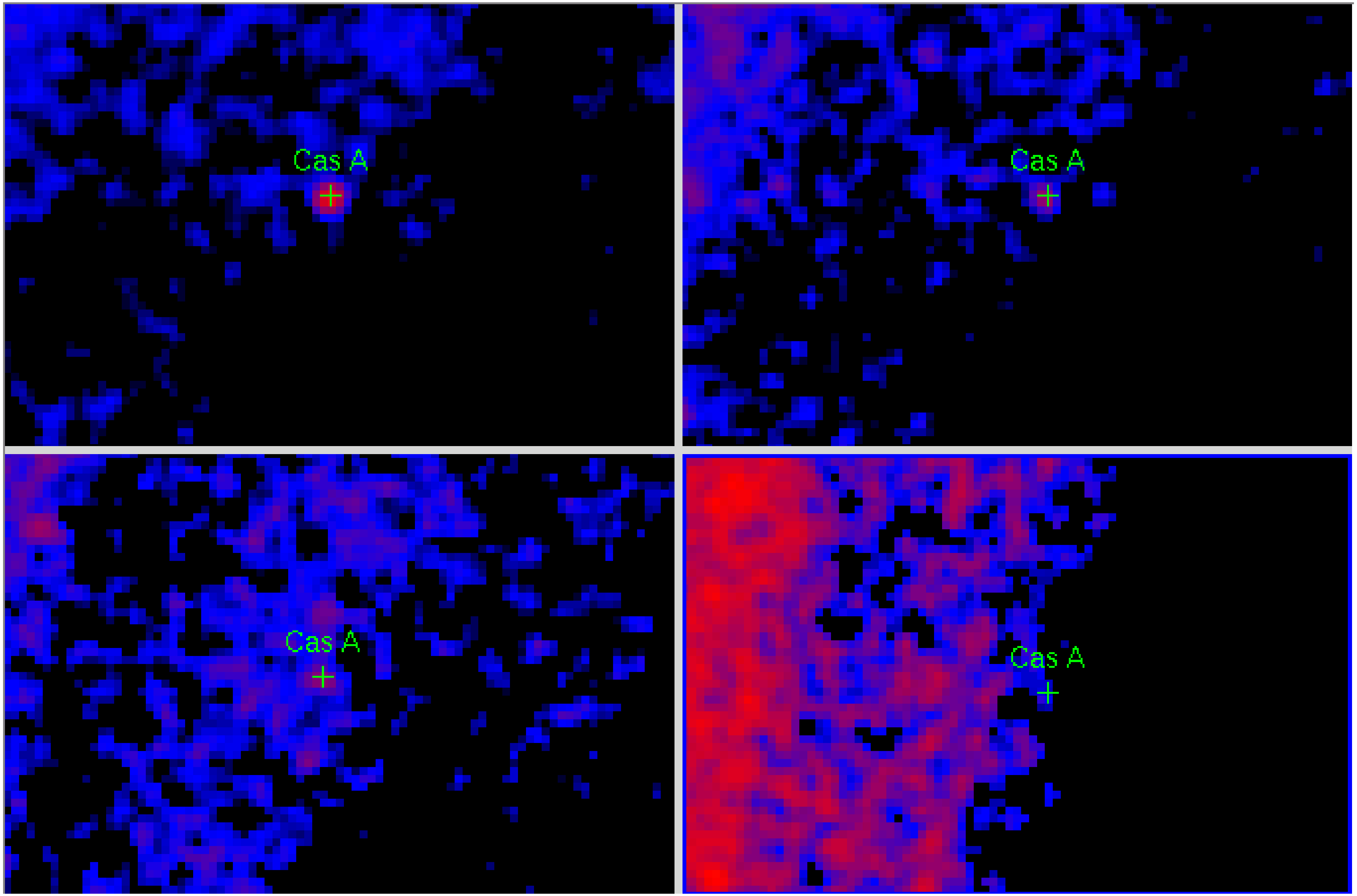

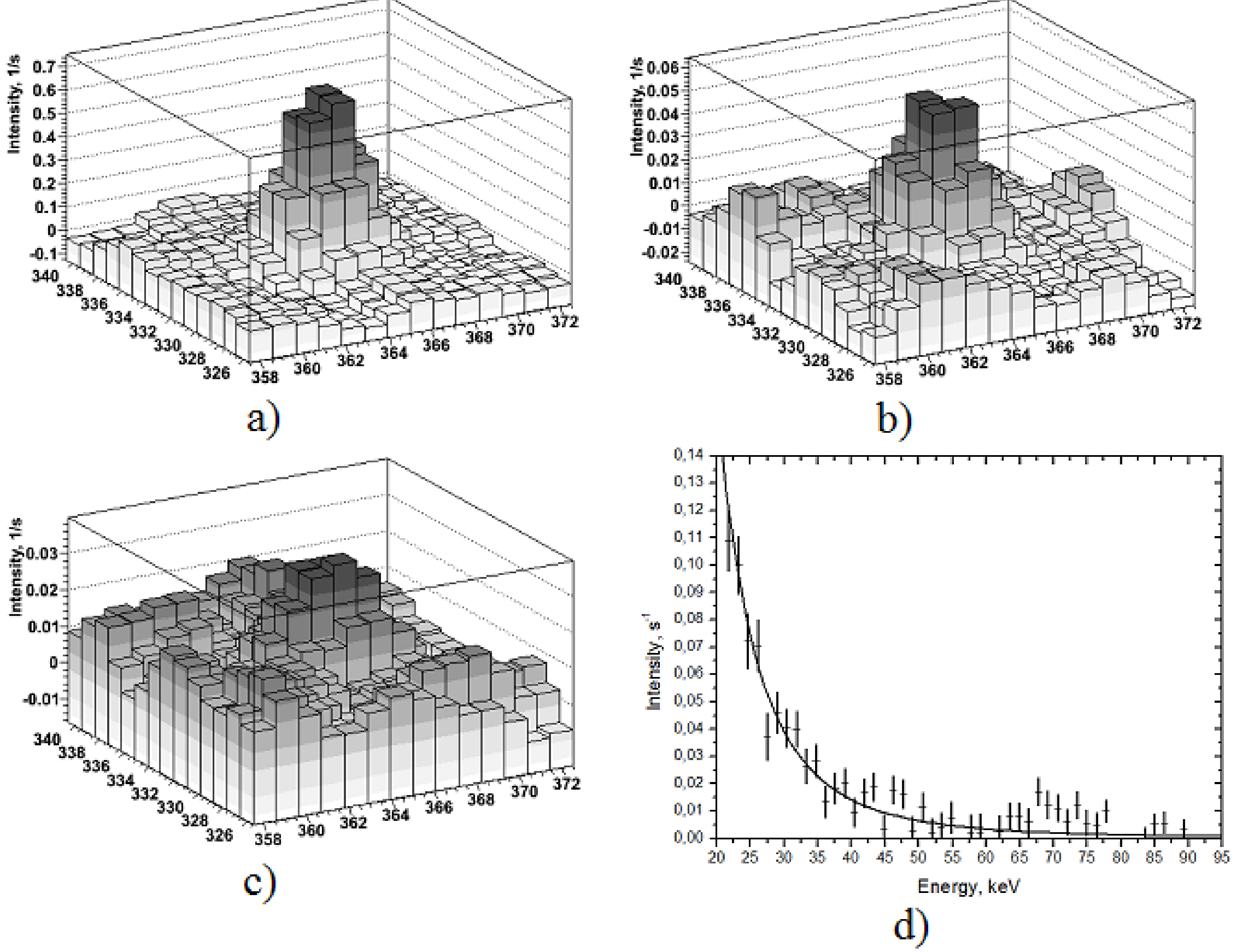

F The direction (i.e.. pixel number) dependence of the registered gamma-ray flux at different energy ranges: **20–62 keV - a, 62–72 keV - b, 72–82 keV – c**; for the angle region containing the Cassiopeia A SN remnant. The right bottom panel (d) represents the spectrum from the Cassiopeia A in the energy range 20–95 keV, the solid line shows the fit with the power law energy *E* dependence, .

Background estimate + Lines

$K \cdot E^a$

a=-3.64 +/- 0.09

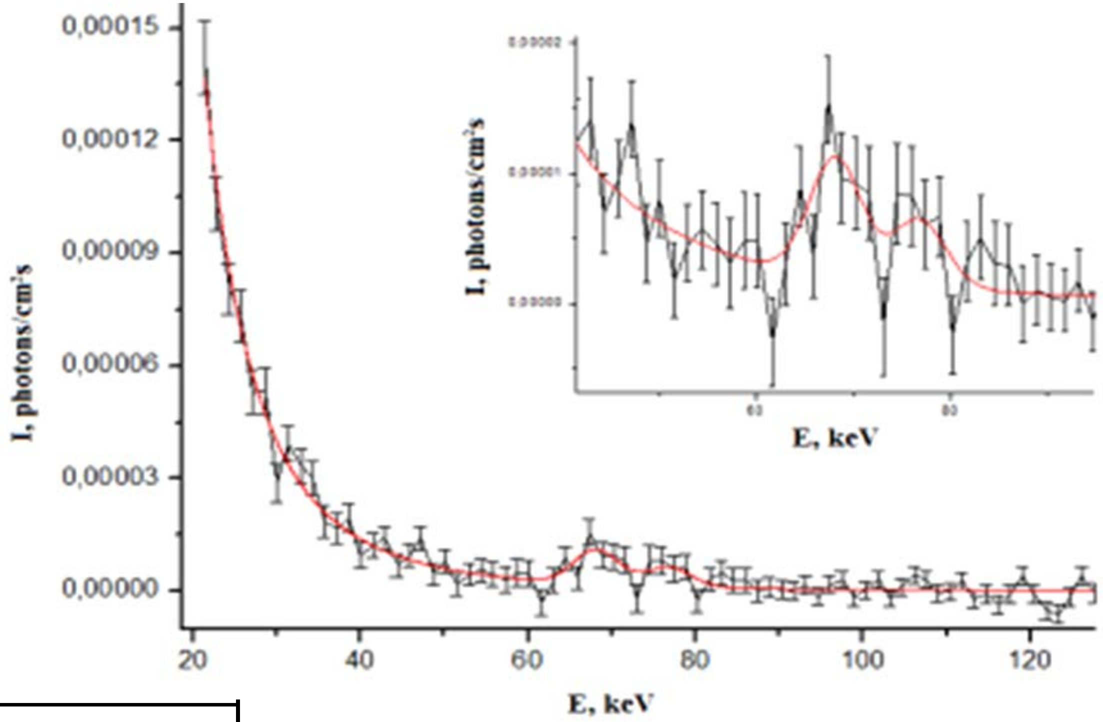

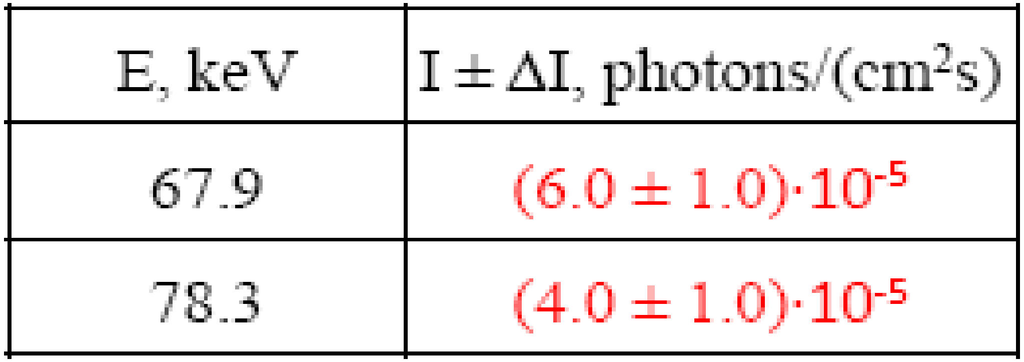

E, keV	I ± ΔI, photons/(cm²s)
67.9	$(6.0 \pm 1.0) \cdot 10^{-5}$
78.3	$(4.0 \pm 1.0) \cdot 10^{-5}$

T= 1.5Ms

SPI detector data

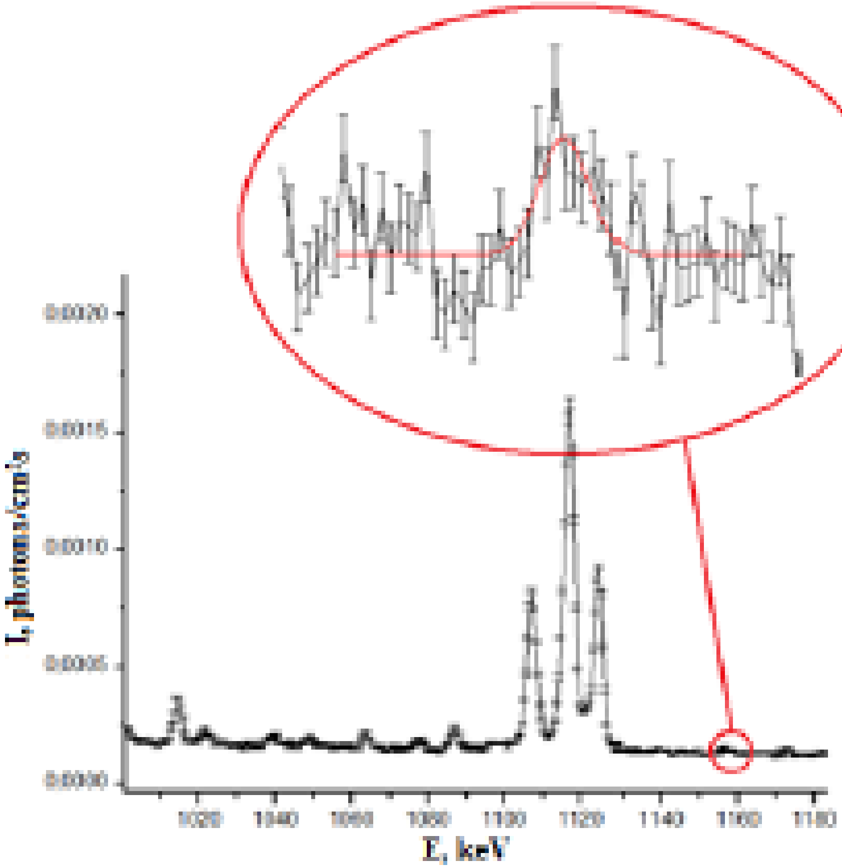

Fit results

$$E = 1157.20 \pm 0.26\ keV$$

$$FWHM = 3.1 \pm 0.7\ keV$$

Flux=(5.1+/-1.0) 10^{-5}ph/cm^2 s

T=1.5 Ms

mass of ^{44}Ti synthesized at Cassiopeia A explosion [VNK et al *‘Nucleus2004’; PhAN (2009)*]

$$m = \frac{4\pi R^2 \cdot T_{1/2} \cdot M \cdot I}{\ln 2 \cdot N_a \cdot p} \cdot 2^{-\frac{t}{T_{1/2}}}$$

R–distance to the object,$T_{1/2}$–the element half-life, N_a–theAvogadro constant,M–mola rmass,I–γ-quanta flux,p-quantum yield, t–remnant age.

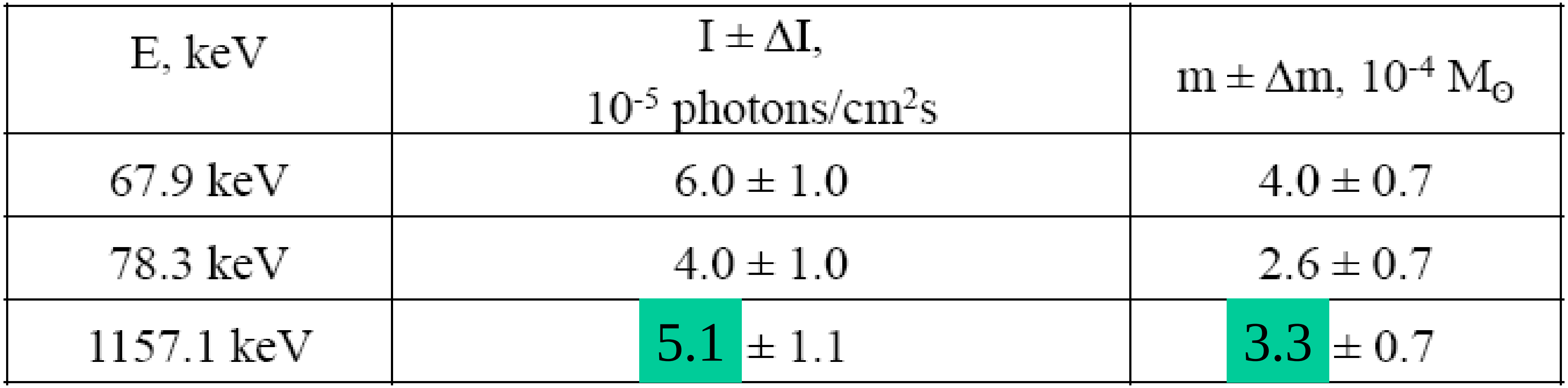

E, keV	$I \pm \Delta I$, 10^{-5} photons/cm^{2}s	$m \pm \Delta m$, 10^{-4} $M_\odot$
67.9 keV	6.0 ± 1.0	4.0 ± 0.7
78.3 keV	4.0 ± 1.0	2.6 ± 0.7
1157.1 keV	5.1 ± 1.1	3.3 ± 0.7

SN1987 A (50kpc)

Energy range (keV): **20-62-72-82-100**

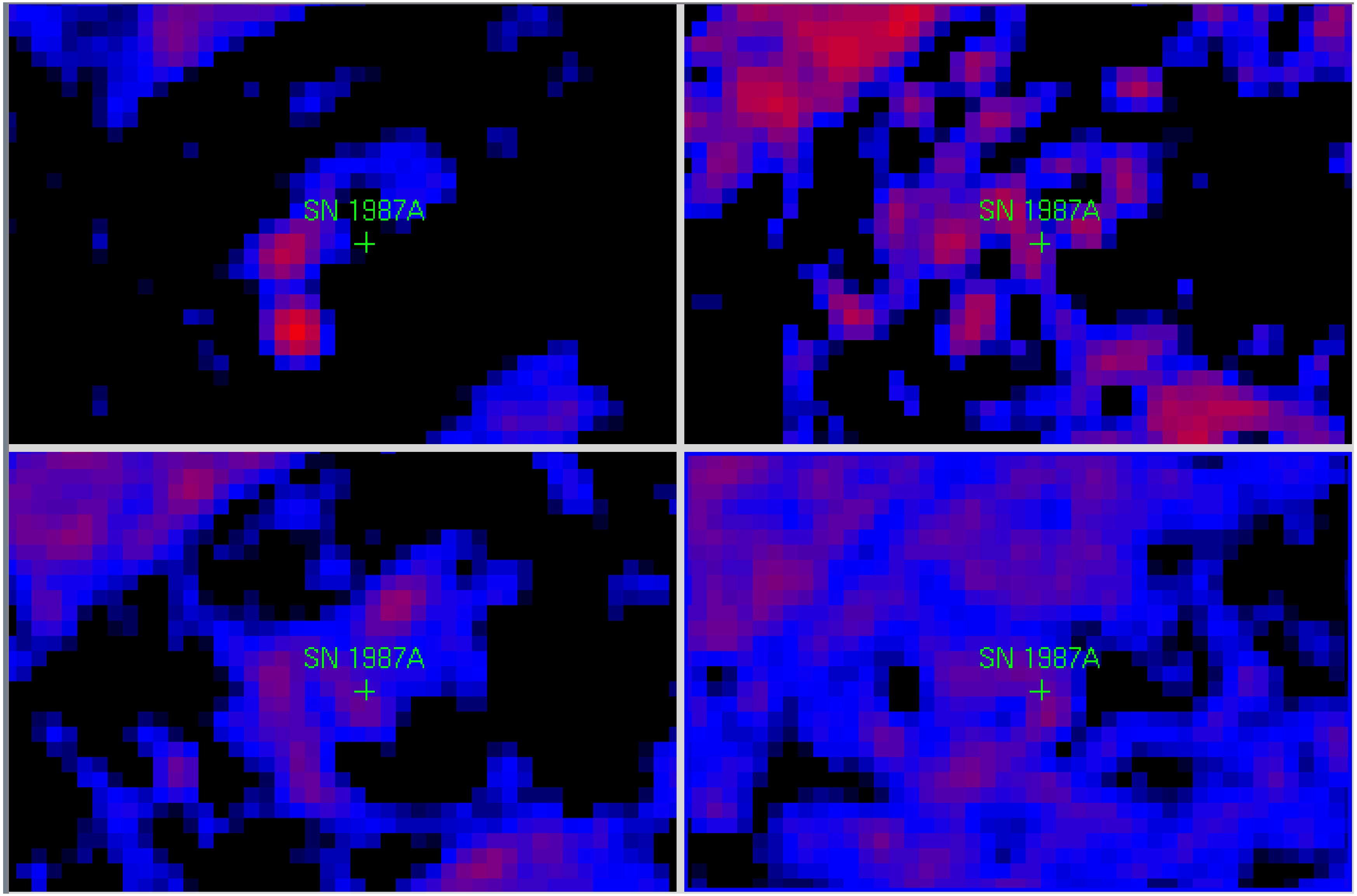

S.A.Grebenev et al *Nature, 490, 373-375 (2012).*

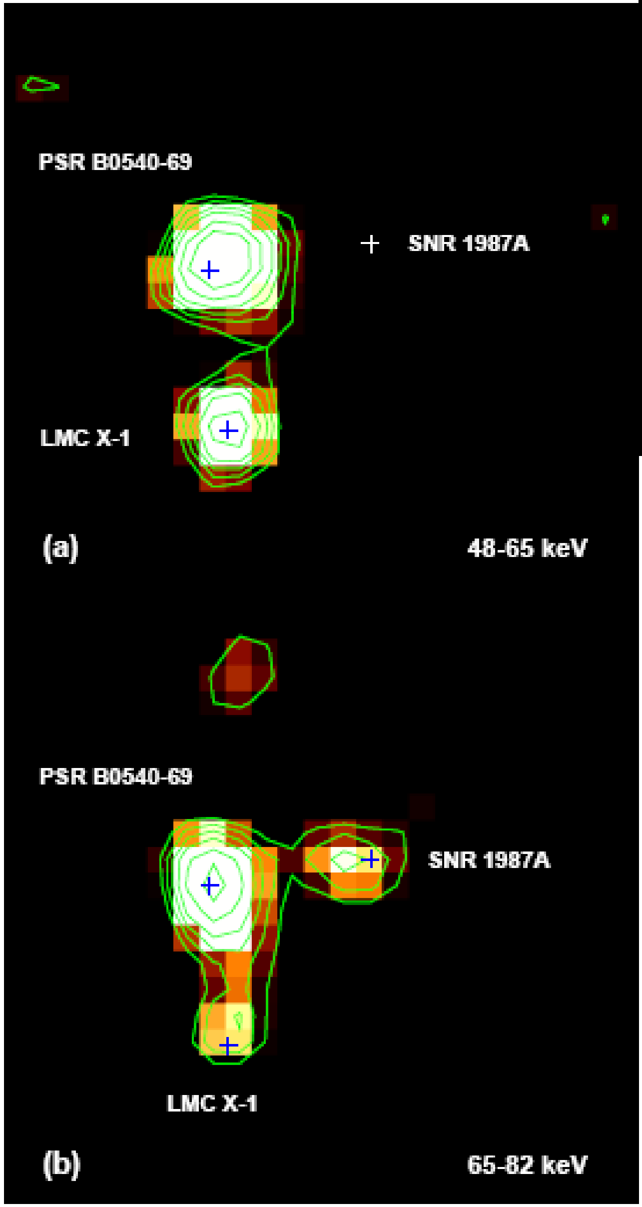

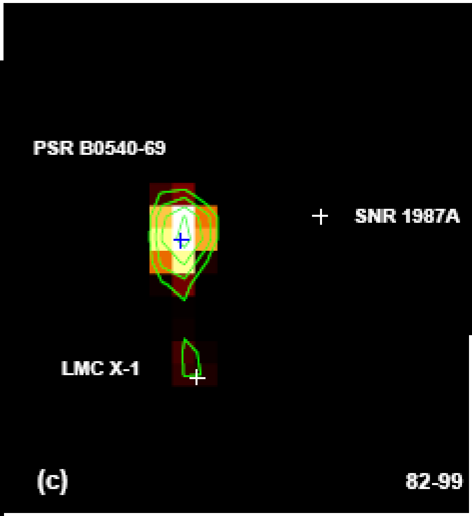

$$(3.1 \pm 0.8) \times 10^{-4} \quad M_\odot$$

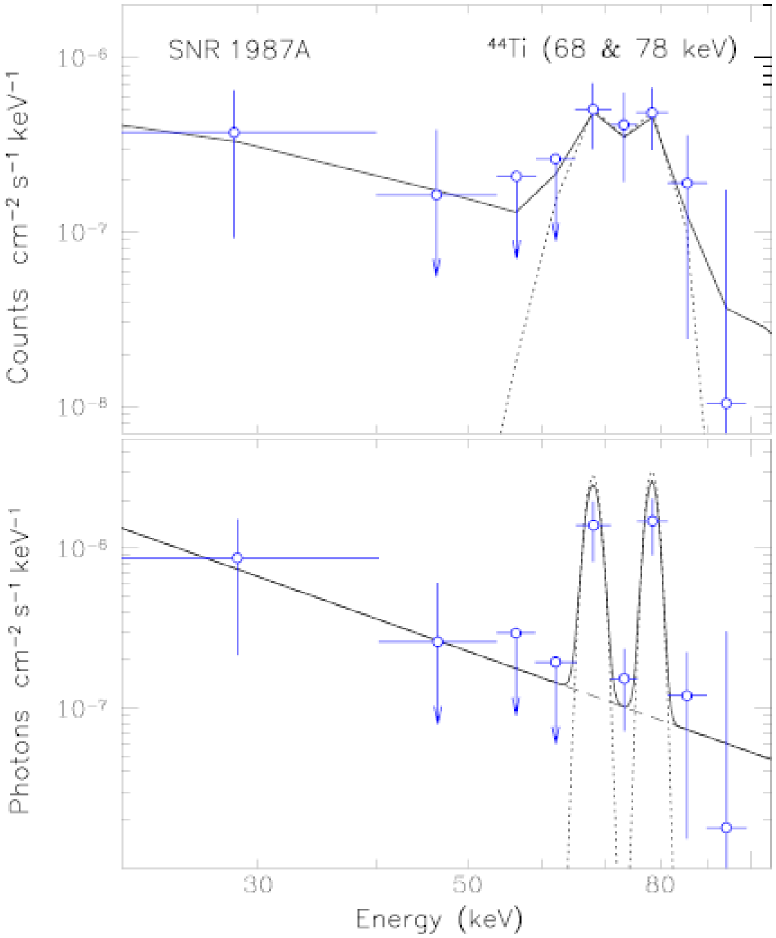

THEORY

$$(0.02 - 2.5) \times 10^{-4} \quad M_{\odot}$$

Thielemann, F.-K., Hashimoto, M. & Nomoto, K. Explosive nucleosynthesis in SN1987A. II. Composition, radioactivities, and the neutron star mass. *Astrophys. J.* ***349, 222–240 (1990)***

Woosley, S.E., & Hoffman, R. D. 57Co and 44Ti production in SN1987A. *Astrophys. J.*, ***368, L31-L34*** (1991).

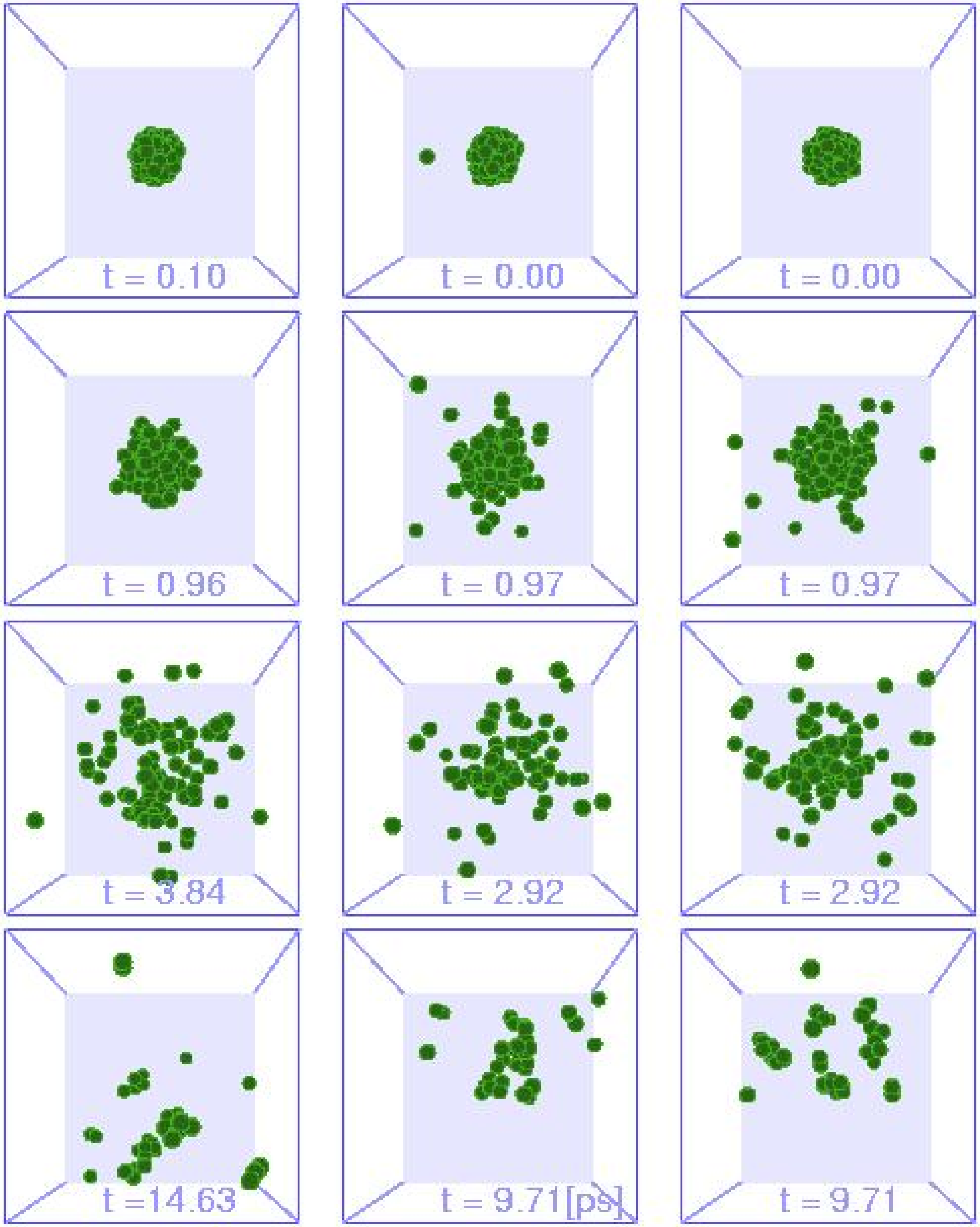
t = 0.10
t = 0.00
t = 0.00
t = 0.96
t = 0.97
t = 0.97
t = 3.84
t = 2.92
t = 2.92
t =14.63
t = 9.71[ps]
t = 9.71

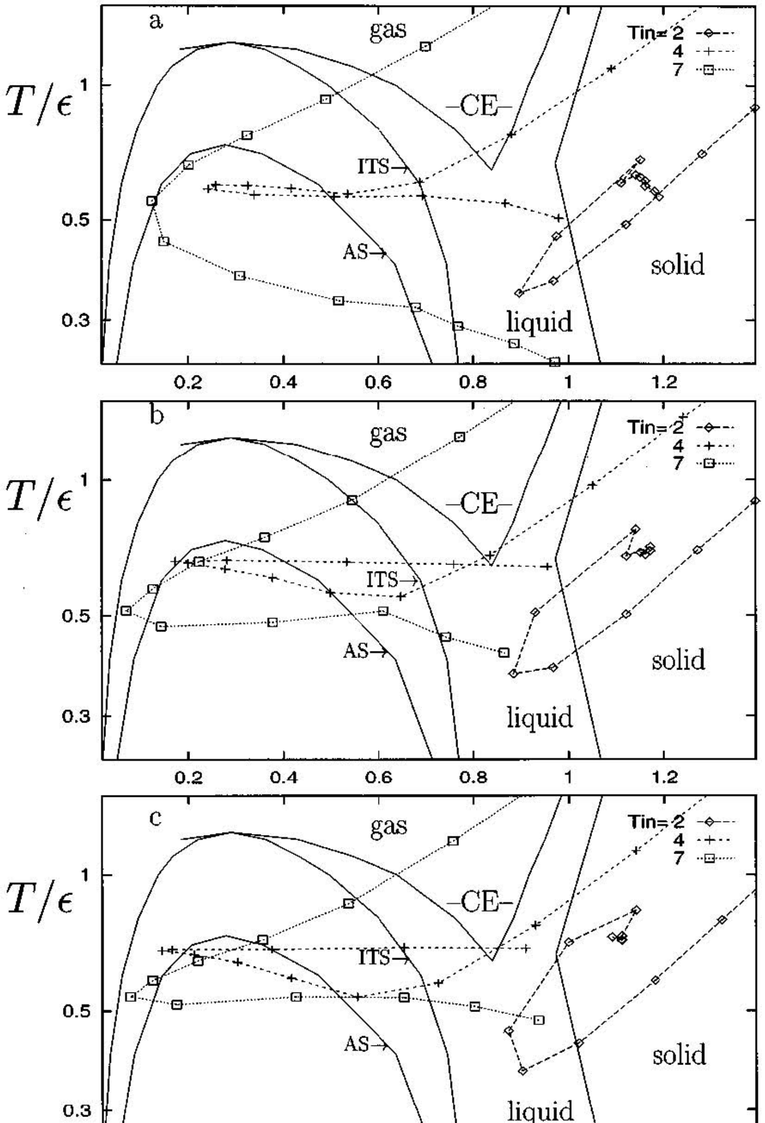
a
b
c
gas
CE
ITS→
AS→
liquid
solid
Tin=2
4
7
T/ϵ
1
0.5
0.3
0.2
0.4
0.6
0.8
1
1.2

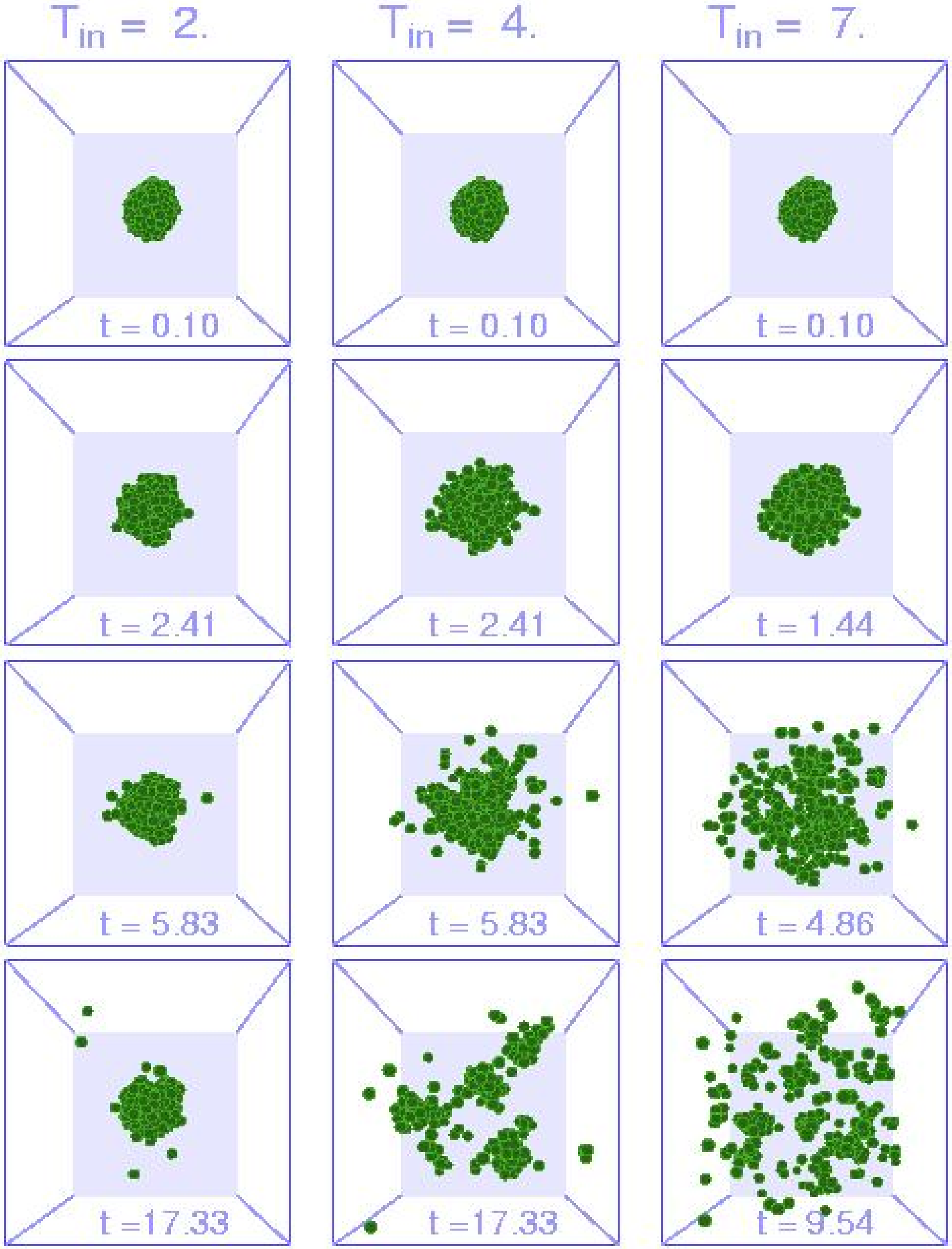
$T_{in} = 2.$
$T_{in} = 4.$
$T_{in} = 7.$
t = 0.10
t = 0.10
t = 0.10
t = 2.41
t = 2.41
t = 1.44
t = 5.83
t = 5.83
t = 4.86
t =17.33
t =17.33
t = 9.54

State Equation (SE): Nuclear Matter *vs* Regular Liquid *(Noble Gas)*

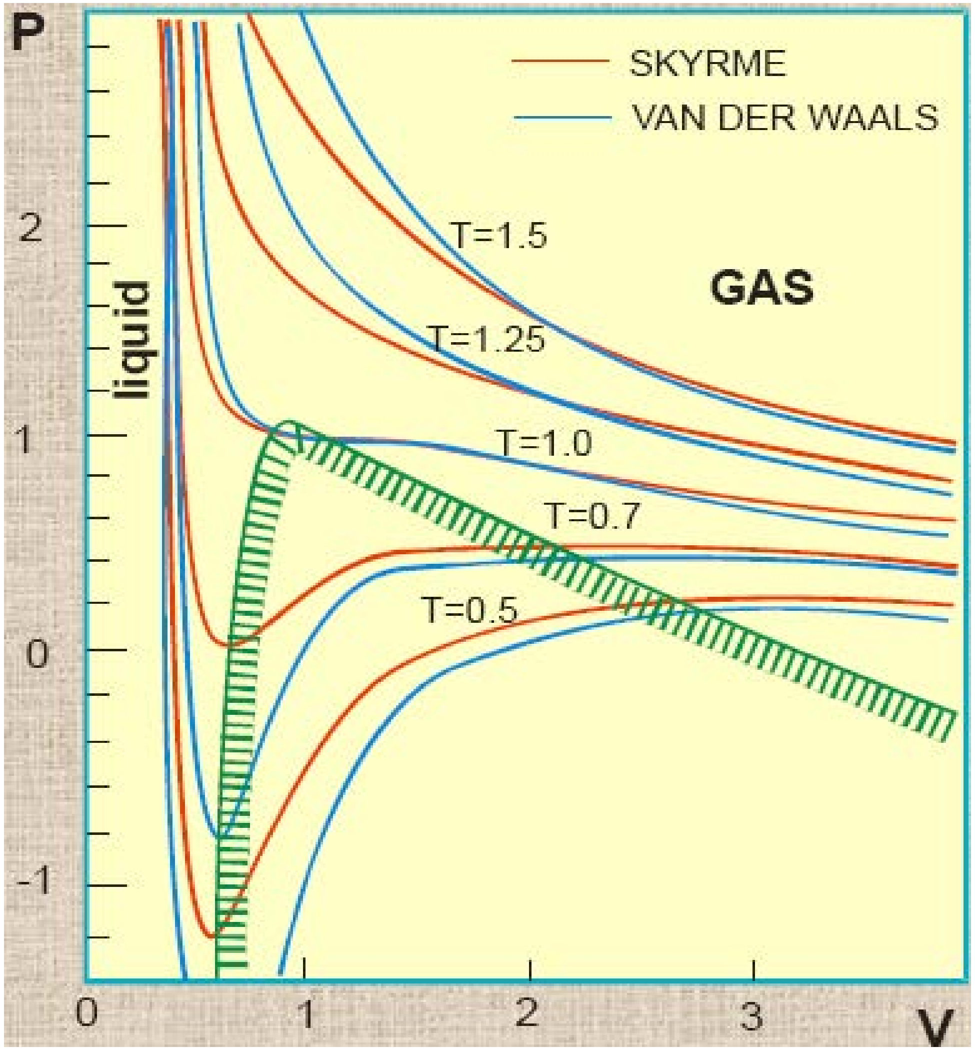

Van der Waals SE *(1875)*
& Nuclear Matter SE
(1983)(relative units:
V/Vc; p/pc ; T/Tc)

Instability region

$$\partial p / \partial V \big|_T > 0$$

H. Jaqaman *et al*., Phys. Rev. C 27 (1983)2782

equation of state *vs* phase diagram

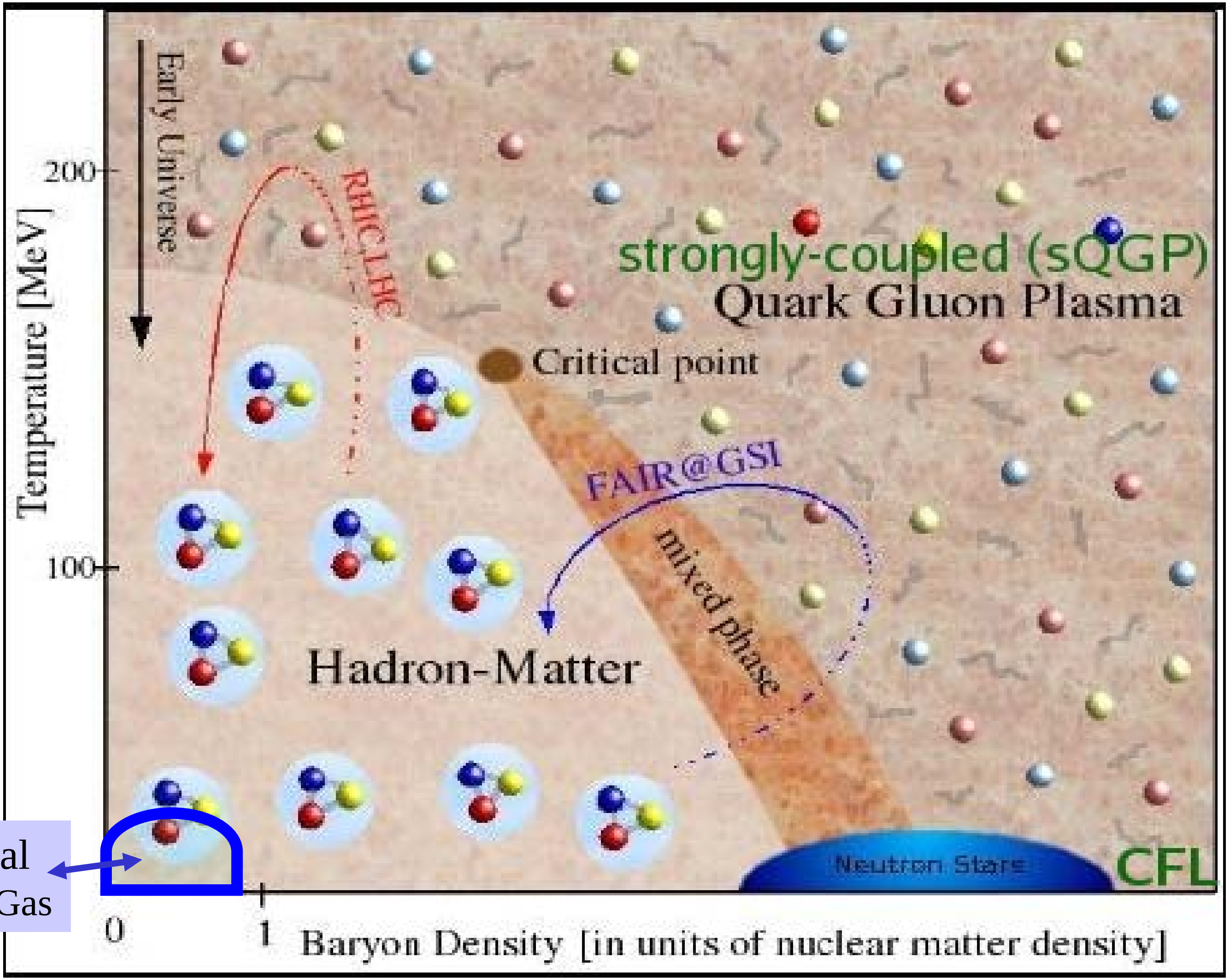

Spinodal
Liquid-Gas

equation of state *vs* phase diagram

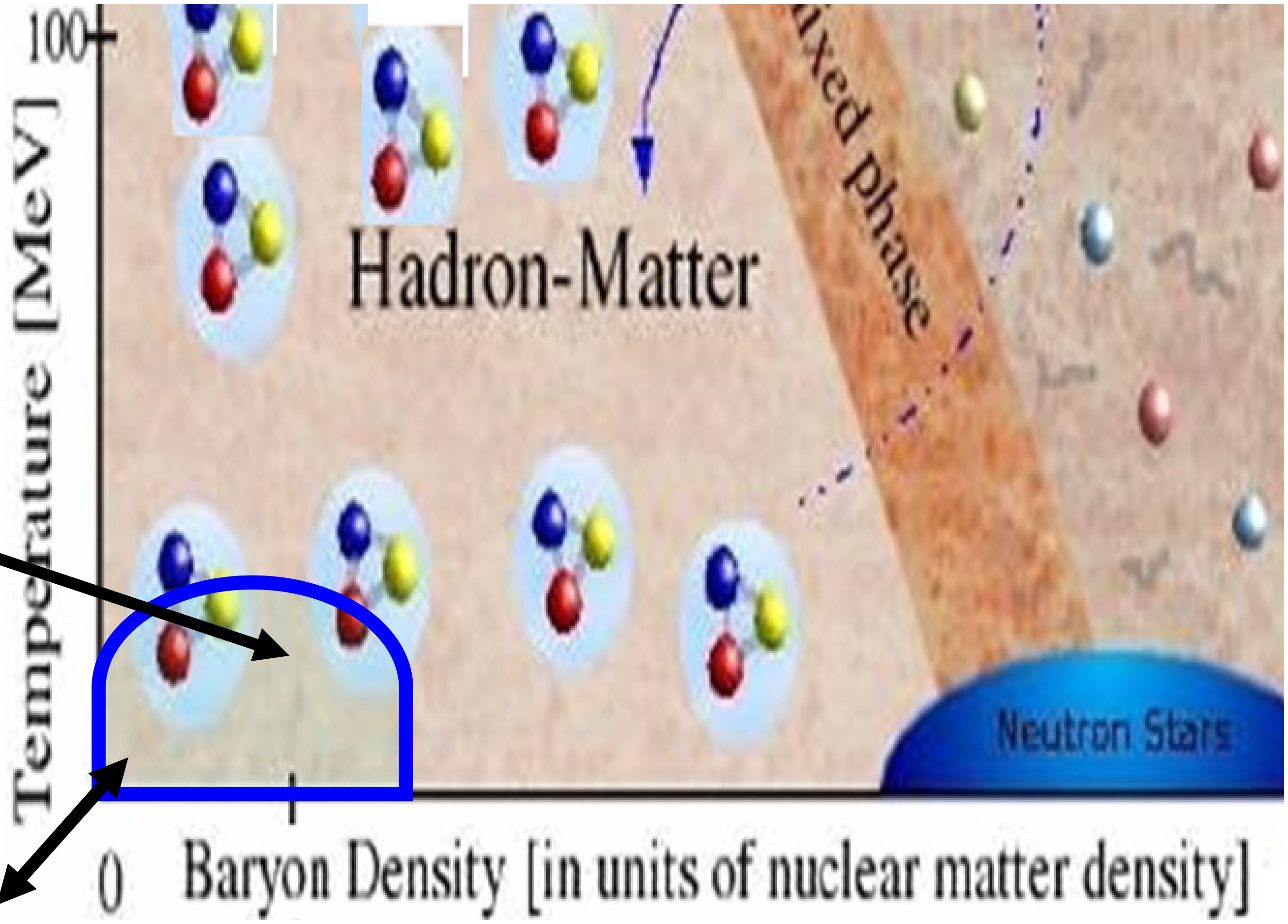

Spinodal
Liquid-Gas

D=10^9 g/cm^3
T=0.5MeV

explosion proceeds through convection processes

ν-sphere

magneto-rotational instabilities & dynamo-action → amplifying

Magnetic fields up to strengths hundred *tera-tesla*

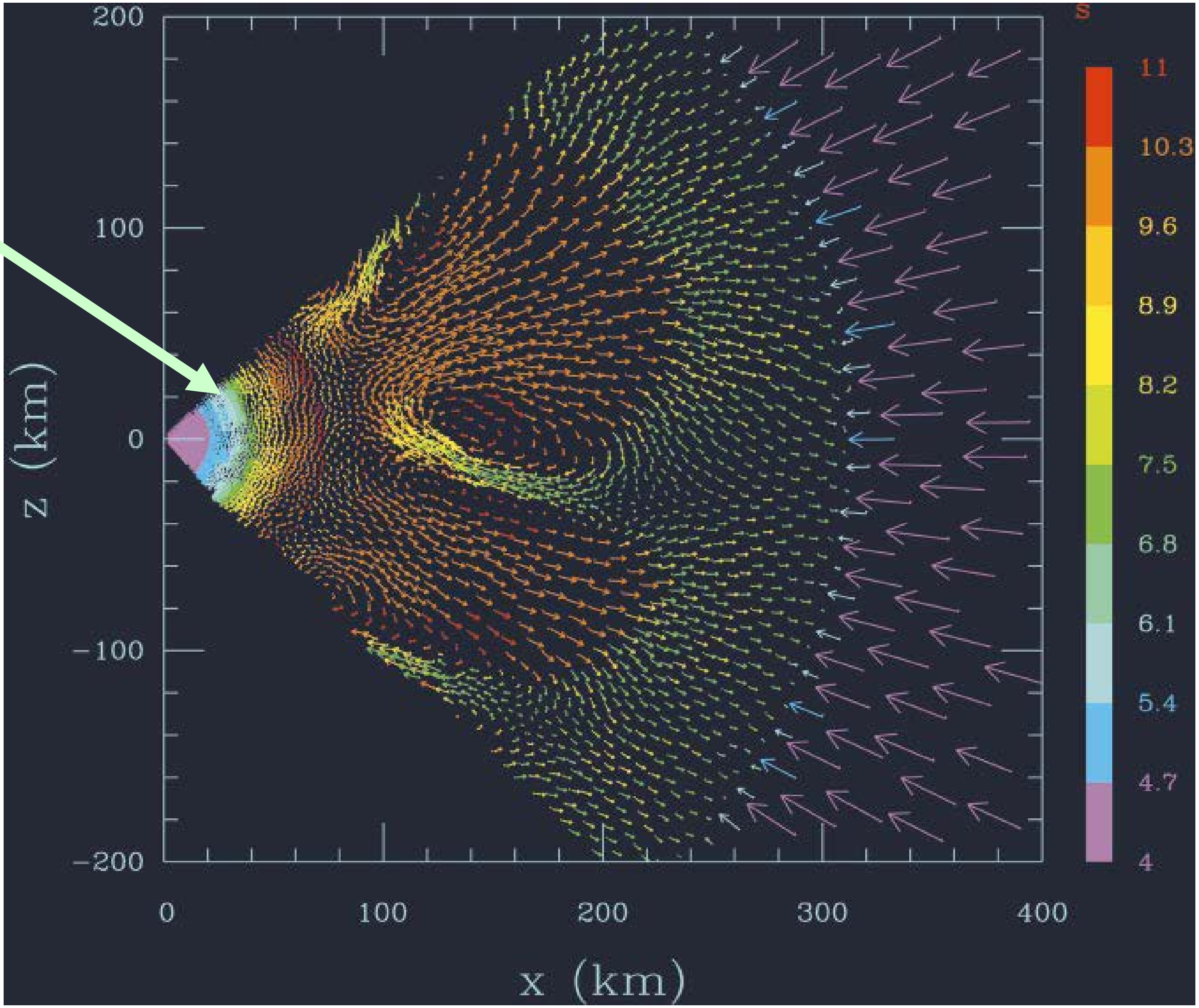

The magnetic field evaluation

(S.G.Moiseenko, G.S.Bisnovatyj-Kogan, N.V.Ardeljan, MNRAS 370 (2006) 501)

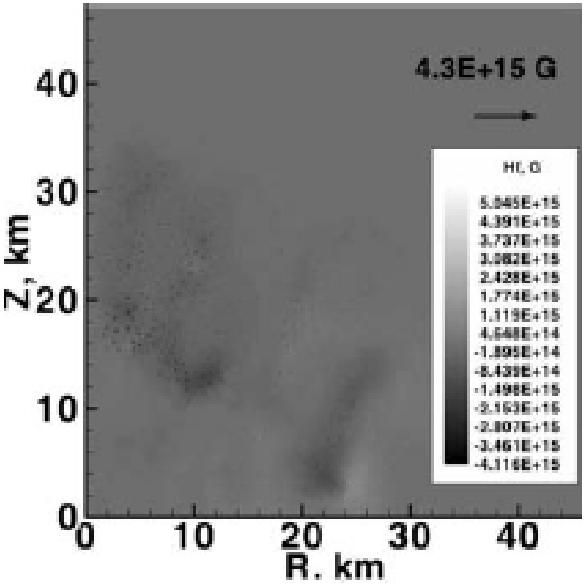

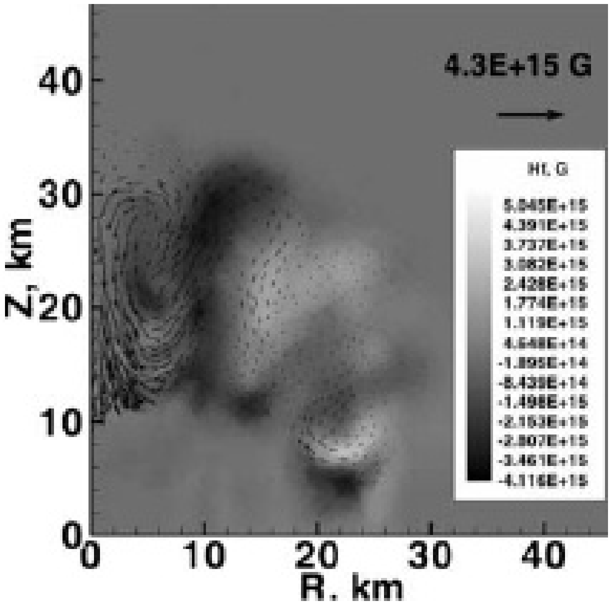

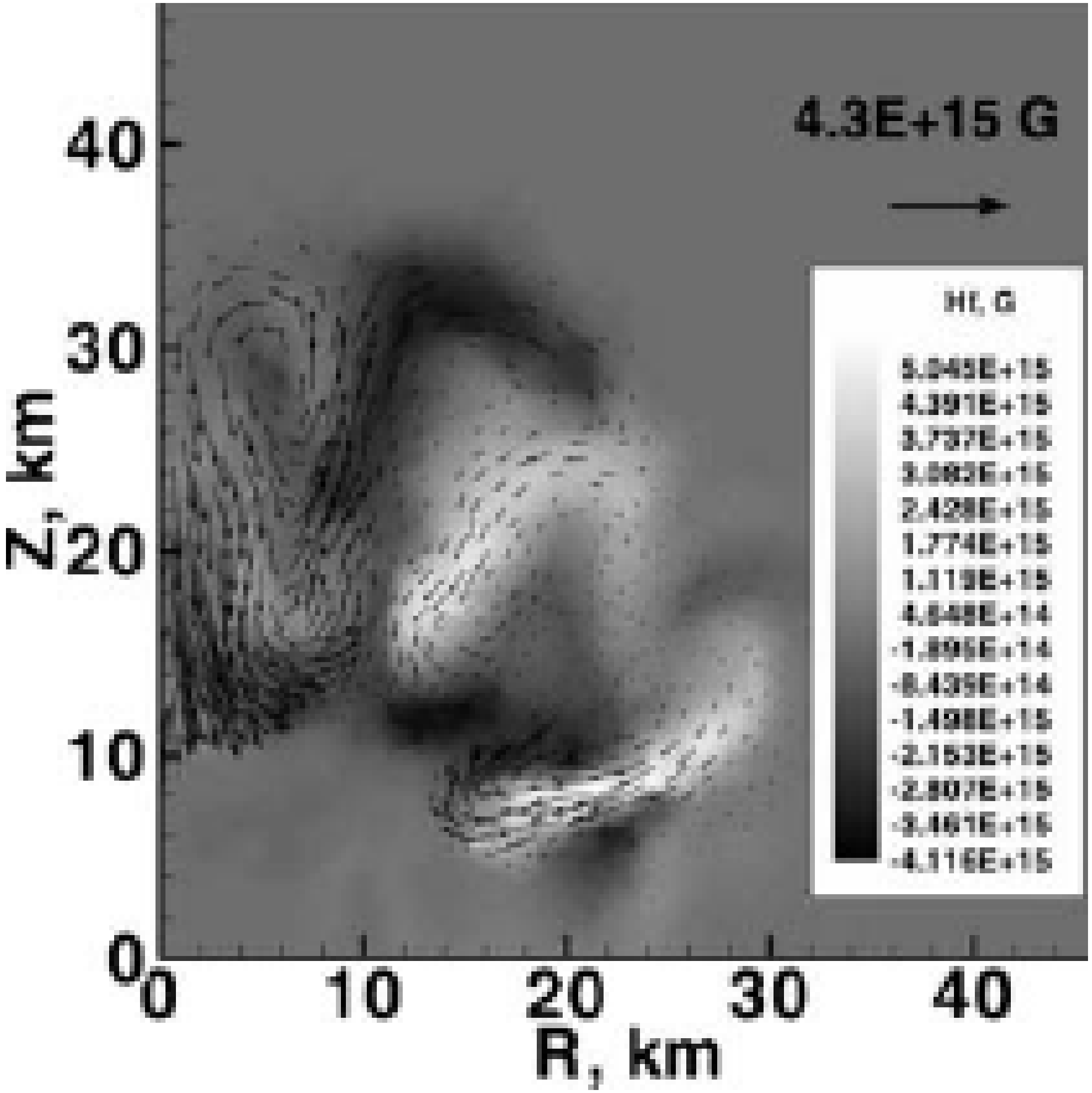

Magnetic field estimates

`predominant energy component of shock wave` E_S `originates from the magnetic pressure`

$$\langle B_\nu^2 \rangle R_\nu^2 \Delta R \sim 2E_S \quad \sim 10^{51,5} \text{ ergs}$$

$R_\nu \sim 40\text{Km};\ \Delta R \sim 1\text{Km}$

$B_\nu \sim 10^1 - 10^2$ TeraTesla

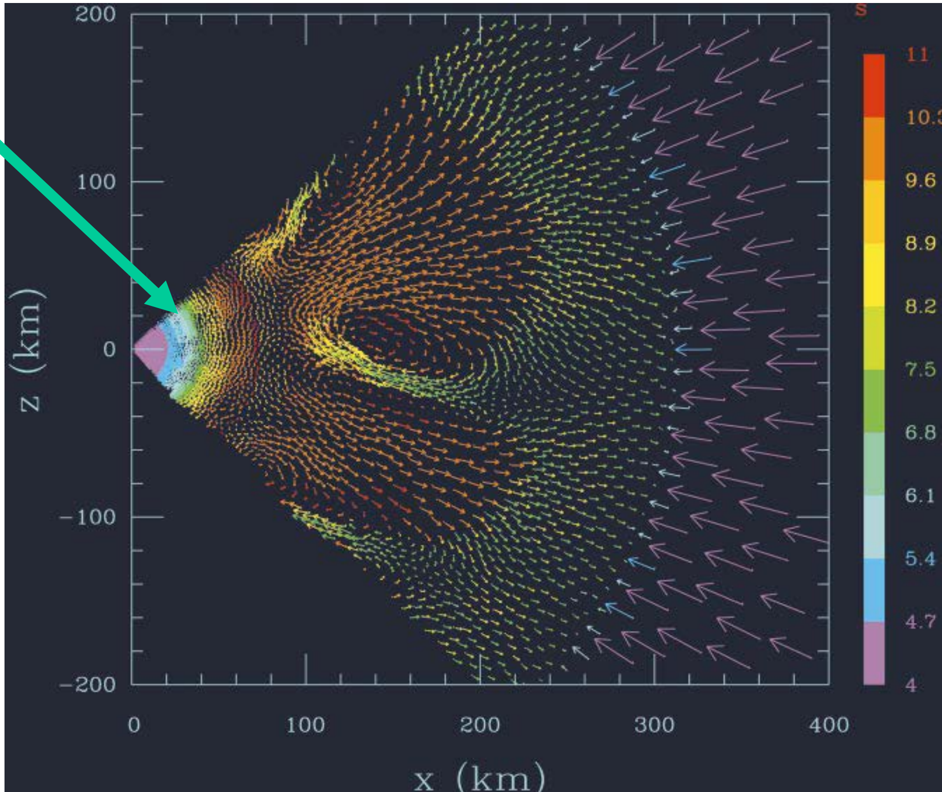

$B(R) \sim B_\nu \square R_\nu / R$

Magnetic field estimates

Magnetic and gravitational forces

$$dB_\nu^2/dR \sim 8\pi\, GM\, n(R)/R^2$$

$4\pi R^2\, n(R) = dM/dR$

$B \sim 10^{1.5}$ TeraTesla $(M/M_o)(10\mathrm{km}/R)^2$

$R_\nu \sim 40$ Km; $\Delta R \sim 1$ Km

$B_\nu \sim 10^1 - 10^2$ TeraTesla

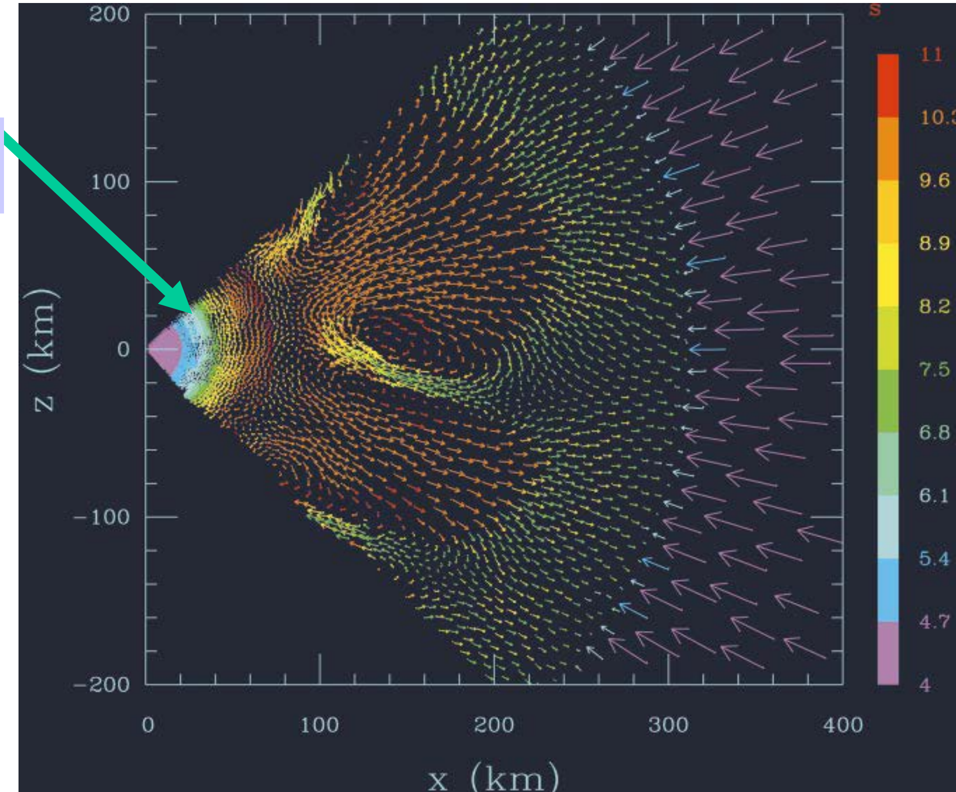

NUCLEAR STATISTICAL EQUILIBRIUM in Ultra-Strong Magnetic Fields

Entropy *S* extremum →

$$TdS = \sum_i \lambda_i dY_i = 0$$

Nuclear composition at temperature *T*

$$Y \propto \frac{G_A}{G_n^N G_p^Z} \exp\{-B/kT\}$$

Binding Energy ***B***

spin-magnetic part in partition function

$$G_i = \sum_M \exp\{g_i M \omega_L / kT\} / (2I_i + 1)$$

$$\omega_\mathrm{L} = \mu_\mathrm{N} H$$

Nuclear Shell Effects at *Ultra-Strong Magnetic Fields*

V.N.K. //PRL 2002. V.88, 221101 // J.Nucl.Sci.Technol. V.1 Sup.2. P.550 // J.Nucl.Radiochem.Sci. 2002. V.3. P.205 // PRC 2004 V.69, 038801/ЯФ. 2012

$$N = \int_{-\infty}^{\varepsilon_F} d\varepsilon \cdot \rho(\varepsilon)$$

Nucleons

Binding Energy $$B = \int_{-\infty}^{\varepsilon_F} d\varepsilon \varepsilon \rho(\varepsilon) = B^{sm} + B^{sh}$$

Level density $$\rho = \sum_n \delta(\varepsilon - \varepsilon_n) = \rho^{sm} + \rho^{sh}$$

With Single particle levels ε_n ***filled up to the Fermi energy*** ε_F

the Hartree self-consistent mean field approach in magnetic field : h

- Single particle Hamiltonian
- $H = H_{MF} + (so)*(ls) +$ *(Magnetic terms)*
- Pauli–spin (S) → **- M (hS)**
- Landau–orbital (l) → **- M (hl)** **:protons**

Neutrons

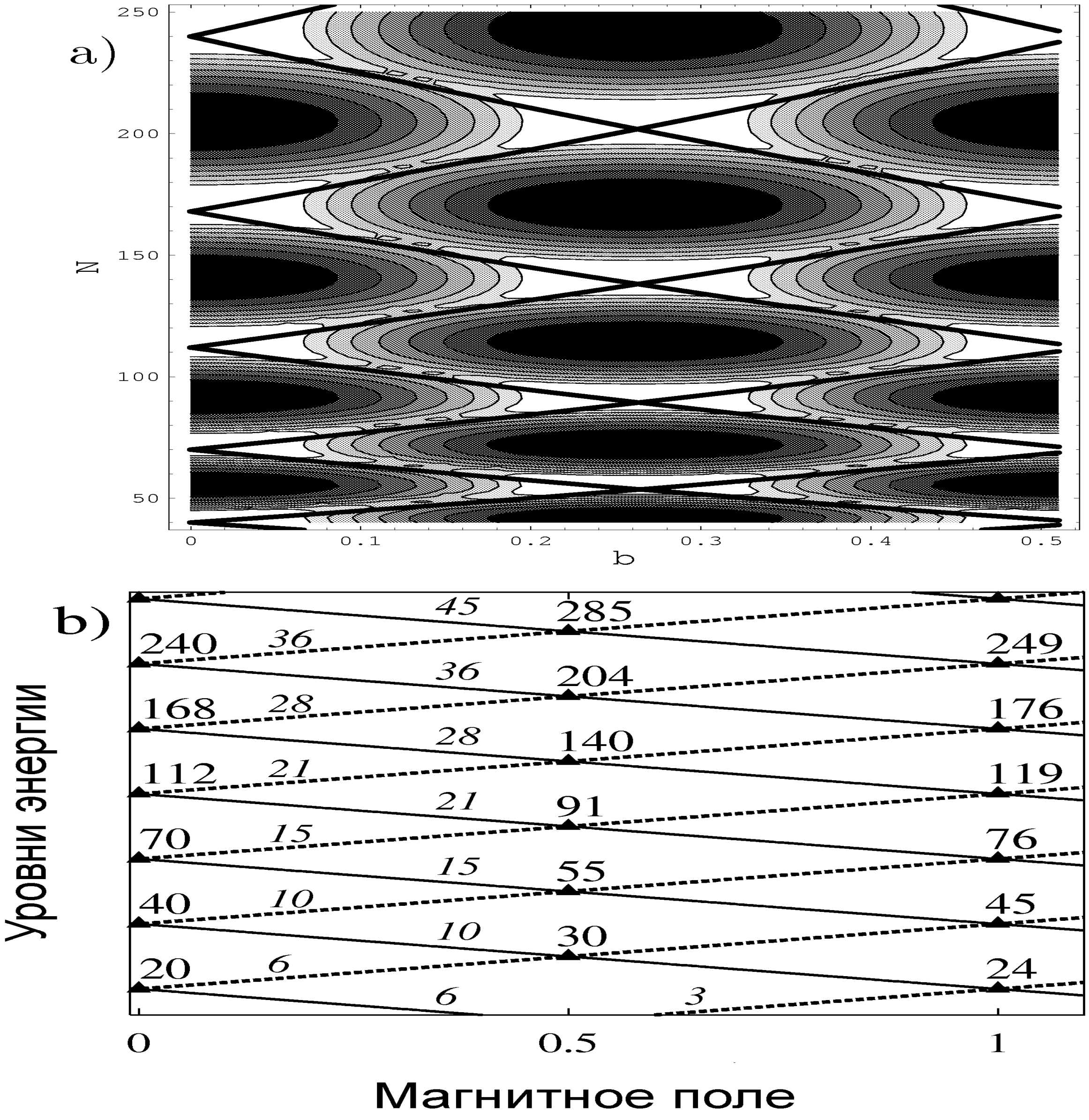

Minority
spin up

Majority
spin down

Binding energy of even-even symmetric nuclei *at magnetic fields h*

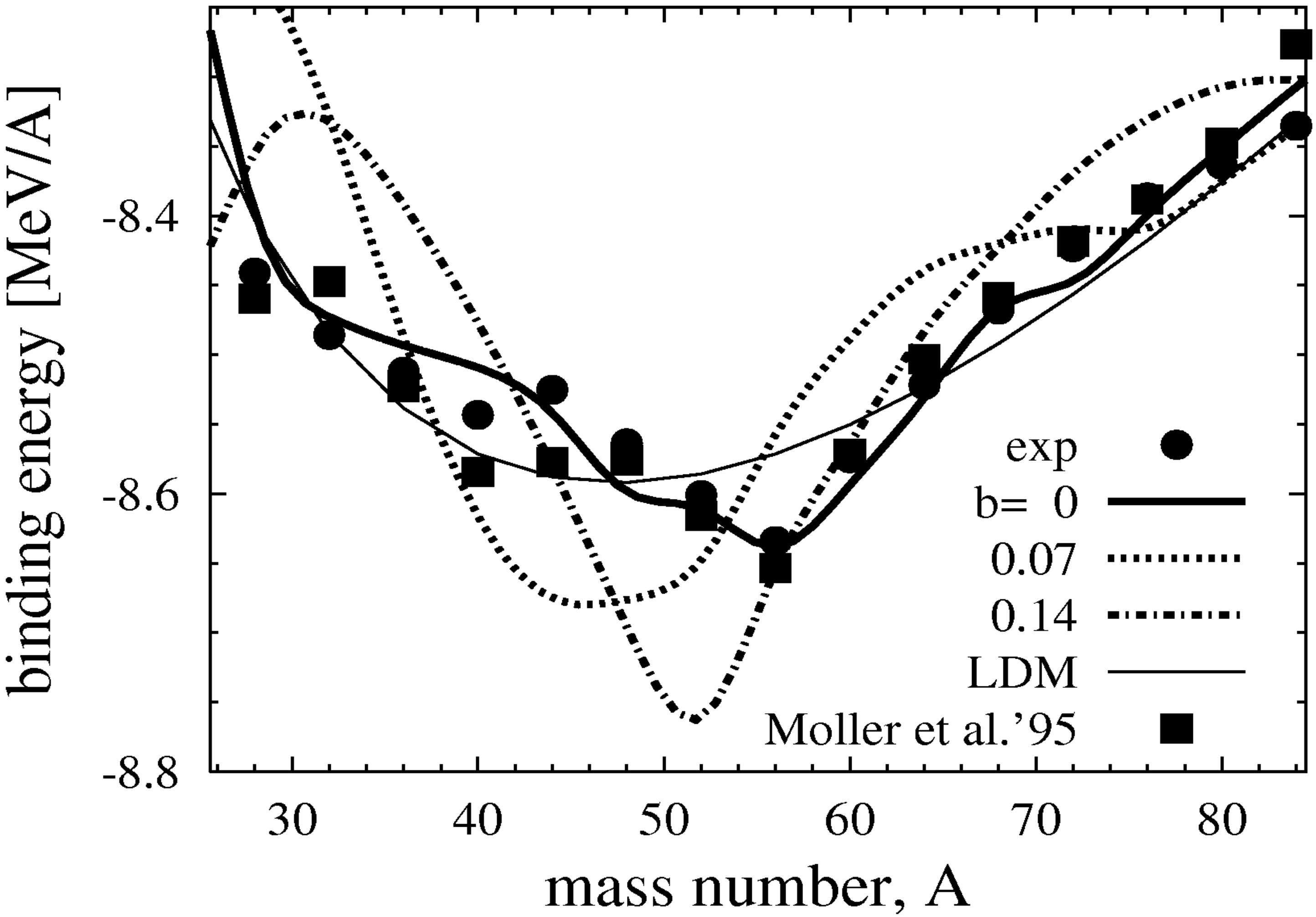

relative yield *y*=*Y(H)/Y(0)*

^{56}Ni(solid) i ^{44}Ti(dashed line)

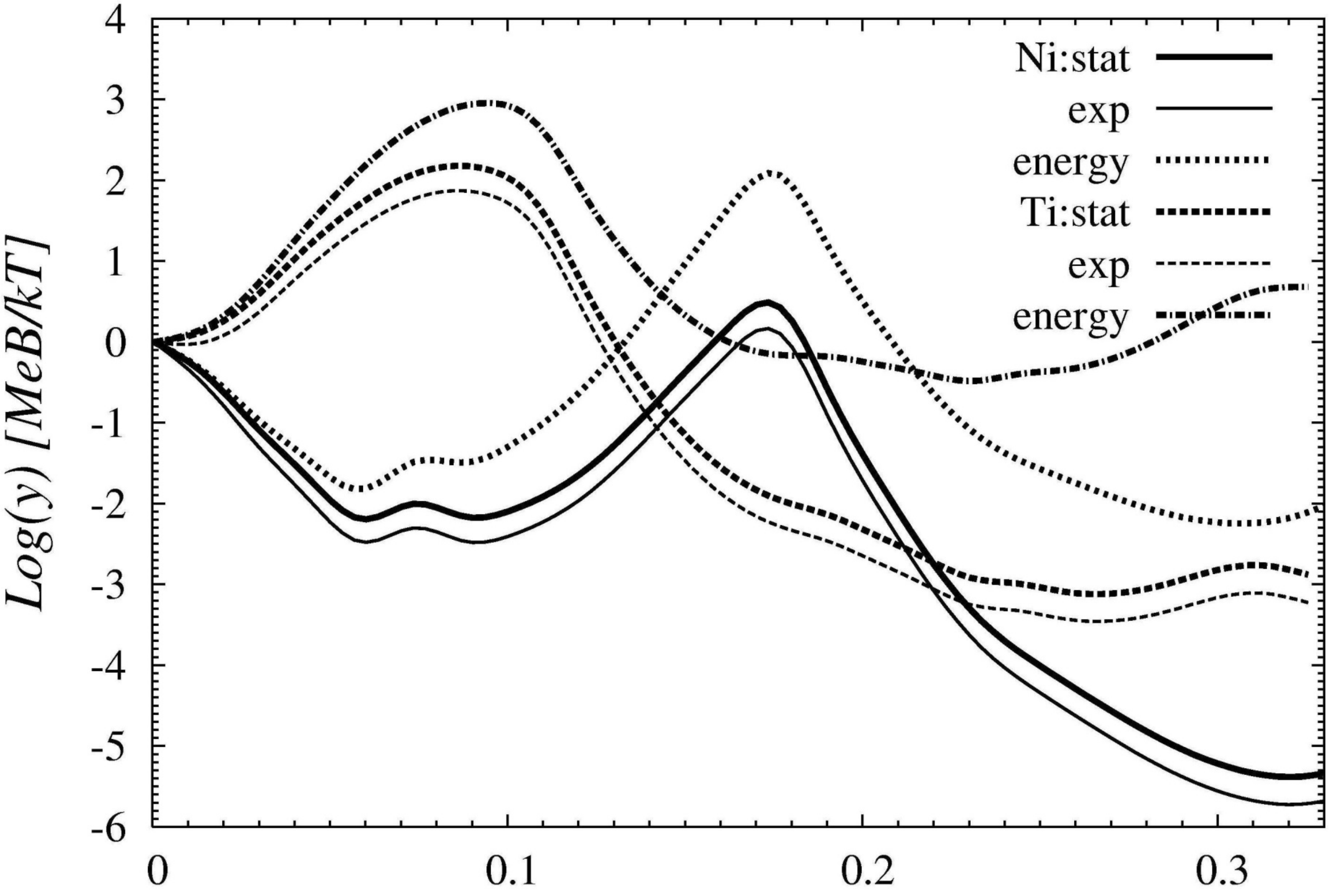

Магнитное поле, *h*

Explosive nucleosynthesis: s-process

- The **s-process** (slow-process) proceeds via neutron-capture (n, ***γ***) reaction chains at low neutron flux.
- Process definition: $T_{\text{beta-decay}} < T_{(n,\ \gamma)}$ -- **new nucleus decays to stable nuclide before further neutron is captured:** (sec vs ~10^3 yrs)
- s-process works through chain of stable nuclides ('beta stability valley') & n-capture much ***slower*** decay times
- Famous s-element Technetium (Z = 43) has no stable isotopes - the longest lived ~10^6 years -- must be produced recently in stars where observed.
- Tc was first observed by Merrill (1952) and provided the first real proof that nucleosynthesis was indeed happening in stars!

slow- or s-process.

Beta-decay faster n-capture rate

weak interactions keep the proton&neutron Fermi levels at equilibrium

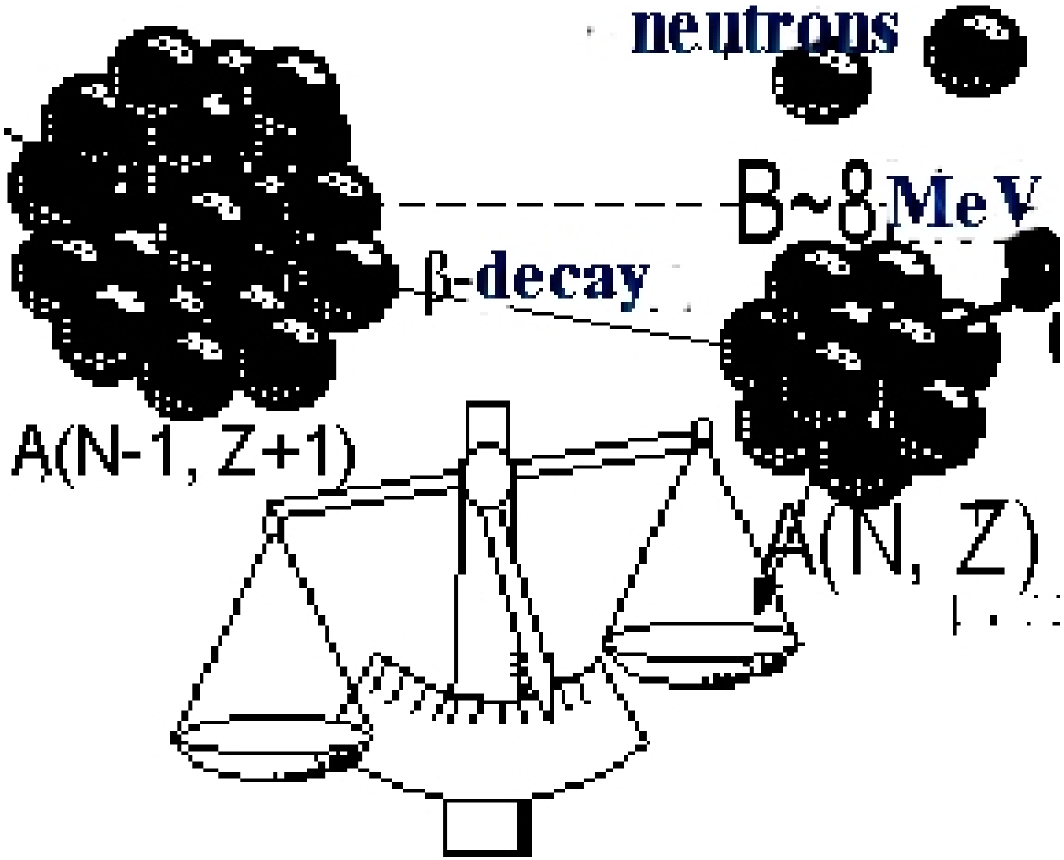

Sample of the s-process:

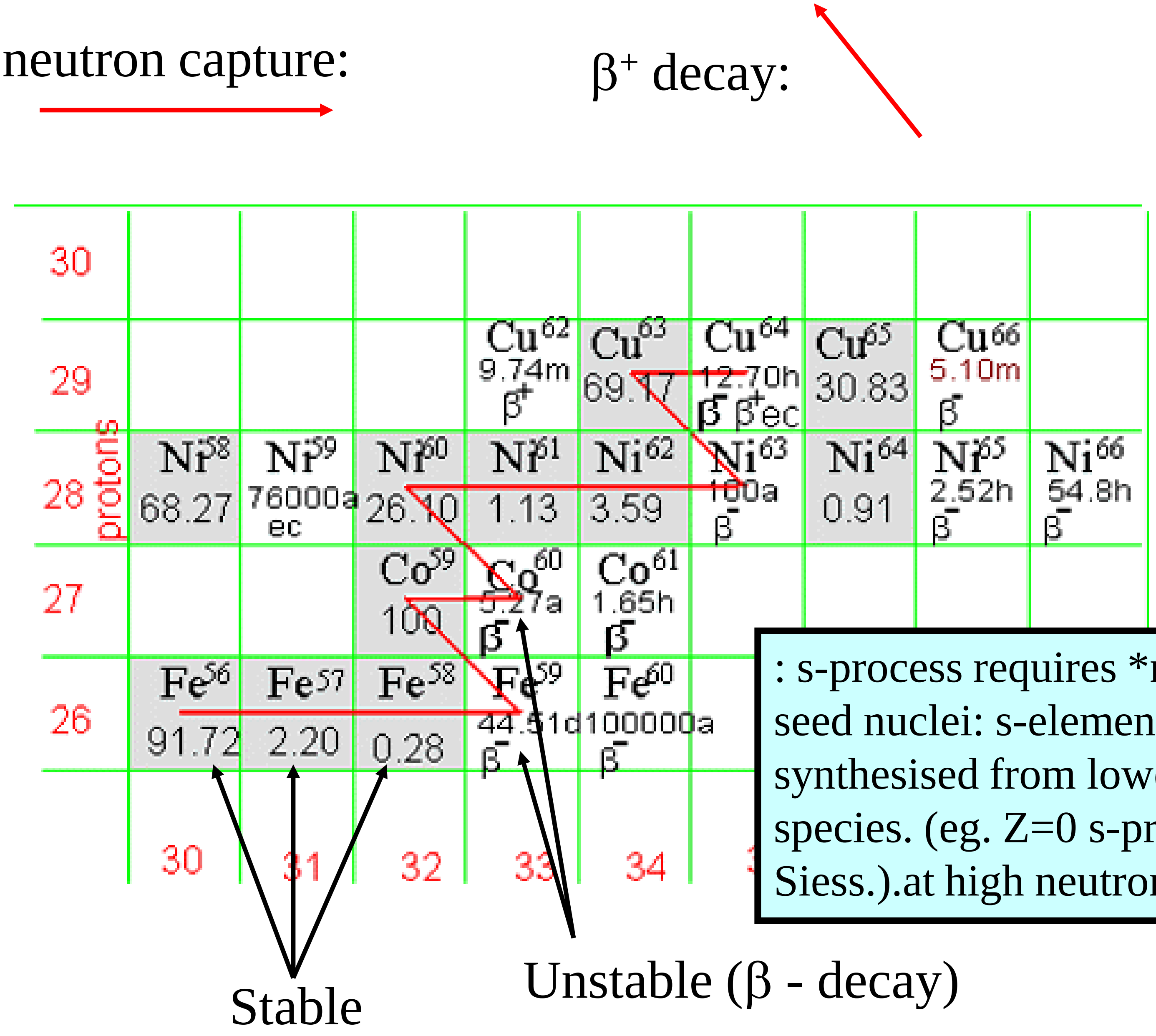

neutron capture:

β^+ decay:

protons									
30									
29				Cu^{62} 9.74m β^+	Cu^{63} 69.17	Cu^{64} 12.70h β^- β^+ec	Cu^{65} 30.83	Cu^{66} 5.10m β^-	
28	Ni^{58} 68.27	Ni^{59} 76000a ec	Ni^{60} 26.10	Ni^{61} 1.13	Ni^{62} 3.59	Ni^{63} 100a β^-	Ni^{64} 0.91	Ni^{65} 2.52h β^-	Ni^{66} 54.8h β^-
27			Co^{59} 100	Co^{60} 5.27a β^-	Co^{61} 1.65h β^-				
26	Fe^{56} 91.72	Fe^{57} 2.20	Fe^{58} 0.28	Fe^{59} 44.51d β^-	Fe^{60} 100000a β^-				
	30	31	32	33	34	3			

Stable

Unstable (β - decay)

: s-process requires *no* Fe group seed nuclei: s-elements can be synthesised from lower-mass species. (eg. Z=0 s-process, Siess.).at high neutron fluxes.

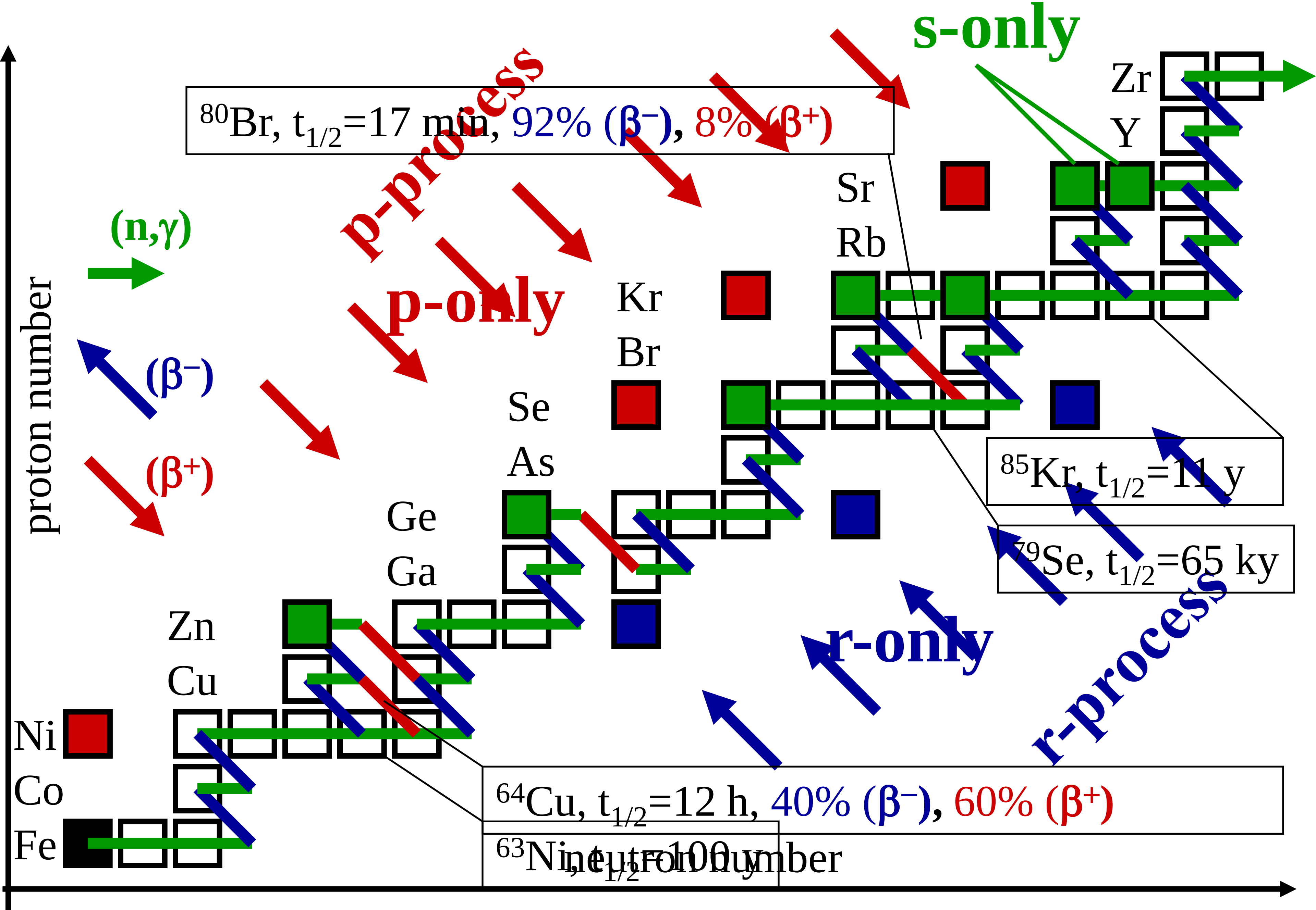

^{80}Br, $t_{1/2}$=17 min, 92% (β−), 8% (β+)

^{85}Kr, $t_{1/2}$=11 y

^{79}Se, $t_{1/2}$=65 ky

^{64}Cu, $t_{1/2}$=12 h, 40% (β−), 60% (β+)

^{63}Ni, $t_{1/2}$=100 y

Nuclear Magics in s-process:

- For certain neutron numbers -- *N* = 28, 50, 82, 126 -- neutron capture cross-sections are much smaller than others.
- When one of these "magic" numbers is reached, the nucleus hardly captures more neutrons.
- significant number of nuclei will build up at magic numbers
- more abundant Elements corresponding to neutron "magic" numbers produce peaks in the observations.
- Solar System as abundance peaks at
  ^{88}Sr, ^{138}Ba, & ^{208}Pb.

$$\boxed{N_A \propto \frac{1}{\langle \sigma \rangle_A}}$$

small capture cross sections at neutron magic numbers

⇔ pronounced abundance peaks

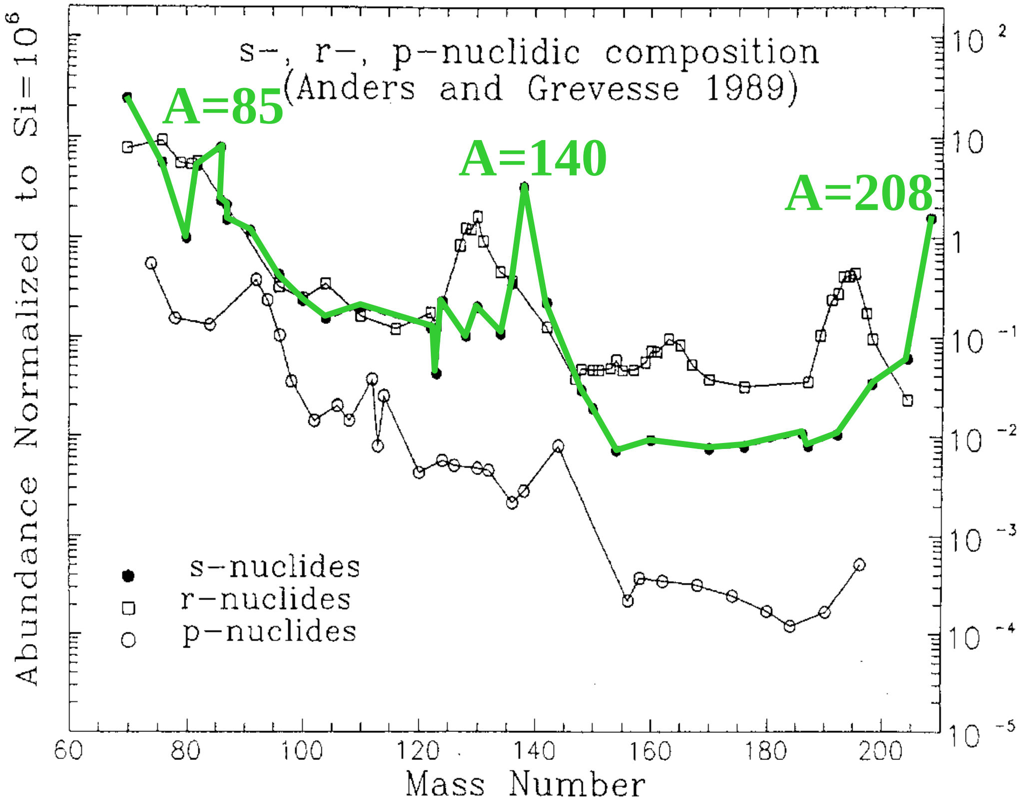

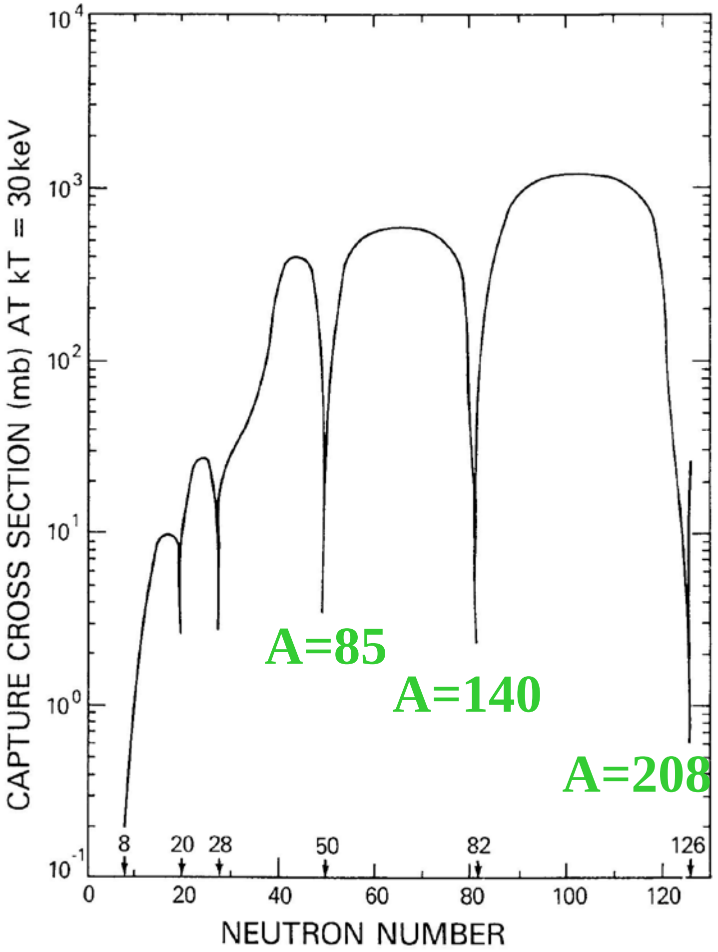

Rolfs & Rodney: Cauldrons in the Cosmos, 1

$$\langle\sigma\rangle_A N_A = \text{constant}$$

condition fulfilled between
magic numbers of neutrons

sudden drops observed at
neutron magic numbers

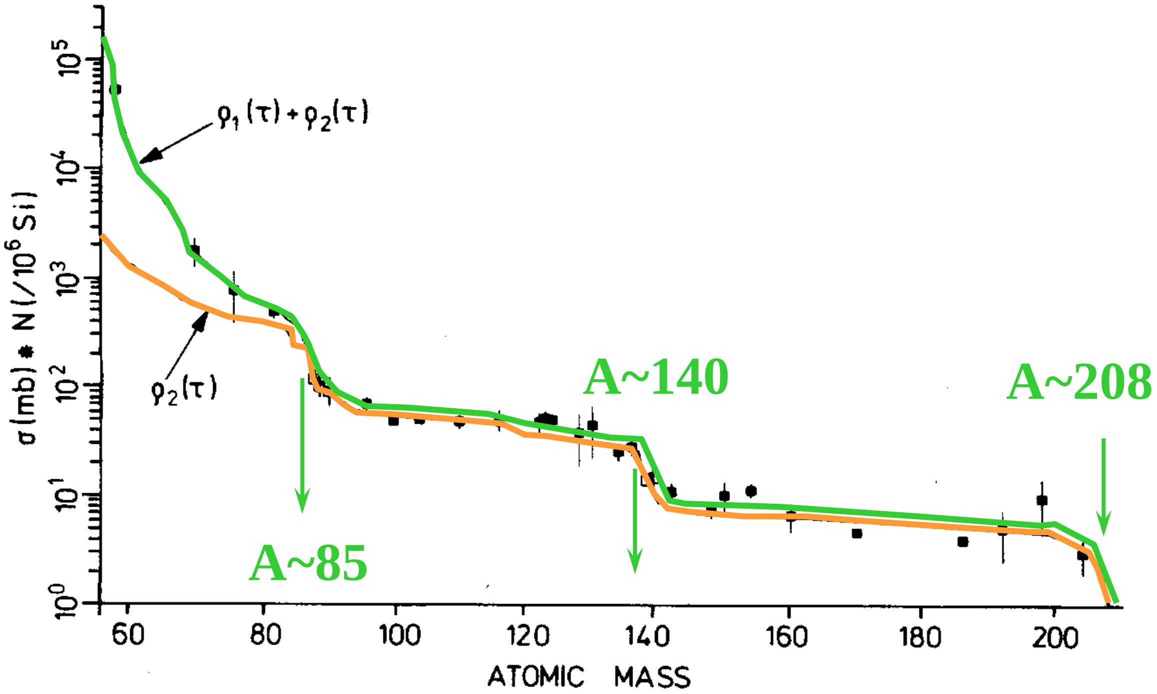

NOTE

a superposition of many neutron irradiations is needed to correctly reproduce the abundance curve

- **main component (A=88-209)**
- **weak component (A<90)**

s-process: best understood nucleosynthesis process from nuclear point of view

The s (& r) processes explain the production of higher mass nuclei (beyond the Fe peak).

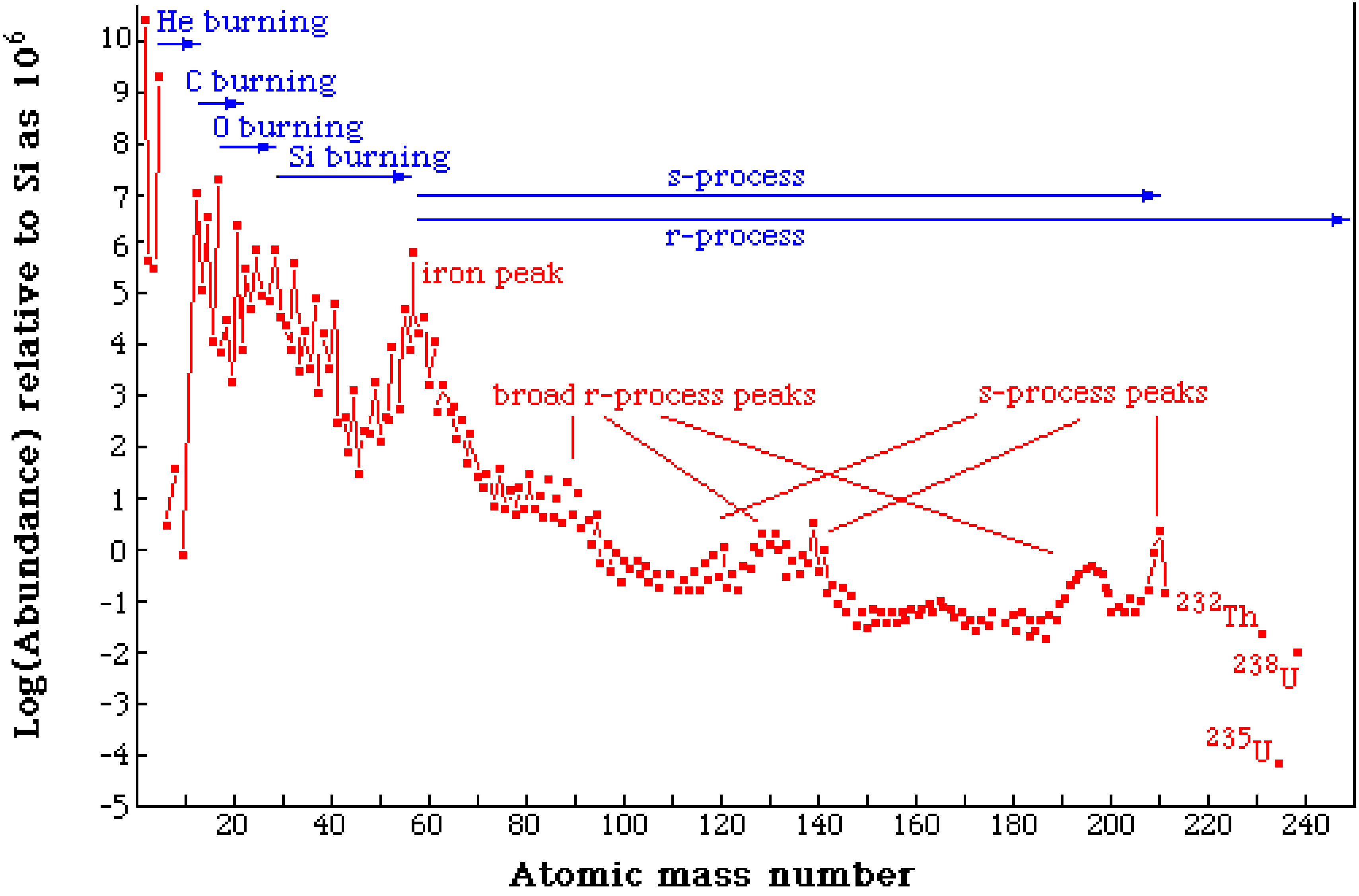

r-process (r = rapid) neutron capture process)

unstable nucleus reacts before the decay $\Leftrightarrow$ $\boxed{\tau_n << \tau_\beta}$

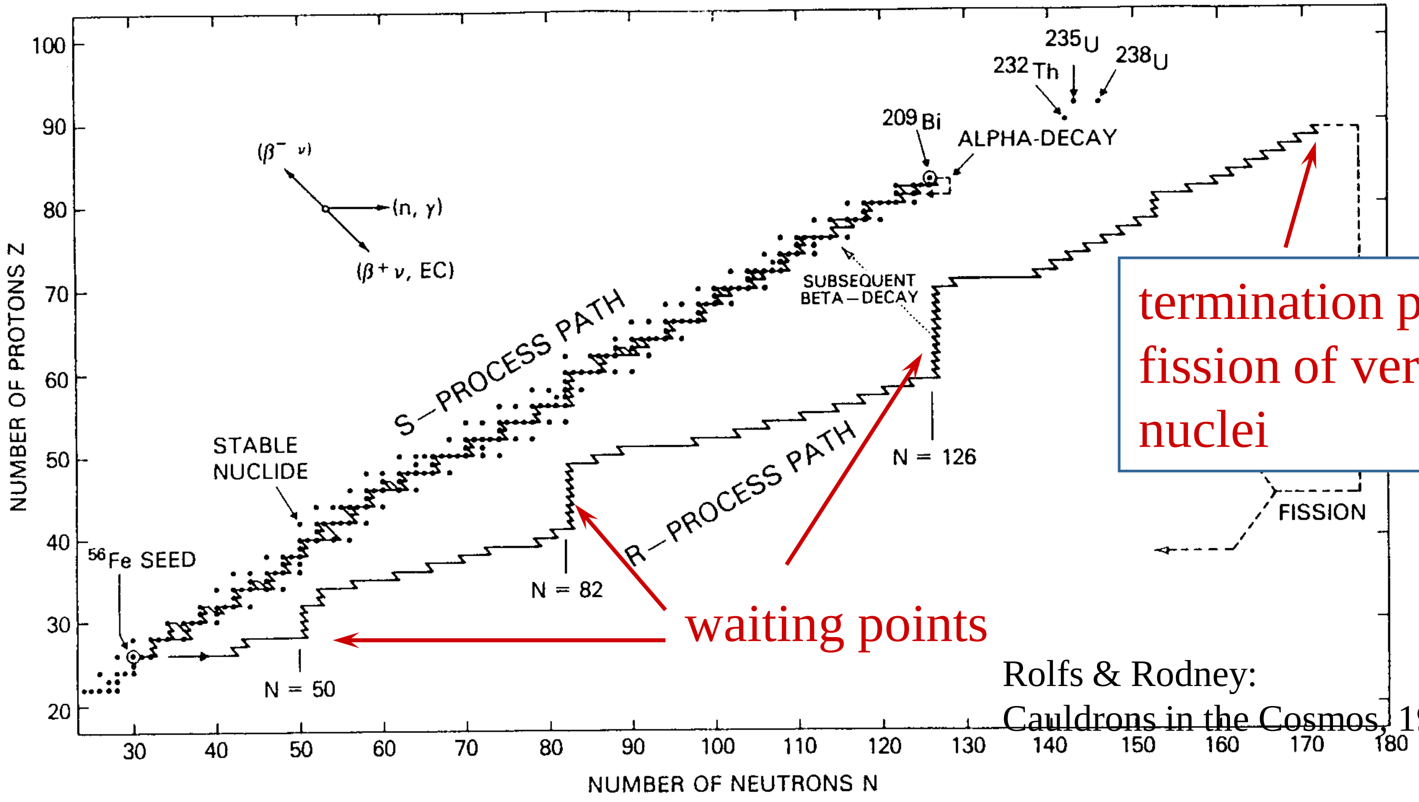

termination point: fission of very heavy nuclei

waiting points

Rolfs & Rodney: Cauldrons in the Cosmos, 1988

typical lifetimes for unstable nuclei far from the valley of β stability: $10^{-6} – 10^{-2}$ s

requiring: $\boxed{\tau_n \sim 10^{-4}\text{ s} \quad \Leftrightarrow \quad N_n \sim 10^{20}\text{ n/cm}^3}$

explosive scenarios needed to account for such high neutron fluxes

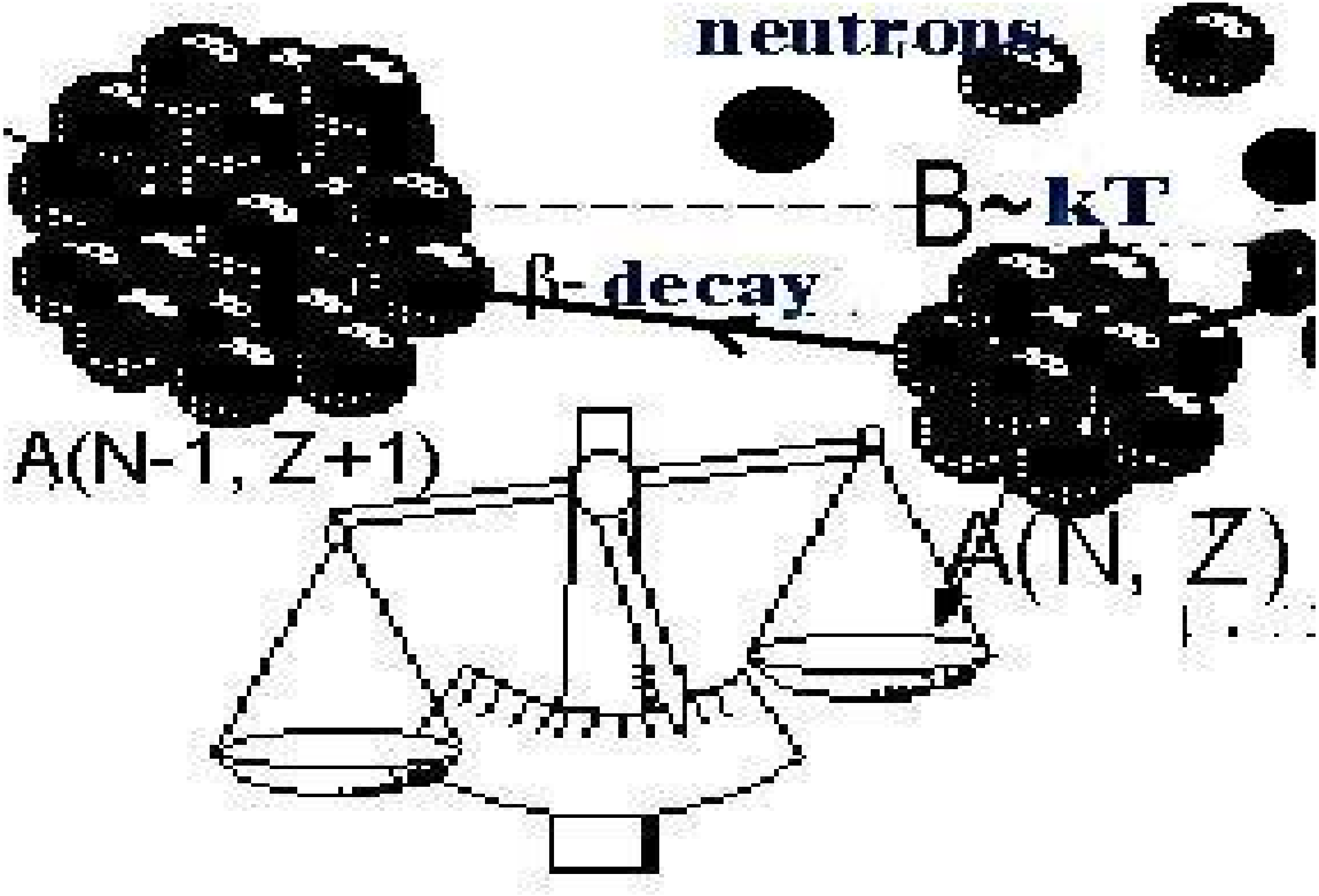

R-process←|exceptionally explosive conditions

N(n)~ 10^{20}/cc : T~ 10^{9}K : t~ 1sec

Transmutations of ultramagnetized atomic nuclei under intensive neutron

nuclear reaction rate

$$r = \int \sigma v dD_x dD_X$$

radiative *neutron*-capture (n,γ) reaction

Hauser-Feshbach statistical approach

$$\sigma_{(n,\gamma)} \,\square\, \Gamma / \kappa^2 \,\square\, 1 / v_n$$

Relative rate

$$r(H) / r(0) = \sigma(H) / \sigma(0)$$

Neutron-capture rate

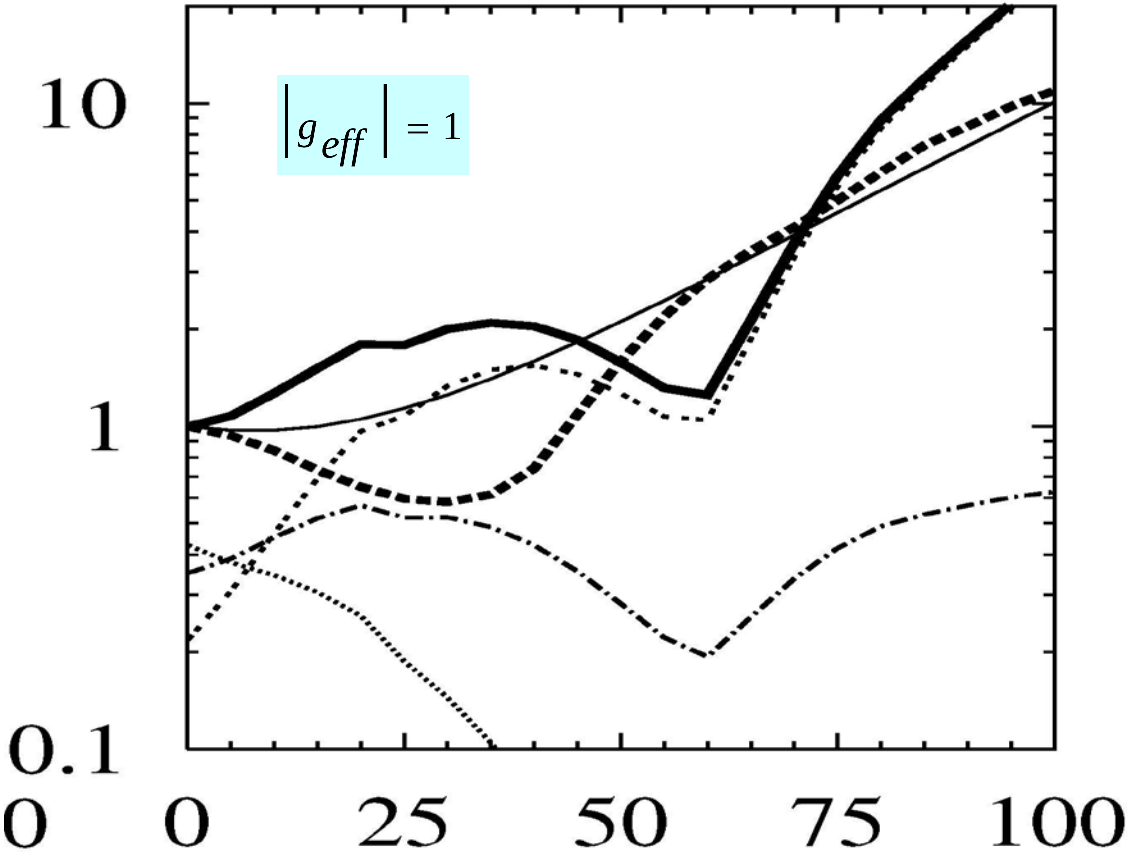

SUMMARY

- We analyze the synthesis and decay of ^{n} nuclides in SNRs
- Obtained the spectra and flux for the specific lines of decay products

SUMMARY

- Magnetism of Atomic Nuclei
  Thermodynamic formalism
- Magnetic field effect on Nuclear Shell Structure
  Phase-shift in shell oscillations of Nuclear Masses
- Pauli type Paramagnetic Response
- Landau-type Orbital Magnetism
- Magnetic fields of Tera-Tesla shift
  Nuclear Magics of Iron region towards
  Smaller Masses approaching Ti-44
- Enhancement in Yield at nucleosynthesis

SUMMARY

- We analyze the synthesis and decay of ^{44}Ti in SNRs
- Obtained the spectra and flux for the lines of ^{44}Sc

Models explaining titanium excess

Motizuki Yuko, Kumagai Shiomi, ^{44}Ti radioactivity in young supernova remnants: Cas A and SN 1987A., New Astr. Rev. 2004. V. 48. P. 69

→

The radioactivity suppression is induced by the high level of ionization of matter. As a result – decreasing of the activity at the early phases of the evolution of the SNR.

Kondratyev V.N., Kadenko I.M., Nucleosynthesis in strong magnetic fields at statistical equilibrium; MNRAS 2005. V.359, P.927

→

Increasing of the Ti-44 synthesis due to astrophysics environment

$1\text{kpc} = 3.08567758 \times 10\text{^}^{19}$ метра